PB98-115959

STATEWIDE CALIBRATION OF ASPHALT TEMPERATURE STUDY FROM 1992 AND 1993 VOLUME I

NOV 97

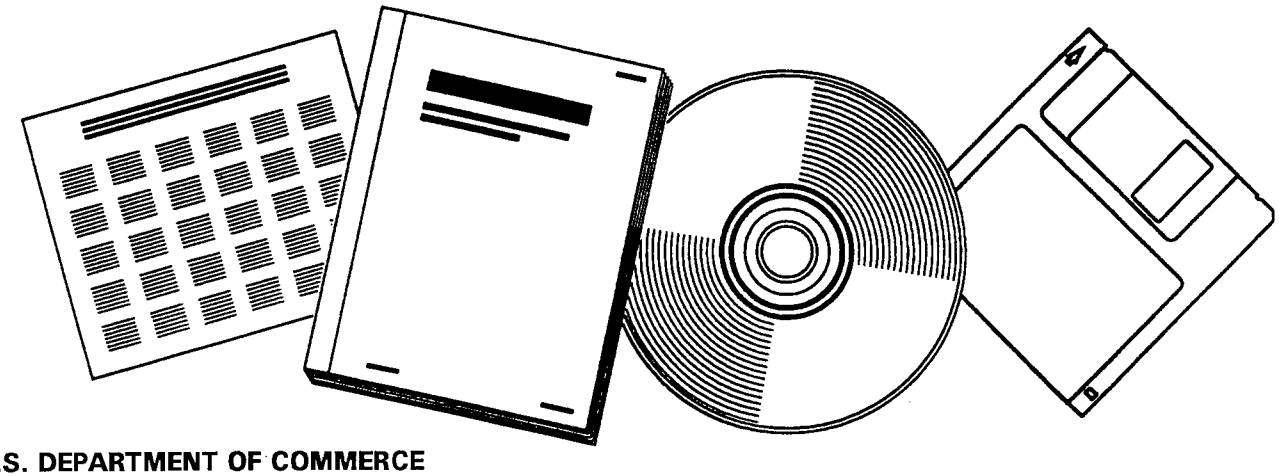

U.S. DEPARTMENT OF COMMERCE
National Technical Information Service

CENTER FOR TRANSPORTATION ENGINEERING STUDIES

DEPARTMENT OF CIVIL ENGINEERING
NORTH CAROLINA STATE UNIVERSITY

STATEWIDE CALIBRATION OF ASPHALT TEMPERATURE STUDY FROM 1992 AND 1993

VOLUME I

by

Y. Richard Kim, PhD, PE
Associate Professor

Sunwoo Park, PhD
Research Associate

Lisheng Shao, PhD
Research Associate

Final Report

November 1997

STATEWIDE CALIBRATION OF ASPHALT TEMPERATURE STUDY FROM 1992 AND 1993

VOLUME I

by

Y. Richard Kim, PhD, PE
Associate Professor

Sunwoo Park, PhD
Research Associate

Lisheng Shao, PhD
Research Associate

Final Report Submitted to the
North Carolina Department of Transportation

Department of Civil Engineering
North Carolina State University
Raleigh, NC

November 1997

Technical Report Documentation Page

1. Report No.	2. Government Accession No.	3. Recipient's Catalog No.
FHWA/NC/97-002		

4. Title and Subtitle	5. Report Date
Statewide Calibration of Asphalt Temperature Study from 1992 and 1993 - Volume I	October 1997
	6. Performing Organization Code
	8. Performing Organization Report No.
7. Author(s) Y. Richard Kim, Sunwoo Park, Lisheng Shao	
9. Performing Organization Name and Address Center for Transportation Engineering Studies Department of Civil Engineering Studies North Carolina State University Raleigh, NC 27695	10. Work Unit No. (TRAIS)
	11. Contract or Grant No. 23241-95-1
	13. Type of Report and Period Covered Final Report 7/1/94 - 6/30/96
12. Sponsoring Agency Name and Address North Carolina Department of Transportation Raleigh, NC 27611	14. Sponsoring Agency Code

15. Supplementary Notes

16. Abstract

The overlay design analysis in the 1993 AASHTO Guide for Design of Pavement Structures introduces nondestructive deflection testing as a primary means of evaluating the in situ structural capacity of existing pavements. In order to use the approaches recommended in the AASHTO Guide, deflection measurements or backcalculated layer properties must be corrected to a particular type of loading system and a standard set of environmental conditions. One of the major environmental factors affecting surface deflection measurements of flexible pavements is the pavement temperature.

Various publications bear witness to incorrect temperature correction factors presented in the 1993 AASHTO Guide, especially at higher temperatures. Based upon an urgent need of developing a more realistic temperature correction procedure for the overlay designs in North Carolina, a research project entitled "Asphalt Paving Material Properties Affected by Temperature" was funded during 1992 and 1993 by the North Carolina Department of Transportation. This project resulted in empirical models for temperature prediction and deflection correction procedures. Although these models were simple in form and practical enough to be implemented in routine deflection analyses, the deflection and temperature measurements used in developing these models were obtained from pavements located in only central region of North Carolina. This limitation necessitated testing of these models against data from other regions within the state for the statewide implementation, resulting in a follow-up project entitled "Statewide Calibration of Asphalt Temperature Study from 1992 and 1993."

17. Key Words	18. Distribution Statement
temperature correction, falling weight, deflectometer, backcalculation, asphalt concrete	No Restrictions 125 copies of this document were printed at a cost of $3.75 per copy.

19. Security Classif. (of this report)	20. Security Classif. (of this page)	21. No. of Pages	22. Price
		177	

Form DOT F 1700.7 (8-72) Reproduction of completed page authorized

ABSTRACT (CONTINUED)

During the course of this study, FWD tests and temperature measurements have been conducted on seven pavement sections at different regions of North Carolina. The field data obtained from four pavements in the central region during the 92/93 study are also included in the analysis. The new temperature correction procedure is composed of the algorithm predicting the AC layer mid-depth temperature as an effective AC layer temperature and the temperature correction procedure for deflections and backcalculated moduli.

The temperature prediction algorithm is based on fundamental principles of heat transfer and uses the surface temperature history since yesterday morning to predict the AC layer mid-depth temperature at the time of FWD testing today. The surface temperature history is determined using the yesterday's maximum air temperature and cloud condition, the minimum air temperature of today's morning, and surface temperatures measured during FWD tests. For the deflection and modulus correction procedure, a new statewide empirical model is recommended due to its simplicity and practicality. However, it needs to be warned that, when mixture properties are much different from the normal mixtures in North Carolina, this empirical model may lead to erroneous correction. Therefore, whenever thermo-mechanical properties of mixtures are available, the analytical procedure described in this report is strongly recommended, which is based on the theory of viscoelasticity and the time-temperature superposition principle.

DISCLAIMER

The contents of this report reflect the views of the authors who are responsible for the facts and the accuracy of the data presented herein. The contents do not necessarily reflect the official views or policies of the North Carolina Department of Transportation. This report does not constitute a standard, specification, or regulation.

ACKNOWLEDGMENTS

This research was sponsored by the North Carolina Department of Transportation and the Federal Highway Administration. The principal investigator wishes to thank several people who have made significant contributions to the research. Several pavement engineers at NCDOT have provided direction, helpful suggestions, constructive criticism, and support throughout the project. They are Dr. Judith Corley-Lay, Mr. Tim Little, Dr. Shin Wu, Mr. Thomas Hearne, Mr. Warren Napowsa, Mr. Josh Holland, and Mr. Mark Tiller of the Pavement Management Unit. The FWD data presented in this report were collected by Mr. Tim Little and Mr. Warren Napowsa for eastern and central regions and by Mr. Josh Holland and Mr. Mark Tiller for western region. Their careful and persistent characteristics were the key factor in the high quality FWD data. Also special thanks are due to the engineers from the Geotechnical Unit for their excellent cooperation in installing gages and obtaining cores.

EXECUTIVE SUMMARY

Nondestructive evaluation using the falling weight deflectometer (FWD) has become a primary means of determining in-situ structural conditions of pavements for design of rehabilitation strategies. The moduli of pavement layer materials, which are used as the indicators of the structural integrity of respective layers, are typically backcalculated from deflection basins obtained from FWD tests. In order to make a fair assessment of the structural condition of pavements, deflections or backcalculated moduli must be corrected to a particular type of loading system (including the type of loading device, frequency of loading, load level, etc.) and a standard set of environmental conditions. The most important environmental factor affecting surface deflections and backcalculated moduli of flexible pavement is the temperature of asphalt layers.

The correction of surface deflections or moduli to a reference temperature requires two major steps. The first is to predict an effective temperature of asphalt layers (a so-called temperature prediction procedure), and the second step is to adjust the measured deflections to a reference temperature using the predicted effective asphalt layer temperature and deflection correction factors (a so-called deflection correction procedure).

The significance of temperature correction on surface deflections has been recognized by AASHTO. The 1986 AASHTO Guide for Design of Pavement Structures presents a set of curves for deflection correction and the temperature prediction procedure requiring the use of the average air temperature for the previous five days in predicting pavement depth temperatures. However, various publications bear witness to incorrect temperature correction factors in the Guide (especially at high temperatures) and to inaccurate and impractical temperature prediction procedure. Based upon an urgent need of developing a more realistic temperature correction procedure for the overlay designs in North Carolina, a research project entitled "Asphalt Paving Material Properties Affected by Temperature" was funded in 1992 by the North Carolina Department of Transportation. As a result of this study, the PI developed empirical models for temperature prediction and temperature correction procedures. These models were simple in form and practical enough to be implemented in routine deflection analyses. However, the deflection and temperature measurements used in developing these models were obtained from pavements located in only central region of North Carolina. This limitation necessitated testing of these models against data from other regions within the state for the statewide implementation, resulting in a follow-up project entitled "Statewide Calibration of Asphalt Temperature Study from 1992 and 1993."

This report presents the findings from the follow-up statewide study. A total of seven pavement sites were selected for temperature data collection: three in the mountains (western), one in the piedmont (central), and three in the coastal (eastern) region. To measure pavement temperatures at varying depths, thermocouples were installed at varying depths of these pavements.

The FWD tests were performed on four locations in wheel path with four different loading levels (26.7, 40.0, 53.4, and 66.7 kN). These tests were repeated at different times of day and in four different seasons. Only 40 kN loading and the corresponding deflections were used in the present analysis. Pavement subsurface temperatures were measured at the time of the FWD testing using the thermocouples. The AC mid-depth temperature is taken as the effective AC temperature. In addition to the temperature measurements during the FWD testing days, pavement and air temperatures and corresponding weather conditions were recorded for seven consecutive days in each of the four seasons.

One asphalt core with 100-mm (4-inch) diameter was retrieved from each of the seven test sites. Out of the seven sites, the cores from three sections were selected for laboratory creep tests to determine the viscoelastic properties as a function of time and temperature. These three sections are New Hanover (eastern), Durham (central), and Wilkes (western).

Analytical study of deflection and temperature data has resulted in the recommended procedure that is composed of two algorithms: (1) the temperature prediction procedure for estimating AC layer mid-depth temperature as the effective AC temperature and (2) the deflection correction procedure for correcting deflections (or moduli) at the effective temperature to the reference temperature of 20°C. The temperature prediction procedure is based on fundamental principles of heat transfer and predicts the AC layer mid-depth temperature at the FWD testing time using the surface temperature history during the period from the morning of the day prior to FWD testing (D-1 day) to the time of FWD testing (D day).

The surface temperature history is constructed by combining two parts. The first part covers the period from when the surface temperature is at the lowest in D-1 day to the morning of D day. This part is predicted from the yesterday's maximum air temperature, the minimum air temperature of today's morning, and cloud conditions of yesterday. The second part of the surface temperature history is for the period between the today's morning time with the lowest surface temperature and the FWD testing time. It is constructed using actual surface temperatures measured prior to the FWD test and their extrapolation back to the time the lowest temperature occurred in today's morning.

For the correction of moduli and deflections, several alternatives have been investigated. They are: (1) new statewide model modified from the 92/93 model to cover different regions in North Carolina; (2) regional empirical models developed using data from each region; and (3) analytical model based on the theory of linear viscoelasticity and the time-temperature superposition principle. Careful comparison of these models for accuracy and practicality resulted in recommending the statewide empirical model for both deflections and backcalculated moduli if the mixture properties are not available and if the mixture properties are not believed to be unusual. However, it needs to be warned that, when mixture properties are much different from the normal mixtures in North Carolina, this empirical model may lead to erroneous correction. Therefore, whenever thermomechanical properties of mixtures are available, the analytical procedure described in this report is strongly recommended, which is based on the theory of viscoelasticity and the time-temperature superposition principle.

TABLE OF CONTENTS

Section		Page
PART I. SUMMARY		1
I.1.	Introduction	1
I.2.	Field Experiments	3
	I.2.1. Selection of pavement sections	3
	I.2.2. Instrumentation	5
	I.2.3. Test program	7
I.3.	Proposed Procedure	9
I.4.	Example	10
PART II. TEMPERATURE PREDICTION IN ASPHALT LAYERS		14
II.1.	Introduction	14
II.2.	Heat Conduction Theory	15
	II.2.1. Theory	16
	II.2.2. Verification of the heat conduction theory	20
II.3.	Surface Temperature Prediction	21
	II.3.1. Prediction of maximum surface temperature	23
	II.3.2. Prediction of minimum surface temperature	26
II.4.	Pavement Depth Temperature Prediction	32
II.5.	Verification of New Temperature Prediction Procedure	45
II.6.	Conclusions	60
PART III. TEMPERATURE CORRECTION OF MODULI AND DEFLECTIONS		61
III.1.	Introduction	61
III.2.	Theoretical Background	63
	III.2.1. Linear viscoelasticity	63
	III.2.2. Time-temperature superposition	65
	III.2.3. Analysis of layered viscoelastic system	67
III.3.	Laboratory Creep Tests on Field Cores	68
III.4.	Temperature Correction of Backcalculated AC Moduli	75
	III.4.1. General	75
	III.4.2. 92/93 model - the empirical model developed from the 92/93 study	84
	III.4.3. Regional model - new empirical model based on regional field data	85
	III.4.4. Statewide model - new empirical model based on statewide field data	96
	III.4.5. Analytical model - new analytical model based on individual mixture properties	96

TABLE OF CONTENTS (Continued)

Section		Page
III.5.	Temperature Correction of FWD Center Peak Deflections	109
	III.5.1. General	109
	III.5.2. 92/93 model - the empirical model developed from the 92/93 study	121
	III.5.3. Regional model - new empirical model based on regional field data	126
	III.5.4. Statewide model - new empirical model based on statewide field data	127
	III.5.5. Analytical model - new analytical model based on individual mixture properties and forward deflection analysis	127
III.6.	Conclusions	147
III.7.	Recommendations	149
III.8.	Implementation and Technology Transfer Plan	150
REFERENCES		152

VOLUME II:

APPENDICES

A.	Materials on Temperature Prediction Modeling	1
	A.1. Statistical analysis on the maximum and minimum surface temperatures	1
	A.2. Sun rise and sun set times	7
	A.3. Statistical analysis on crossing times	14
	A.4. Weather records	20
	A.5. Temperature prediction programs	26
	A.6. Examples	46
	A.7. An application of heat conduction theory to predict subsurface temperatures in an asphalt pavement system	53
B.	Analysis of stresses and displacements in layered viscoelastic system with varying temperature	99
C.	Backcalculated AC moduli and center peak deflections (for P = 40 kN)	158

LIST OF TABLES

Table		Page
Table I.1	Selected seven test sections	4
Table I.2	Thermocouple burial depths (in mm)	6
Table I.3	FWD testing and seven-day temperature measurement period	8
Table I.4	Predicted temperature profile during FWD tests	12
Table I.5	Deflection correction work sheet	12
Table II.1	Statistical results of times at maximum and minimum surface temperature	28
Table II.2	Statistical results of crossing times	31
Table II.3	Input data for the temperature prediction program	42
Table III.4.1	Backcalculated AC moduli and center peak deflections (for P=40 kN)	76
Table III.4.2	The negative slope (m-value) of the linear fit of log E versus T data for each site, region, and the state	82
Table III.5.1	The slope (n-value) of the linear fit of log w versus T data for each site, and the C-value (Eq. III.27) for each region and the state.	116

LIST OF FIGURES

Figure		Page
Figure II.1	One dimensional heat conduction in a semi-infinite solid	17
Figure II.2	Representation of a random boundary temperature variation by a piece-wise linear function	19
Figure II.3	Comparison between the predicted and the measured mid-depth pavement temperatures	22
Figure II.4	Records of temperature measurement (Pitt County, February 1996)	33
Figure II.5	Flow chart of the AC layer temperature prediction procedure	37
Figure II.6	Flow chart of the pavement surface temperature prediction procedure	39
Figure II.7	Definition of solar and surface angles (Solaimanian and Kennedy, 1993)	43
Figure II.8	Plane of the ecliptic and the celestial equator	44
Figure II.9	Declination angle between the ecliptic plane and the celestial equator	44
Figure II.10	Zenith angles for the period from May to August in Northern latitudes (Solaimanian and Kennedy, 1993)	46
Figure II.11	Comparison between the predicted and the measured pavement temperatures (Durham County, August 13 and 14, 1995)	47
Figure II.12	Sensitivity analysis on the values of crossing temperature (Durham County, August 12 and 13, 1995)	49
Figure II.13	Comparison between the predicted and the measured pavement temperatures (Pitt County, May 18 and 19, 1996)	50
Figure II.14	Comparison between the predicted and the measured pavement temperatures (Wilkes County, August 22 and 23, 1995)	52
Figure II.15	Comparison between the predicted and the measured pavement temperatures (Pitt County, February 12 and 13, 1996)	53
Figure II.16	Comparison between the predicted and the measured pavement temperatures (Carteret County, February 22 and 23, 1996)	55
Figure II.17	Comparison between the predicted and the measured pavement temperatures (Carteret County, April 4 and 5, 1996)	56
Figure II.18	Comparison between the predicted and the measured pavement temperatures (New Hanover, November 17 and 18, 1996)	57
Figure II.19	Comparison between the predicted and the measured pavement temperatures (Polk County, April 2 and 3, 1996)	59
Figure III.3.1.	Isothermal and master creep compliances of the asphalt mixtures from three test sites: (a) New Hanover; (b) Durham; (c) Wilkes	69
Figure III.3.2.	Master relaxation moduli of the asphalt mixtures from three test sites	72
Figure III.3.3.	Time-temperature shift factors of the AC mixtures from three test sites	73
Figure III.4.1.	Variation of backcalculated AC modulus with temperature: (a) eastern region; (b) central region; (c) western region; (d) all regions	76

LIST OF FIGURES (Continued)

Figure		Page
Figure III.4.2.	A typical linear regression and the negative slope (m-value) of the linear fit of log E versus T data (Pitt site)	81
Figure III.4.3.	The negative slope (m-values) of the linear fit of log E versus T data for all regions	83
Figure III.4.4.	Temperature-corrected AC moduli using the 92/93 empirical model: (a) east region; (b) central region; (c) west region; (d) all regions	86
Figure III.4.5.	The temperature correction factors for AC moduli from various empirical models: (a) on the semi-log scales; (b) on the linear scales	90
Figure III.4.6.	Temperature-corrected AC moduli using the regional empirical models: (a) east region; (b) central region; (c) west region; (d) all regions	92
Figure III.4.7.	Temperature-corrected AC moduli using the statewide empirical model: (a) east region; (b) central region; (c) west region; (d) all regions	97
Figure III.4.8.	The temperature correction factors for AC moduli from new analytical model in comparison with the empirical models: (a) New Hanover; (b) Durham;(c) Wilkes	102
Figure III.4.9.	Temperature-corrected AC moduli using new analytical model in comparison with the empirical models: (a) New Hanover; (b) Durham; (c) Wilkes	106
Figure III.5.1.	Variation of center peak deflection with temperature: (a) east region; (b) central region; (c) west region; (d) all regions	110
Figure III.5.2.	A typical linear regression and the slope (n-value) of the linear fit of log w versus T data (Pitt site)	114
Figure III.5.3.	The variation of n-value with AC layer thickness: (a) east region; (b) central region; (c) west region; (d) all regions	117
Figure III.5.4.	Temperature-corrected deflections using the 92/93 model: (a) east region; (b) central region; (c) west region; (d) all regions	122
Figure III.5.5.	Temperature-corrected deflections using the regional empirical models: (a) east region; (b) central region; (c) west region; (d) all regions	128
Figure III.5.6.	The temperature correction factors for center peak deflections from the statewide empirical model for three different AC layer thicknesses: (a) on the semi-log scales; (b) on the linear scales	132
Figure III.5.7.	Temperature-corrected deflections using the statewide empirical model: (a) east region; (b) central region; (c) west region; (d) all regions	134
Figure III.5.8.	The temperature correction factors for center peak deflections from new analytical model in comparison with the empirical models: (a) New Hanover; (b) Durham; (c) Wilkes	141
Figure III.5.9.	Temperature-corrected deflections using new analytical model in comparison with the empirical models: (a) New Hanover; (b) Durham; (c) Wilkes	144

LIST OF SYMBOLS

The following symbols are used in this study:

c = specific heat (per unit mass)

$\underline{g}$ = temperature gradient vector

$G(x)$, $F(t)$, $F_1(t)$, $F_2(t)$= prescribed scalar-valued functions

$H(t)$ = the Heaviside step function

k = thermal conductivity

P = period of the temperature wave

$\underline{q}$ = heat flux vector

q_I = rate of internal heat generation per unit volume

S_1 = temperature-prescribed boundary

S_2 = heat flux-prescribed boundary

t = time

$T = T(\underline{x},t)$ = temperature field as a function of $\underline{x}$ and t

T_i = uniform initial temperature

T_0 = constant surface temperature or the mean surface temperature

ΔT = amplitude of the surface temperature wave

$$\dot{T} = \frac{DT}{Dt} = \frac{\partial T}{\partial t} + \frac{\partial T}{\partial \underline{x}} \cdot \frac{d\underline{x}}{dt}$$

$\frac{\partial T}{\partial n} = \underline{n} \cdot \frac{\partial T}{\partial \underline{x}}$ ($\underline{n}$ is the unit outward normal vector)

v = propagation speed of the temperature wave

V = spatial domain of the problem

$\underline{x}$ = spatial coordinates (= $x\underline{i} + y\underline{j} + z\underline{k}$ in Cartesian coordinates)

α = thermal diffusivity

β = phase angle

λ = wavelength

ρ = mass density

ρc = thermal capacity (per unit volume)

ω = angular frequency

$\underline{\nabla}$ = *del* operator (= $\frac{\partial}{\partial x}\underline{i} + \frac{\partial}{\partial y}\underline{j} + \frac{\partial}{\partial z}\underline{k}$ in Cartesian coordinates)

a = radius of loaded area

A_k = Prony series coefficients

a_T = time-temperature shift factor

a_T^{eff} = effective time-temperature shift factor

$D(t)$ = uniaxial creep compliance

$E(t)$ = uniaxial relaxation modulus

h_i = thickness of layer i

$H(t)$ = Heaviside unit step function

$I(t)$ = input

$J_0(\ )$ = Bessel function of the first kind and order zero

$J_1(\ )$ = Bessel function of the first kind and order one

q = load

$R(t)$ = response

$R_H(t)$ = unit response

t = time

T = temperature

T_R = reference temperature

u, w = r- and z-components of a displacement vector

ε_{rr}, $\varepsilon_{\theta\theta}$, ε_{zz}, γ_{rz} = normal and shear components of a strain tensor

ϕ = Love's stress function

ν = Poisson's ratio

ρ_k = time constants in a Prony series

ρ'_k = reduced time constants in a Prony series

σ_{rr}, $\sigma_{\theta\theta}$, σ_{zz}, τ_{rz} = normal and shear components of a stress tensor

ξ = reduced time

PART I. SUMMARY

I.1. Introduction

Nondestructive evaluation using the falling weight deflectometer (FWD) has become a primary means of determining in-situ structural conditions of pavements for design of rehabilitation strategies. The moduli of pavement layer materials, which are used as the indicators of the structural integrity of respective layers, are typically backcalculated from deflection basins obtained from FWD tests. In order to make a fair assessment of the structural condition of pavements, deflections or backcalculated moduli must be corrected to a particular type of loading system (including the type of loading device, frequency of loading, load level, etc.) and a standard set of environmental conditions. The most important environmental factor affecting surface deflections and backcalculated moduli of flexible pavement is the temperature of asphalt layers.

The correction of surface deflections or moduli to a reference temperature requires two major steps. The first is to predict an effective temperature of asphalt layers (hereinafter called temperature prediction procedure), and the second step is to adjust the measured deflections to a reference temperature using the predicted effective asphalt layer temperature and deflection correction factors (hereinafter called deflection correction procedure).

The significance of temperature correction on surface deflections has been recognized by AASHTO. The 1986 AASHTO Guide for Design of Pavement Structures (1993) presents a set of curves for deflection correction and the temperature prediction procedure requiring the use of the average air temperature for the previous five days in predicting pavement depth temperatures. However, various publications bear witness to incorrect temperature correction factors in the Guide (especially at high temperatures) and to inaccurate and impractical temperature prediction

procedure. Based upon an urgent need of developing a more realistic temperature correction procedure for the overlay designs in North Carolina, a research project entitled "Asphalt Paving Material Properties Affected by Temperature" was funded in 1992 (hereinafter called the 92/93 study) by the North Carolina Department of Transportation. As a result of this study, Kim et al. (1995, 1995a) developed empirical models for temperature prediction and temperature correction procedures. These models were simple in form and practical enough to be implemented in routine deflection analyses. However, the deflection and temperature measurements used in developing these models were obtained from pavements located in only central region of North Carolina. This limitation necessitated testing of these models against data from other regions within the state for the statewide implementation, resulting in a follow-up project entitled "Statewide Calibration of Asphalt Temperature Study from 1992 and 1993."

This report presents the findings from the follow-up statewide study. Before detailed information on the temperature prediction and deflection correction procedures are given, this section describes field experiments conducted to collect necessary data to develop statewide models and the structure of data base developed as a result, and summarizes the proposed temperature prediction and deflection and moduli correction procedures. Then, an actual example of temperature correction of deflections and moduli is given to aid understanding of these procedures. Parts II and III of this report discuss the details involved in the development of the temperature prediction and the deflection correction procedures, respectively.

I.2. Field Experiments

I.2.1. Selection of pavement sections

There are a number of factors to be considered in selecting test sections for temperature and deflection measurements, including climatic conditions, asphalt layer thicknesses, temperature susceptibility of asphalt mixtures, material types and thicknesses of subsurface layers, moisture conditions of subsurface layers, etc. Before details on selected pavements are given, a general description is made on three distinctive climatic regions in North Carolina; the eastern coastal plain, the central piedmont, and the western mountains.

The coastal plain occupies about 45% of the land area of North Carolina, and its soil is composed of sandy to clayey marine and fluvial deposits. Elevations range from sea level to about 200 meters. The piedmont occupies nearly 39% of the state and is a rolling to hilly area between the coastal plain and mountains. Its altitudes range from 90 m on the east to 460 m near the mountains. The mountains occupy about 16% of North Carolina, with altitudes varying from 460 m to 2037 m. In the piedmont and coastal plain, the mean annual soil temperature is in the range of 15 to 20^{o}C at 0.5 m below the surface. The mountain soils have two temperature regimes: mesic, 8-15^{o}C, and frigid, less than 8^{o}C. The mesic temperature regime in North Carolina starts at 400 m and ends at an elevation of about 1400 m. The mesic temperature regime covers soil temperatures similar to those at lower elevations from central Virginia to central or north central New York State. The soil temperatures in the frigid regime, elevation above 1400 m, are similar to those found in northern New York, Michigan and much of Canada.

A total of seven pavement sites were selected for temperature data collection: three in the mountains, one in the piedmont, and three in the coastal region. Characteristics of the selected sections are given in Table I.1.

Table I.1. Selected seven test sections

Region	County	AC Thickness (mm)	Route
Eastern	Pitt	114	US264
	Carteret	229	NC24
	New Hanover	305	US17
Central	Durham	254	NC54
Western	Polk	165	US74
	Buncombe	203	US25
	Wilkes	241	US421

I.2.2. Instrumentation

To measure pavement temperatures at varying depths, thermocouples were installed through a 152 mm diameter hole drilled to a depth of 2 m below the bottom of the AC layer. Depths of installed thermocouples are listed in Table I.2. According to the field study by Zhou and Elkins (1994) as a part of the FHWA Long Term Pavement Performance (LTTP) seasonal monitoring program, a depth gradient of pavement temperatures remains relatively constant below 2 m. During the drilling process, aggregates and soils obtained from different depths were stored in separate plastic buckets, so that the original materials could be used in backfilling various depths in the hole. A 51 mm diameter plastic tube with thermocouples attached at designed depths was placed at the bottom of the hole with the thermocouples facing and touching one side of the hole. Then, the hole was backfilled and compacted in layers using original materials.

After the compaction of base and subgrade materials, thermocouples in asphalt concrete layers were installed by drilling horizontal holes to the core wall using a drill with a pivoting nose. Epoxy was injected into each horizontal hole followed by thermocouple attached to strands of insulated wire. The wires from the plastic tube and thermocouples in the AC layers were taken across the pavement through a trench slit cut transversely from the core hole to the pavement edge. The core hole was backfilled with hot mix and the trench in the pavement filled with epoxy.

Wires from instrumentation were placed in a junction box located outside of the shoulder area. All the temperatures were measured at the time of FWD testing and at least seven consecutive days a season per section during one year period using automatic data loggers. The use of data loggers allowed continuous temperature measurements without an operator.

Table I.2. Thermocouple burial depths (in mm)

Thermo-couple ID	Pitt Co.	Carteret	New Hanover	Durham	Polk	Buncom-be	Wilkes
1A	Air	Air	Air	Air	Air	Air	Air
1B	0*	0*	0*	0*	0*	0*	0*
1C	25*	25*	25*	25*	25*	32*	30*
1D	50*	50*	40*	40*	50*	64*	60*
2A	80*	75*	80*	80*	75*	89*	80*
2B	115*	105*	130*	130*	105*	121*	130*
2C	145	140*	190*	190*	165*	140*	190*
2D	225	229*	305*	254*	248	203*	240*
3A	305	299	375	324	328	235	245*
3B	385	379	455	404	428	315	334
3C	525	529	605	554	558	465	414
3D	675	729	805	754	808	665	564
4A	825	979	1055	1004	1058	915	764
4B	1075	1229	1305	1254	1318	1165	1164
4C	1455	1629	1705	1654	1578	1565	1664
4D	1875	2029	2105	2054	1978	1965	2064

1. Depth of zero corresponds to AC surface.
2. Probe depths marked with * indicate that those probes are located within the AC layer.

I.2.3. Test Program

The FWD tests were performed on four locations in wheel path with four different loading levels (26.7, 40.0, 53.4, and 66.7 kN or 6000, 9000, 12000, and 15000 lbs). These tests were repeated at different times of day and in four different seasons. Only 40 kN loading and the corresponding deflections were used in the present analysis. Pavement subsurface temperatures were measured at the time of the FWD testing using the thermocouples installed at different depths from the pavement surface down into the subgrade. The AC mid-depth temperature is taken as the effective AC temperature.

In addition to the temperature measurements during the FWD testing days, pavement and air temperatures and corresponding weather conditions were recorded for seven consecutive days in each of the four seasons. The periods for FWD testing and seven-day temperature measurement are summarized in Table I.3. One site was selected from each climatic region for the seven-day temperature measurement program (New Hanover for eastern, Durham for central, and Wilkes for western). Some additional measurements were made from other pavement sections whenever the personnel help from NCDOT was available for the collection of data. The seven-day temperature data are not available from Buncombe county because problems were encountered in downloading the data from the logger. All the FWD deflection data and corresponding temperatures are summarized in Appendix B.

One asphalt core with 100-mm (4-inch) diameter was retrieved from each of the seven test sites. Out of the seven sites, the cores from three sections were selected for laboratory creep tests to determine the viscoelastic properties as a function of time and temperature. These three sections are New Hanover (eastern), Durham (central), and Wilkes (western). The reason for

Table I.3 FWD testing and seven-day temperature measurement period

Region	Test Site	FWD Testing Days				7-Days Temperature Measurement			
		1994	1995			1995		1996	
		Fall	Winter	Spring	Summer	Summer	Fall	Winter	Spring
Eastern	Pitt	12/1	1/26	4/10	7/20	N/A	N/A	2/9-2/15	5/14-5/27
	Carteret	12/6	1/31	4/12	7/25	N/A	N/A	2/17-2/28	4/3-4/11
	New Hanover	12/8	2/1	5/3	7/26	8/22-8/30	11/14-11/25	1/31-2/6	4/22-4/30
Central	Durham	11/30	1/24	4/6	7/18	8/11-8/18	10/30-11/6	1/23-1/30	N/A
Western	Polk	11/22	1/24	4/24	8/10	N/A	N/A	2/7-2/14	4/1-4/10
	Buncombe	11/15	2/22	4/20	7/14	N/A	N/A	N/A	N/A
	Wilkes	11/14	1/18	4/26	7/25	8/21-8/30	10/30-11/6	1/29-2/6	4/22-4-30

selecting these pavements is that the AC core heights are long enough for uniaxial creep tests (typical requirement of 203 mm).

I.3. Proposed Procedure

In this section, the proposed temperature correction procedure for deflections and backcalculated moduli is summarized. Technical details of this procedure and validation results are not presented in this section for simplicity and can be found in Parts II and III and appendices of this report. The specific purpose of this section is to illustrate the procedure in a stepwise manner to aid NCDOT understanding and implementing the proposed procedure.

The proposed procedure is composed of two algorithms: (1) the temperature prediction procedure for estimating AC layer mid-depth temperature as the effective AC temperature and (2) the deflection correction procedure for correcting deflections (or moduli) at the effective temperature to the reference temperature of 20°C. The temperature prediction procedure is based on fundamental principles of heat transfer and predicts the AC layer mid-depth temperature at the FWD testing time using the surface temperature history during the period from the morning of the day prior to FWD testing (D-1 day) to the time of FWD testing (D day).

The surface temperature history is constructed by combining two parts. The first part covers the period from when the surface temperature is at the lowest in D-1 day to the morning of D day. This part is predicted from the yesterday's maximum air temperature, the minimum air temperature of today's morning, and cloud conditions of yesterday. The second part of the surface temperature history is for the period between the today's morning time with the lowest surface temperature and the FWD testing time. It is constructed using actual surface

temperatures measured prior to the FWD test and their extrapolation back to the time the lowest temperature occurred in today's morning.

For the correction of moduli and deflections, several alternatives have been investigated. They are: (1) new statewide model modified from the 92/93 model to cover different regions in North Carolina; (2) regional empirical models developed using data from each region; and (3) analytical model based on the theory of linear viscoelasticity and the time-temperature superposition principle. Careful comparison of these models for accuracy and practicality resulted in recommending the statewide empirical model for both deflections and backcalculated moduli if the mixture properties are not available and if the mixture properties are not believed to be unusual. However, it needs to be warned that, when mixture properties are much different from the normal mixtures in North Carolina, this empirical model may lead to erroneous correction. Therefore, whenever thermomechanical properties of mixtures are available, the analytical procedure described in this report is strongly recommended, which is based on the theory of viscoelasticity and the time-temperature superposition principle.

In the next section, an example is given to illustrate these procedures in a stepwise manner.

I.4. Example

On February 13, 1996, FWD tests are performed on a pavement with 114 mm (4.5-inch) thick AC layer. The pavement surface temperatures were measured during FWD tests.

Temperature Prediction Procedure:

The crew consulted local newspapers for February 13 and 14 and found that it was clear and the maximum air temperature was 12.8°C on February 12. The minimum air temperature in

the morning of February 13 was -7.6°C. During FWD tests, the crew found no shade on the test position. Also, the pavement surface is horizontal at the test site.

Based on the field records, the input data file was generated for the temperature prediction program, "PD.for." The detailed description of the input file is given in Appendix A.6. The predicted temperature profile within the AC layer is listed in Table I.4.

Temperature Correction of AC Modulus and Deflections:
(Columns referred in each step are from Table I.5.)

(a) An Illustration of temperature correction of backcalculated AC modulus using the new statewide empirical model

Step 1. Secure an uncorrected AC modulus (typically from a backcalculation program using an FWD deflection basin) as shown in column (1).

Step 2. Find the effective AC temperature at the time of FWD test (typically predicted by a method described in Part II) as shown in column (3). An effective AC temperature of T = 7.58°C at 10:00 a.m. given in Table I.4 was used.

Step 3. Determine the modulus correction factor according to the formula given in Part III as shown in column (5).

Step 4. Multiply the modulus correction factor by the original uncorrected modulus to obtain the corrected modulus as shown in column (7).

(b) An Illustration of temperature correction of FWD center peak deflection using the new statewide empirical model

Step 1. Secure an uncorrected FWD deflection under 9000 lbs load as shown in column (2).

Table I.4. Predicted temperature profile during FWD tests

Time	Temperature (°C)	
	Surface	Mid-depth
8.2	2.23	2.13
8.6	3.84	2.81
9.0	5.8	3.78
9.5	9	5.44
10.0	12.7	7.58
10.5	14.6	9.59
11.0	17.3	11.45
11.5	19.7	13.38
12.0	21	15.02
12.5	22.7	16.47
13.0	23.4	17.68
13.5	23.5	18.47
14.0	23.2	18.89
14.5	22.7	19.03
15.0	20.7	18.64
15.5	18	17.58
16.0	15	16.04

Table I.5 Deflection correction work sheet

(1) Backcalculated AC Modulus, E@T (MPa)	(2) FWD Center Peak Deflection, w@T (mm)	(3) Mid-Depth AC Temperature, T (C)	(4) Thickness of AC Layer, hAC (mm)
2959	0.37	7.58	114
(5) Modulus Correction Factor, $10^{0.0262(T-20)}$	(6) Deflection Correction Factor, $10^{-4.65E-5\ (hAC)(T-20)}$	(7) Corrected Modulus, E@20C (MPa)	(8) Corrected Deflection, w@20C (mm)
0.47	1.16	1391	0.43

Step 2. Find the effective AC temperature at the time of FWD test (typically predicted by a method described in Part II) as shown in column (3). An effective AC temperature of T = 7.58°C at 10:00 a.m. given in Table I.4 was used.

Step 3. Find the thickness of the AC layer under consideration as shown in column (4).

Step 4. Determine the deflection correction factor according to the formula given in Part III as shown in column (6).

Step 5. Multiply the deflection correction factor by the original uncorrected deflection to obtain the corrected deflection as shown in column (8).

PART II. TEMPERATURE PREDICTION IN ASPHALT LAYERS

II.1. Introduction

The 1986 AASHTO Guide presents a temperature prediction procedure requiring the use of the average air temperature for the previous five days in predicting pavement depth temperatures. However, researchers and practitioners have challenged the accuracy of the AASHTO temperature prediction procedure. Inge and Kim (1994) and Baltzer and Jansen (1994) have demonstrated that the temperature prediction procedure in the 1986 AASHTO Guide can not account for different temperature-depth gradients between the heating (morning) and the cooling (afternoon) cycles, which have a significant effect on the effective pavement temperature. Also the requirement of the average air temperature for the previous five days was considered impractical for routine deflection analysis in state highway agencies. The 1993 AASHTO Guide does not recommend any specific procedure for the prediction of the effective AC layer temperature.

Based on urgent needs of developing a more accurate and practical temperature-deflection correction procedure for overlay designs in North Carolina, the NCDOT embarked upon a research project in 1992. New temperature prediction and deflection correction procedures have been developed as a result of this study (Kim et al. 1995, Inge and Kim 1995). In their study, an empirical approach based on the data base developed from the field measurements was used for temperature prediction.

Although Inge and Kim's temperature prediction model is capable of accounting for the difference in temperature gradients between the heating and cooling cycles with practical input requirements, model coefficients were determined using only the data obtained from the central

region of North Carolina. Since the temperature prediction procedure could be sensitive to climatic conditions, geologic conditions, and local-specific material types, suitability of the temperature prediction algorithm needs to be tested for other regions, such as the eastern coastal area and the western mountain area, for the NCDOT to fully implement the model.

To develop a model that is applicable to more general climatic conditions, the researchers felt that the empiricality had to be minimized without loosing practicality in the model. One of the primary objectives of this study is to develop a practical, but fundamentally sound procedure for the prediction of the AC layer mid-depth temperature. The predicted mid-depth temperature will be used as an effective AC layer temperature for the FWD deflection correction analysis. In the following sections, a brief review is made on two background theories that are used in the model development; heat conduction theory and earlier work done by Solaimanian and Kennedy (1993) on the prediction of surface temperature from air temperature. A new prediction procedure based on the theories and the temperature data base developed from field tests is then presented. Finally, the verification results are presented using case studies in North Carolina.

II.2 Heat Conduction Theory

Details in heat conduction theory and examples demonstrating how the theory works are presented in Appendix A.7. In the following, major heat conduction equations that govern the proposed temperature prediction procedure are summarized to aid readers' understanding.

II.2.1. Theory

A one-dimensional heat conduction problem for a semi-infinite solid (Figure II.1) with a constant thermal conductivity and without an internal heat generation may be defined by the following equations and conditions:

Field Equations:

$$\frac{\partial^2 T}{\partial x^2} = \frac{1}{\alpha}\frac{\partial T}{\partial t} \qquad \text{for } x>0,\ t>0. \tag{II.1}$$

Initial Condition:

$$T = G(x) \qquad \text{for } x\geq 0,\ t=0. \tag{II.2}$$

Boundary Condition:

$$T = F(t) \qquad \text{for } x=0,\ t>0. \tag{II.3}$$

where α is the thermal diffusivity with a dimension of m^2/sec or m^2/hour, and G and F are prescribed functions of depth (x) and time (t), respectively. The solution to the problem defined by (II.1)-(II.3) is known and given by (e.g., Carslaw and Jaeger 1959)

$$T(x,t) = \frac{1}{2\sqrt{\pi\alpha t}}\int_0^\infty G(\xi)\left[\exp\left(-\frac{(x-\xi)^2}{4\alpha t}\right) - \exp\left(-\frac{(x+\xi)^2}{4\alpha t}\right)\right]d\xi + \frac{2}{\sqrt{\pi}}\int_{\frac{x}{2\sqrt{\alpha t}}}^\infty F\left(t-\frac{x^2}{4\alpha\eta^2}\right)e^{-\eta^2}\,d\eta \tag{II.4}$$

where ξ and η are dummy variables of integration.

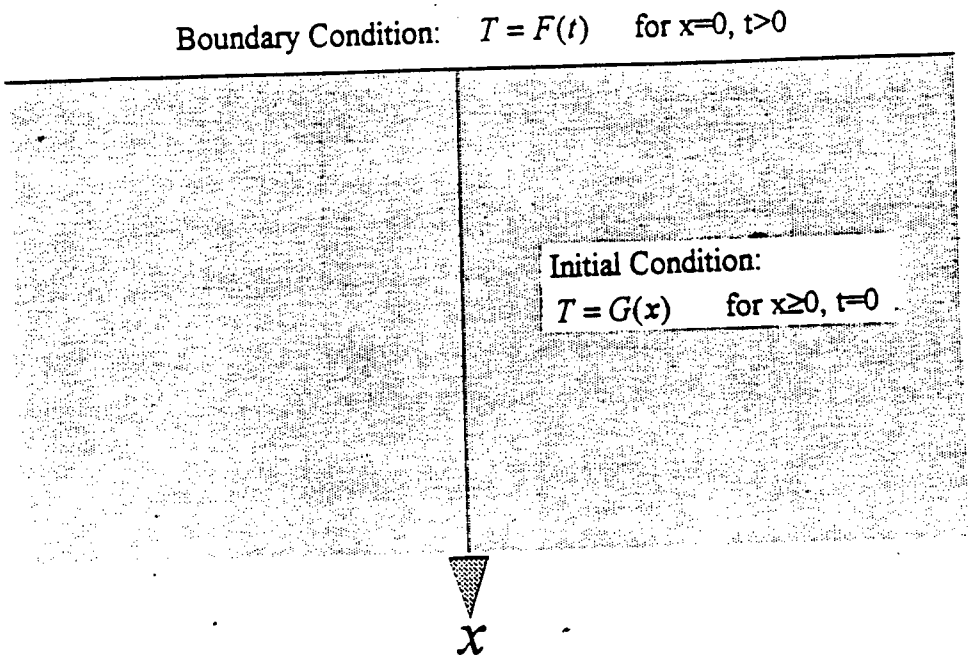

Governing Differential Equations: $\frac{\partial^2 T}{\partial x^2} = \frac{1}{\alpha}\frac{\partial T}{\partial t}$ for x>0, t>0

Figure II.1 One dimensional heat conduction in a semi-infinite solid.

We shall consider a special case of a uniform initial temperature distribution and a random piece-wise linear surface temperature variation (typically characterized by actual surface temperature measurements in the field), as shown in Figure II.2, i.e.,

$$G(x) = T_0 \quad and \quad F(t) = \sum_{i=1}^{n} F_i(t)[H(t-t_i) - H(t-t_{i+1})] \tag{II.5}$$

where T_0 is constant,

$$F_i(t) = A_i + B_i t \quad for \quad t_i \le t < t_{i+1} \quad (i = 1, 2, \ldots, n),$$

$$B_i = \frac{T_{i+1} - T_i}{t_{i+1} - t_i}, \quad A_i = T_i - B_i(t_i - t_1) \quad (no\ sum\ on\ i;\ i = 1, 2, \ldots, n),$$

$$H(t) = \begin{cases} 1 & for \quad t > 0 \\ 0 & for \quad t < 0 \end{cases} \quad \text{(the Heaviside step function),}$$

and T_i = measured surface temperature at the corresponding time t_i, with $t_1 = 0$ and $t_{n+1} = t$ (the current time) where (n+1) is the total number of measurements up to the current time. Now, substituting (II.5) into (II.4) and rearranging (details are given in Appendix A.7)

$$T(x,t) = T_0\, erf\left(\frac{x}{2\sqrt{\alpha t}}\right) + \sum_{i=1}^{n}\left[\left\{(A_i + B_i t)erfc(X_i) + 2B_i(t-t_i)\left(X_i^2 erfc(X_i) - \frac{X_i}{\sqrt{\pi}}e^{-X_i^2}\right)\right\}\right. \tag{II.6}$$
$$\left. - \left\{(A_i + B_i t)erfc(X_{i+1}) + 2B_i(t-t_{i+1})\left(X_{i+1}^2 erfc(X_{i+1}) - \frac{X_{i+1}}{\sqrt{\pi}}e^{-X_{i+1}^2}\right)\right\}\right]$$

where

$$X_i = \frac{x}{2\sqrt{\alpha(t-t_i)}} \quad and \quad X_{i+1} = \frac{x}{2\sqrt{\alpha(t-t_{i+1})}},$$

$$F(t) = \sum_{i=1}^{n} F_i(t)[H(t-t_i) - H(t-t_{i+1})]$$

where

$$F_i(t) = A_i + B_i\, t \quad for \quad t_i \le t < t_{i+1} \quad (i = 1,2,\ldots,n)$$

$$B_i = \frac{T_{i+1} - T_i}{t_{i+1} - t_i}, \quad A_i = T_i - B_i(t_i - t_1)$$

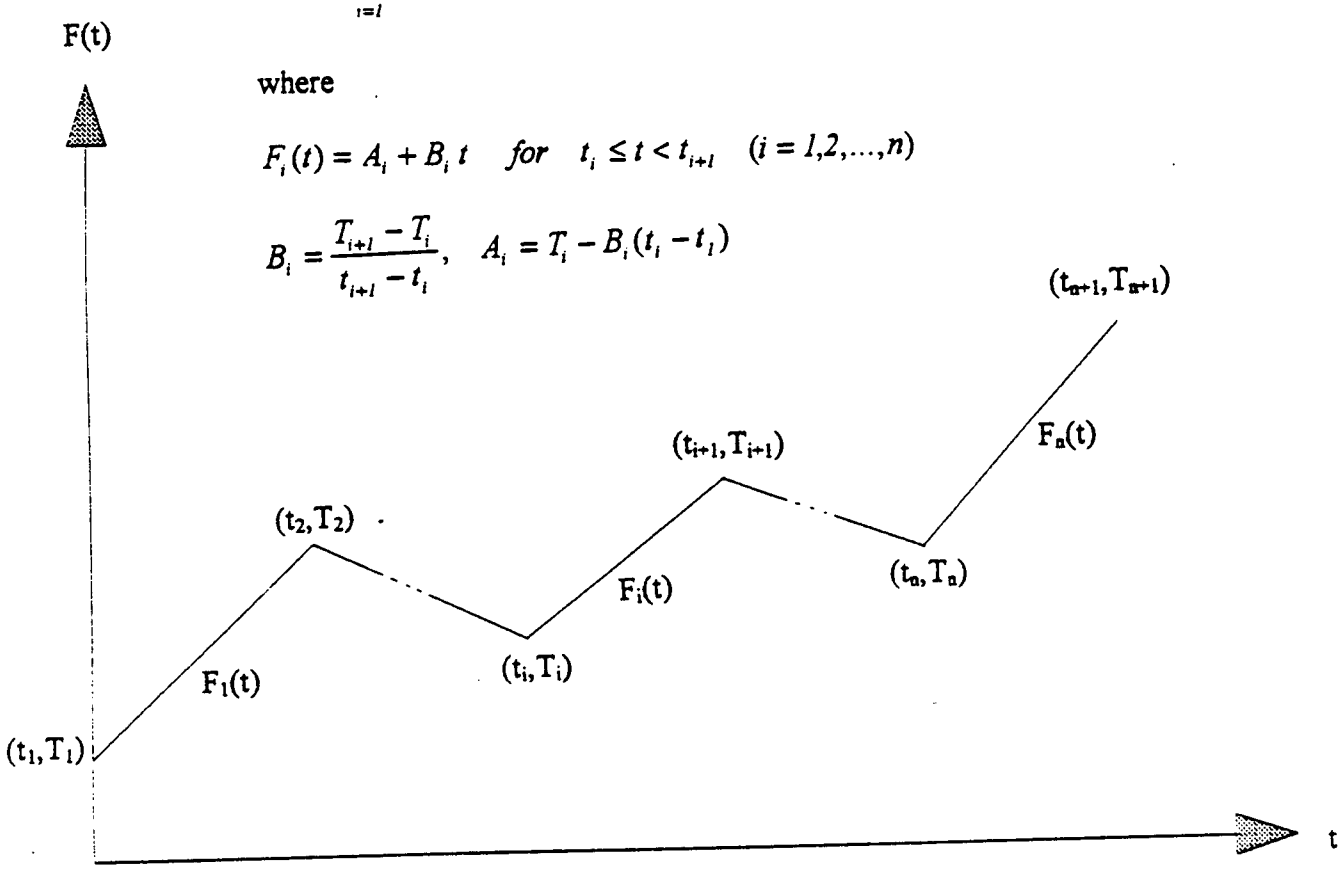

Figure II.2 Representation of a random boundary temperature variation by a piece-wise linear function.

$$erf(X) = \frac{2}{\sqrt{\pi}} \int_0^X e^{-\xi^2} d\xi = \textit{error function,}$$

and $$erfc(X) = \frac{2}{\sqrt{\pi}} \int_X^{\infty} e^{-\xi^2} d\xi = \textit{complementary error function.}$$

II.2.2. Verification of the heat conduction theory

It is understood from (II.6) that the influence of the initial temperature is not significant at shallow depths beneath the surface and the uniform distribution of initial temperature is not a critical assumption. It can be also seen that the influence of the remote past history of the surface temperature on the current subsurface temperature is negligible, and therefore, in practice, only the surface temperature history for a limited past duration needs to be known to predict the subsurface temperature. Detailed discussions are provided in Appendix A.7, and a sensitivity analysis is presented in section II.6, Case 1. This observation is important because the further we have to go back in time the more impractical the model becomes due to more difficult data collections.

It has been observed from most of the records that the time history curves of temperatures at the surface and mid-depth of the asphalt layer cross each other at approximately the same time each morning. Hereafter, this time is called the *crossing time*. The nature of near-uniform distribution of the temperature within the asphalt layer at the crossing time is important to apply the heat conduction theory described above to our problem. The crossing time and the corresponding *crossing temperature* will be used in our subsurface prediction procedure as the initial time (t_0) and the initial temperature (T_0) respectively.

For the crossing time concept to be applicable to the prediction of pavement temperatures, it is not necessary to have these temperatures cross at a fixed time of day. As a matter of fact, under some special weather conditions, such as snowing or long term raining, these temperature curves may not cross at all. A statistical analysis of the crossing time based on the field temperature records will be presented in Appendix A.3.

To illustrate the theory discussed above, the temperature within an asphalt layer was predicted using (II.6) and the initial and boundary conditions expressed by (II.5) and then compared with the measured data. Figure II.3 compares the predicted mid-depth asphalt layer temperatures and the field measurements at one of the test sites. It was assumed that the initial temperature distribution was uniform (T_0 = 30 °C) throughout the entire depth of the semi-infinite system and the system was subjected to a random surface temperature variation which was defined by the actual temperature readings taken on the pavement surface. The theoretical prediction was in good agreement with the measurements. Some discrepancies observed at the peaks and the bottoms of the curves are believed to be due to the use of an estimated value for the thermal diffusivity. A thermal diffusitivity, α, of 0.0037 m^2/hour was used, given by Yoder and Witczak (1975) for typical asphalt mixtures.

II.3. Surface Temperature Prediction

As can be seen from our heat conduction model in Section II.2.1, the temperature profile inside the pavement is a function of time and the surface temperature as a boundary condition. The surface temperature one week ago has little effect on the current pavement temperature, but

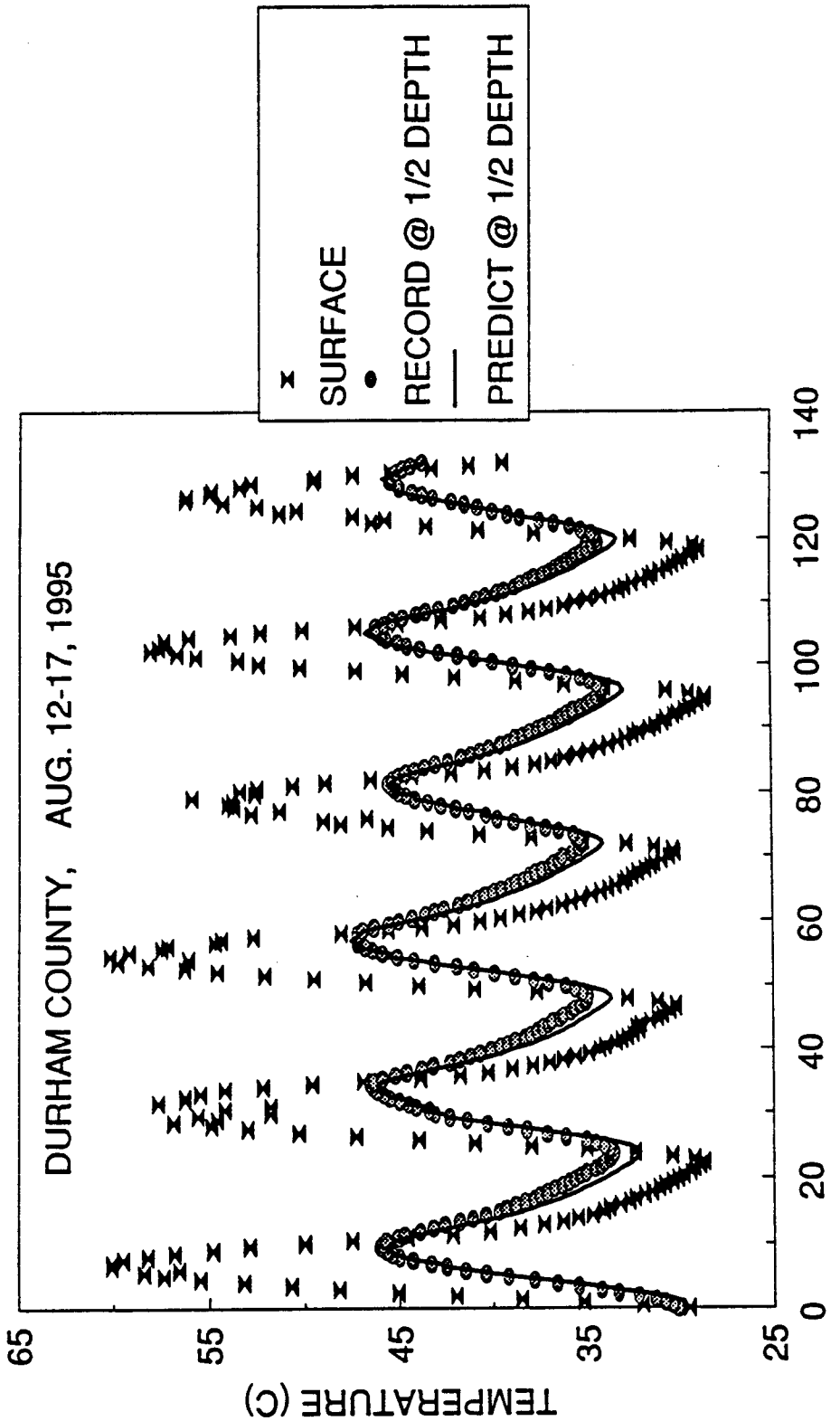

Figure II.3 Comparison between the predicted and the measured mid-depth pavement temperature

the surface temperature an hour ago has significant influence. Fortunately, during FWD tests, the surface temperature can be measured accurately at different times, yielding an accurate short term surface temperature history.

For the surface temperature-time history before the first measurement of the surface temperature at the day of FWD testing, a modified sine-wave function is used. Following, we use "D day" to indicate the day when FWD tests are performed, and "D-1 day" to represent the day before FWD tests. To generate this modified sine-wave function, D-1 day's maximum surface temperature and D day's early morning minimum surface temperature are required. In the following, heat transfer theories for prediction of the maximum and minimum surface temperatures from air temperatures are briefly reviewed.

II.3.1. Prediction of maximum surface temperature

Solaimanian and Kennedy (1993) proposed a simple method to determine the maximum pavement temperature with a minimal amount of input. The method is based on the theory of heat transfer and takes the effect of latitude on solar radiation into account. For the convenience of discussion for the prediction of minimum surface temperature and case studies presented later in the paper, some important equations and definitions from Solaimanian and Kennedy's work are presented here. The fundamental equation of heat equilibrium in a pavement is,

$$q_{net} = q_s + q_a - q_c - q_k - q_r = 0 \qquad \text{(II.7)}$$

where

q_s = energy absorbed from direct solar radiation,

q_a= energy absorbed from diffuse radiation (scattered from atmosphere),

q_c= energy transferred to or from the body due to convection,

q_k= energy transferred to or from the body due to conduction, and

q_r= energy emitted from the body through outgoing radiation.

The energy absorbed by an horizontal pavement can be expressed as,

$$R_s = R_0 \alpha_1 \tau_a^{1/\cos z} \, Cosz \qquad \text{(II.8)}$$

where

R_0= solar constant = 442 Btu/(hr.sq.ft.),

z= the zenith angle (Solaimanian and Kennedy suggested that at the noon 12 sun time and in the region with latitude larger than 25°, z ≅ latitude-20 ° from May to August),

α_1= the surface absorbtivity (For asphalt concrete α_1= 0.85~0.93), and

τ_a= transmission coefficient for unit air mass, ranging from 0.81 on a clear day to 0.62 on a cloudy one.

If the pavement surface is tilted to the horizontal, a more sophisticated solar radiation equation was provided by Solaimanian and Kennedy (1993).

The energy absorbed by the pavement from the atmospheric radiation may be calculated by the following equation developed by Gieger and reported by Solaimanian and Kennedy (1993):

$$q_a = \varepsilon_a \sigma T_{air}^4 \qquad \text{(II.9)}$$

where

ε_a= the coefficient for atmospheric radiation,

σ= Stefan- Boltzman constant = $0.1714*10^{-8}$ Btu/(hr.sq.ft.$^{\circ}R^4$), and

T_{air}= the air temperature in Rankine.

The heat flow by the convection to the surrounding air, q_c, is given by,

$$q_c = h_c(T_s - T_{air}) \qquad \text{(II.10)}$$

where

T_s= the pavement surface temperature in Rankine, and

h_c= the surface coefficient of heat transfer. For an average wind velocity of about 10 mph (4.5 m/sec), the value of h_c is calculated between 3.0 and 4.0 Btu/(hr.sq.ft. F) for typical ranges of maximum air and pavement temperatures during day times.

The heat conduction rate below the pavement surface can be given as,

$$q_k = -k\frac{T_x - T_s}{x} \qquad \text{(II.11)}$$

where

k= thermal conductivity, and

T_x= the temperature at depth x.

The outgoing radiation energy from the pavement surface can be calculated by,

$$q_r = \varepsilon\sigma T_s^4 \qquad \text{(II.12)}$$

where

ε= the emissivity of the pavement surface.

By substituting Equation (II.7) with Equations (II.8), (II.9), (II.10), (II.11), and (II.12), Solaimanian and Kennedy obtained the following equation, by which the surface temperature can be calculated from the air temperature, T_a:

$$422\alpha_1\tau_a^{1/\cos z}\cos z + \varepsilon_a\sigma T_a^4 - h_c(T_s - T_a) - \frac{k}{x}(T_s - T_x) - \varepsilon\sigma T_s^4 = 0 \qquad \text{(II.13)}$$

Using this equation, maximum surface temperatures were calculated for our test sites in the three climatic regions. The input for the parameters in Equation (II.13) were assumed values within the ranges proposed by Solaimanian and Kennedy. As will be presented later in the verification section, the calculated surface maximum temperatures agreed reasonably well with the field measurements.

Solaimanian and Kennedy assumed that the maximum temperature difference between the surface and at a depth of two inches is 15°F during hot summer days. This assumption may not be correct in some regions or during other seasons. The calculated temperature inside the pavement was used to improve the prediction accuracy for the maximum surface temperature.

II.3.2. Prediction of minimum surface temperature

The energy balance equation, Equation (II.7), is valid at any time. During the night, the solar radiation energy is zero. We extended Equation (II.7) for night time as follows:

$$q_{net} = q_a - q_c + q_k - q_r \qquad \text{(II.14)}$$

The equilibrium equation can be derived as,

$$\varepsilon_a\sigma T_a^4 - h_c(T_s - T_a) - \frac{k}{x}(T_s - T_x) - \varepsilon\sigma T_s^4 = 0 \qquad \text{(II.15)}$$

During the night, the temperature is usually lower on the surface than that inside the pavement; therefore, q_k is positive, meaning that the heat flows upward from the bottom of the pavement to the surface. The thermal conductivity (k) and the emissivity of the pavement surface (ε) remain the same as those during day time. However, the surface coefficient of heat transfer (h_c) and the coefficient for atmospheric radiation (ε_a) are changed. The surface coefficient of heat transfer (h_c) depends on the surface and air temperatures, as well as the wind speed. Solaimanian and Kennedy (1993) recommended following empirical formula for determining h_c for a pavement surface:

$$h_c = 122.93\left\{0.00144T_m^{0.3}U^{0.7} + 0.00097\left(T_s - T_{air}\right)^{0.3}\right\} \qquad \text{(II.16)}$$

where

h_c = surface coefficient of heat transfer in Btu/(hr.sq.ft. °F)

T_m = average of the surface and air temperature in °K

U = average daily wind velocity in m/sec

T_s = surface temperature

T_{air} = air temperature.

During night time, both the surface and air temperatures are much lower than those during the day. Using above empirical formula, h_c value was calculated to be 1.4 to 2.5 Btu/(hr.sq.ft.°F).

The times when the surface temperature reaches its maximum and minimum values are investigated from our field temperature records. The summary of statistical results is presented in Table II.1. The detailed statistical analysis is provided in Appendix A.1 for each test day in

Table II.1 Statistical Results of Times at Maximum and Minimum Surface Temperature

Location		Time	1995				1996					
			Summer		Fall		Winter		Spring		All Season	
			Average	STD	Average	STD	Average	STD	Average	STD	Average	STD
Eastern	Pitt	TIME@MIN					0.2919	0.0000	0.2112	0.0069	0.2332	0.0364
		TIME@MAX					0.5558	0.0099	0.5445	0.0193	0.5476	0.0180
		R.T@MIN					0.0305	0.0018	0.0259	0.0128	0.0271	0.0112
		R.T@MAX					0.6267	0.0223	0.5963	0.0329	0.6046	0.0332
	Carteret	TIME@MIN					0.2314	0.0529	0.2132	0.0212	0.2244	0.0444
		TIME@MAX					0.5074	0.0275	0.5257	0.0504	0.5144	0.0390
		R.T@MIN					-0.0881	0.1144	-0.0322	0.0369	-0.0666	0.0965
		R.T@MAX					0.5139	0.0603	0.5617	0.0953	0.5323	0.0792
	New Hanove	TIME@MIN	0.2416	0.0098	0.2911	0.0103	0.3134	0.0000	0.2283	0.0155	0.2671	0.0340
		TIME@MAX	0.6027	0.0170	0.5550	0.0249	0.5530	0.0104	0.5513	0.0222	0.5608	0.0282
		R.T@MIN	0.0391	0.0200	0.0601	0.0233	0.0759	0.0020	0.0318	0.0276	0.0500	0.0276
		R.T@MAX	0.7067	0.0310	0.6838	0.0594	0.6279	0.0228	0.6162	0.0403	0.6614	0.0594
Central	Durham	TIME@MIN	0.2459	0.0078	0.2755	0.0000	0.2520	0.0400			0.2546	0.0257
		TIME@MAX	0.5792	0.0222	0.5046	0.0614	0.5750	0.0173			0.5607	0.0462
		R.T@MIN	0.0636	0.0135	0.0517	0.0029	-0.0720	0.0949			0.0192	0.0811
		R.T@MAX	0.6601	0.0392	0.5713	0.1386	0.6928	0.0422			0.6497	0.0879
Western	Polk	TIME@MIN					0.2944	0.0090	0.2365	0.0354	0.2596	0.0399
		TIME@MAX					0.5756	0.0172	0.5733	0.0200	0.5742	0.0190
		R.T@MIN					0.0639	0.0221	0.0373	0.0672	0.0479	0.0554
		R.T@MAX					0.7020	0.0382	0.6800	0.0382	0.6888	0.0397
	Wilkes	TIME@MIN	0.2425	0.0167	0.2713	0.0000	0.2957	0.0000	0.2462	0.0084	0.2509	0.0196
		TIME@MAX	0.5592	0.0339	0.5630	0.0000	0.5665	0.0000	0.5670	0.0156	0.5634	0.0243
		R.T@MIN	0.0614	0.0316	0.0513	0.0000	0.0539	0.0000	0.0844	0.0142	0.0695	0.0259
		R.T@MAX	0.6416	0.0618	0.7213	0.0000	0.6808	0.0000	0.6603	0.0278	0.6593	0.0490

each season at each site. It was observed from the analysis that times when maximum and minimum temperatures occur are functions of weather condition and season. During rainy or snowy days, the times when the surface temperature reaches its maximum and minimum have large variations. When the weather is clear or partly cloudy, these times are fairly unique. The statistical values in Table II.1 are based on the temperature records in clear or partly cloudy weather. To normalize the seasonal effects, we calculated the time ratio at the maximum and minimum surface temperatures as,

$$RT_{max} = \frac{Time\ @\ Maximum\ Surface\ Temperature - Sun\ Rise\ Time}{Sun\ Set\ Time - Sun\ Rise\ Time} \qquad \text{(II.17)}$$

$$RT_{min} = \frac{Time\ @\ Minimum\ Surface\ Temperature - Sun\ Rise\ Time}{Sun\ Set\ Time - Sun\ Rise\ Time} \qquad \text{(II.18)}$$

The sun rise time, which varies in different seasons, has significant influence to the time at the minimum surface temperature as shown in Table II.1. The surface temperature reaches its minimum value around sun rise time. However, the time at the maximum surface temperature is almost constant in different seasons. Based on the statistical analysis results, we recommend to use the time value in Table II.1 for the maximum surface temperature, and RT_{min} value for calculating the time at the minimum surface temperature.

The sun rise and set times can be easily obtained from local newspaper or yearly astronomical almanac. For the simplicity, the sun rise and sun set times of twelve major cities in North Carolina are listed in Appendix A.2. The sun rise and sun set times at FWD test sites can be approximately estimated by using the times at the closest city in Appendix A.2. These times are calculated for an unobstructed horizon, with normal atmospheric conditions, at zero elevation

above the Earth's surface in a level region. The times used in this report are the regional standard times. The day light saving time needs to be converted before the temperature prediction procedure.

The surface temperature-time history used in the temperature prediction model begins at D-1 day's crossing time. The values of crossing time are obtained from the statistical analysis from the field temperature records of all the test sites. Table II.2 lists statistical results of crossing times at different weather conditions. In Table II.2, the time is represented by a value between 0 and 1 (i.e., 1.0 represents for 24:00 pm; 0.25 represents 6:00 am). The detailed analytical results of crossing time are included in Appendix A.3, which provides crossing times on each day in each season at each site. It was observed from the field records that the value of crossing time depends on the weather condition and sun rise time. Although the crossing time may not exist in rainy or snowy days, the values of the crossing time during clear or partly cloudy days are fairly uniform as shown in Table II.2. The value of crossing time varies in heavy cloudy day or at a site with shade.

With the help from NCDOT, whenever temperatures were recorded using the logger, the weather conditions were also documented of three times a day in all seasons at all sites. These valuable information enabled us to perform more detailed statistical analysis from different weather conditions. A weather index was developed for our database. The clear weather is defined as 100 and the sky fully covered with cloud as 0. The number between 0 to 100 represents the percent of sky which could be seen. Rain is symbolized by -1, and snow or ice weather by -2. Number 500 indicates no weather record. All the weather records are included in Appendix A.4.

Table II.2 Statistical Results of Crossing Times

Location		Weather Index	Crossing Time		Delta t		Delta t Ratio		Number o Days
			Mean	STD	Mean	STD	Mean	STD	
Eastern	Pitt	ALL	0.3245	0.0644	0.0980	0.0532	0.1293	0.0712	19
		100-50	**0.2996**	**0.0348**	**0.0760**	**0.0195**	**0.0996**	**0.0242**	**12**
		50 - 0	0.3136	0.0272	0.0901	0.0346	0.1175	0.0420	3
		0 - -2	0.3717	0.0694	0.1489	0.0784	0.1945	0.0983	3
	Carteret	ALL	0.3175	0.0755	0.0630	0.0797	0.0844	0.1084	20
		100-50	**0.3250**	**0.0276**	**0.0947**	**0.0252**	**0.1252**	**0.0336**	**4**
		50 - 0	0.3056	0.0000	0.0773	0.0000	0.1021	0.0000	1
		0 - -2	0.3423	0.0003	0.1118	0.0010	0.1478	0.0012	2
	New Hanover	ALL	0.3686	0.0576	0.1252	0.0370	0.1734	0.0551	29
		100-50	**0.3565**	**0.0476**	**0.1145**	**0.0225**	**0.1585**	**0.0365**	**18**
		50 - 0	0.3918	0.0894	0.1431	0.0589	0.1981	0.0856	5
		0 - -2	0.3753	0.0193	0.1541	0.0196	0.2028	0.0257	2
Central	Durham	ALL	0.3743	0.0907	0.1273	0.0856	0.1774	0.1234	20
		100-50	**0.3700**	**0.0519**	**0.1296**	**0.0257**	**0.1783**	**0.0432**	**14**
		50 - 0	0.3818	0.1976	0.1148	0.2053	0.1645	0.2925	4
		0 - -2	0.3893	0.0579	0.1365	0.0583	0.1970	0.0841	2
Western	Polk	ALL	0.3252	0.0962	0.0875	0.1028	0.1193	0.1424	16
		100-50	**0.3189**	**0.1147**	**0.0843**	**0.1248**	**0.1139**	**0.1727**	**11**
		50 - 0	0.3421	0.0213	0.0938	0.0251	0.1300	0.0325	3
		0 - -2	0.3843	0.0000	0.1195	0.0000	0.1687	0.0000	2
	Wilkes	ALL	0.3734	0.0564	0.1424	0.0499	0.1957	0.0674	28
		100-50	**0.3594**	**0.0345**	**0.1322**	**0.0149**	**0.1814**	**0.0226**	**15**
		50 - 0	0.3710	0.0846	0.1473	0.0595	0.2023	0.0881	6
		0 - -2	0.3942	0.0606	0.1540	0.0907	0.2114	0.1142	6

Note: The time is represented by a value between 0 and 1 (i.e., 1.0 represents for 24:00 pm; 0.25 represents 6:00 am.

In order to normalize the seasonal effect, we calculated Δt and Δt ratio, which are defined as;

$$\Delta t = cross\ \ time - sun\ \ rise\ \ time \tag{II.19}$$

$$\Delta t\ ratio = \frac{cross\ \ time - sun\ \ rise\ \ time}{sun\ \ rise\ \ time - sun\ \ set\ \ time} \tag{II.20}$$

Because the crossing time is related to the sun rise time, Δt ratio can give a better prediction of the crossing time.

II.4. Pavement Depth Temperature Prediction

Based on a series of sensitivity analyses using varying durations of surface temperature history, it was determined that the method optimizing the practicality and the accuracy is to use the surface temperature time history since the crossing time of D-1 day. The surface temperature history can then be used for the prediction of AC layer mid-depth temperature using heat conduction theory (i.e., Equation II.6). The surface temperature history since the crossing time of D-1 day can be divided into two time zones. The first one is between Points A and C in Figure II.4, i.e., between the crossing time of D-1 day and sun rise time of D day. The other is from D day's sun rise time till the time of FWD testing. As can be seen from Figure II.4, D day's surface temperature history can be determined by measuring surface temperatures at several different times in the morning and extrapolate the trend backward to the sun rise time of this morning.

Developing a function representing the surface temperature history between Points A and C requires careful observation of the characteristic shape of surface temperature time histories. As can be seen from Figure II.4, the shape of surface temperature history within a day seems to

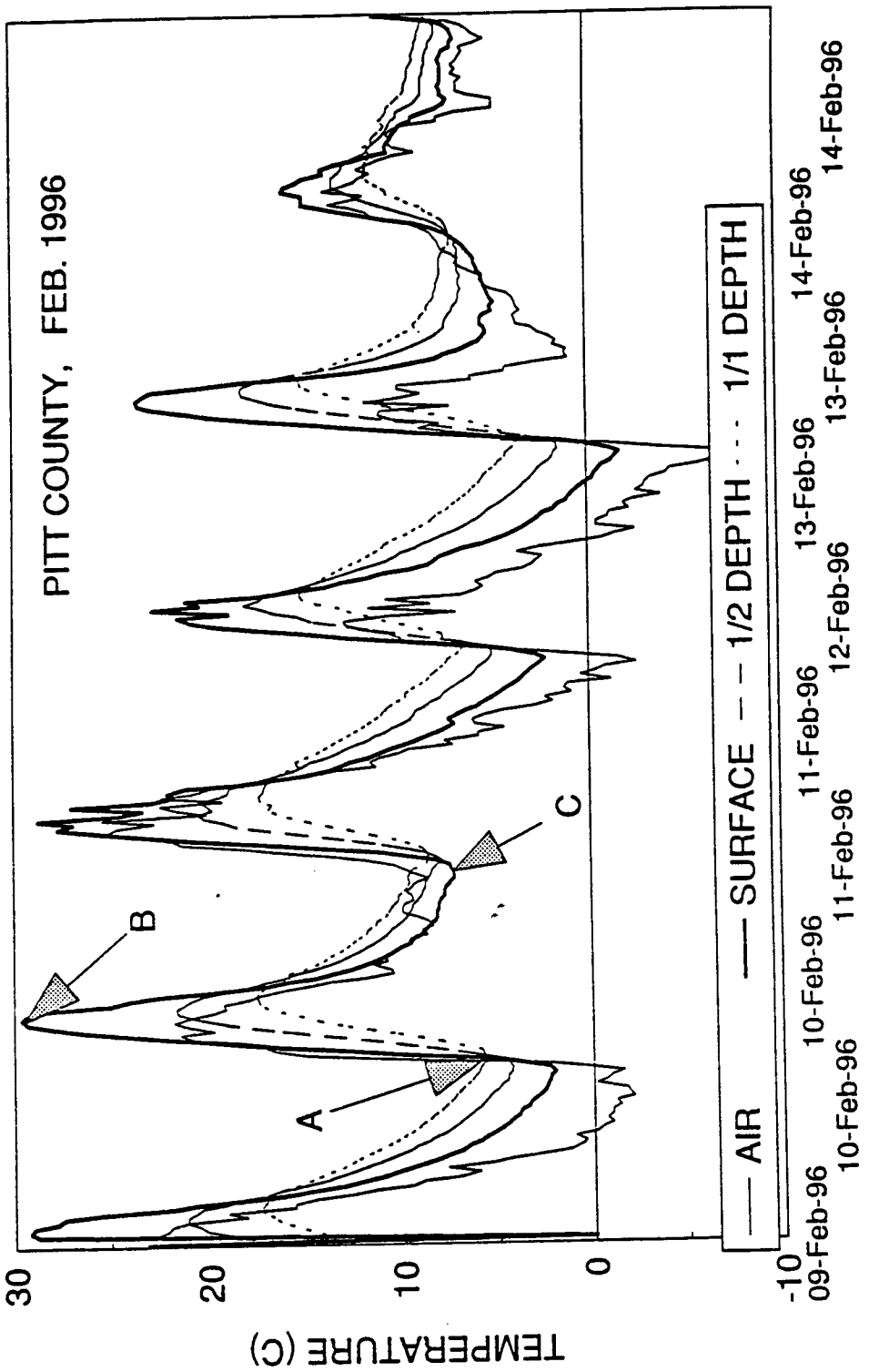

Figure II.4 Records of temperature measurement (Pitt County, February 1996).

follow the sine curve except the rate of temperature rise during the heating cycle and the rate of temperature drop during the cooling cycle are different. Therefore, the surface temperature history within a day can be modeled using a sine curve with two different periods for the heating and cooling cycles which add up to be equal to 24 hours. To find an analytical representation of this nonsymmetric sine curve, time-temperature coordinates of Points A, B, and C in Figure II.4 need to be defined. As long as times are concerned, Point A is the crossing time of D-1 day. Point B is when the surface temperature is the maximum, and Point C is defined as the time when the surface temperature reaches the minimum (in a normal weather condition, around the sun rise time). Actual time for Point C can be determined using a simple astronomical relationship between the sun rise time and the latitude and longitude of the test location. The times for Points A and B are obtained from the regression analysis of measured temperature data in the data base.

Vertical positions (i.e., temperature levels) of these points are much more difficult to determine because they are dependent on maximum and minimum air temperatures, weather conditions, test locations, etc. The approach taken in this study to handle this complexity is to normalize all the surface temperatures within 24 hours with the maximum and the minimum surface temperatures and to obtain the sine function with the normalized surface temperature time history. This normalized sine function is expanded to real values later as the maximum and the minimum surface temperatures are determined from the maximum and the minimum air temperatures respectively using the heat transfer theories described earlier.

The surface temperature history from D-1 day's sun rise time to D-1 day's peak temperature time (point B in Figure II.4) can be expressed as,

$$T(t) = \frac{T_{max} - T_{min}}{2} \sin\left[\frac{\pi(t - t_{min})}{t_{max} - t_{min}} - \frac{\pi}{2}\right] + \frac{T_{max} + T_{min}}{2} \qquad \text{(II.21)}$$

where

T_{min} = the minimum surface temperature at time t_{min},

T_{max} = the maximum surface temperature at time t_{max}.

From D-1 day's peak temperature time to D day's minimum temperature time, the surface temperature function is given by,

$$T(t) = f(t)\left\{ \frac{T_{max} - T_{min}}{2} \sin\left[\frac{\pi(t - t_{max})}{24 - t_{max} + t_{min}} + \frac{\pi}{2}\right] + \frac{T_{max} + T_{min}}{2} \right\} \qquad \text{(II.22)}$$

where f(t) is defined as a shape function to modify the sine curve in the B-C section in Figure II.4 and expressed as,

$$f(t) = \frac{1 - p}{2} \cos\left(2\pi \frac{t - t_{max}}{24 - t_{max} + t_{min}}\right) + \frac{1 + p}{2} \qquad \text{(II.23)}$$

The shape factor, p, equals 0.85.

From D day's minimum temperature to the first temperature record during the FWD test, the surface temperature-time history can be modeled by,

$$T(t) = \frac{T^*_{max} - T_{min}}{2} \sin\left[\frac{\pi(t - t_{min})}{t^*_{max} - t_{min}} - \frac{\pi}{2}\right] + \frac{T^*_{max} + T_{min}}{2} \qquad \text{(II.24)}$$

In order to pass both D day's minimum temperature point and the first temperature recorded in FWD test, the above curve function must have,

$$T^{*}_{max} = \frac{2\left(T(t_1) + 0.5T_{min}V\right)}{U} \qquad \text{(II.25)}$$

where $T(t_1)$ is the first surface temperature value measured at time t_1. U and V values are expressed by,

$$U = \sin\left[\frac{\pi\left(t_1 - t_{min}\right)}{t^{*}_{max} - t_{min}} - \frac{\pi}{2}\right] + 1 \qquad \text{(II.26)}$$

$$V = \sin\left[\frac{\pi\left(t_1 - t_{min}\right)}{t^{*}_{max} - t_{min}} - \frac{\pi}{2}\right] - 1 \qquad \text{(II.27)}$$

t^{*}_{max} is the time when the maximum surface temperature is measured during the FWD test day. If this time is not available, the statistical value, t_{max}, can be used as the same time at D-1 day's maximum surface temperature.

Since the heat conduction phenomenon in pavement systems is time dependent in nature, effects of inaccurate representation of first 24 hour surface temperature history on the prediction accuracy of the effective pavement temperature at the time of FWD testing are much smaller than those due to misrepresentation of this morning's surface temperature history. It is fortunate that surface temperatures in the morning of FWD testing day can be obtained accurately with a little additional effort, if there is any.

Details involved in the proposed temperature prediction procedure can be categorized into three major steps. A FORTRAN program, PD.FOR, is developed to automatically perform these temperature prediction procedures. The flow charts of the main program and a subroutine are plotted in Figures II.5 and II.6, respectively.

Flow Chart of the Main Program
PD.FOR

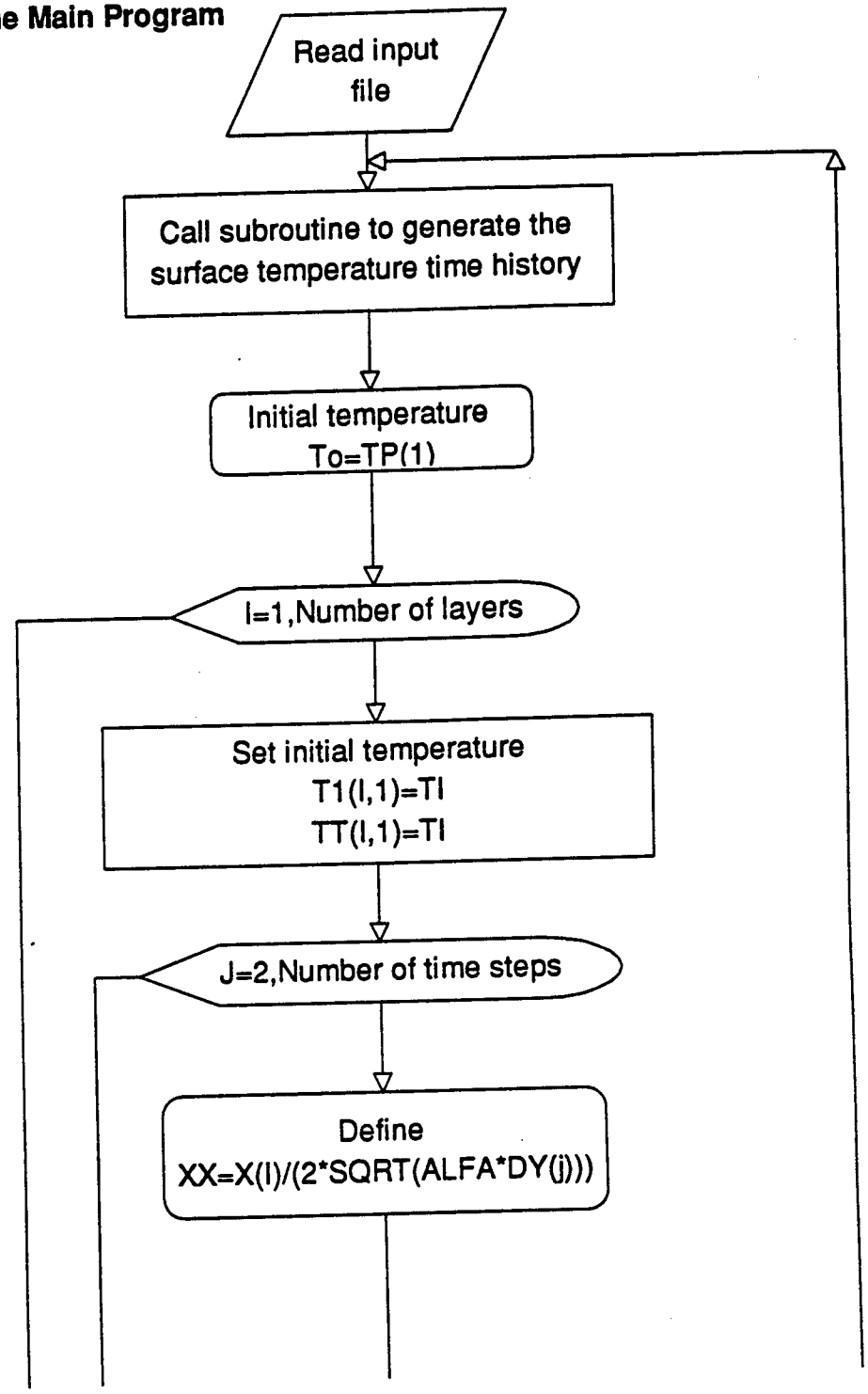

Figure II.5 Flow chart of the AC layer temperature prediction procedure.

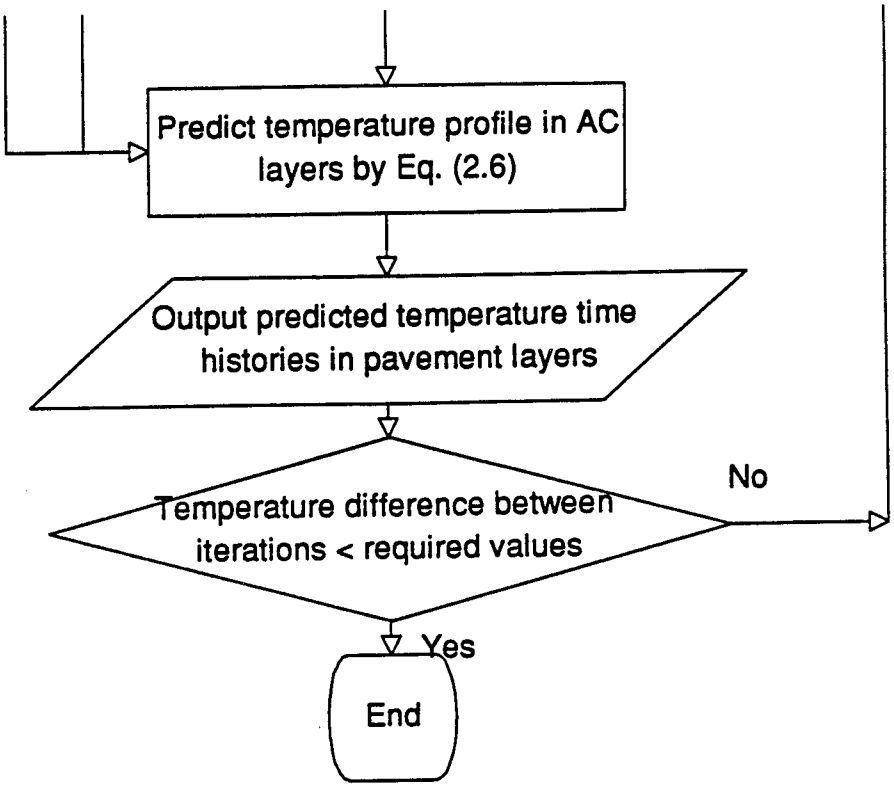

Figure II.5 Continue

Flow Chart of the Subroutine

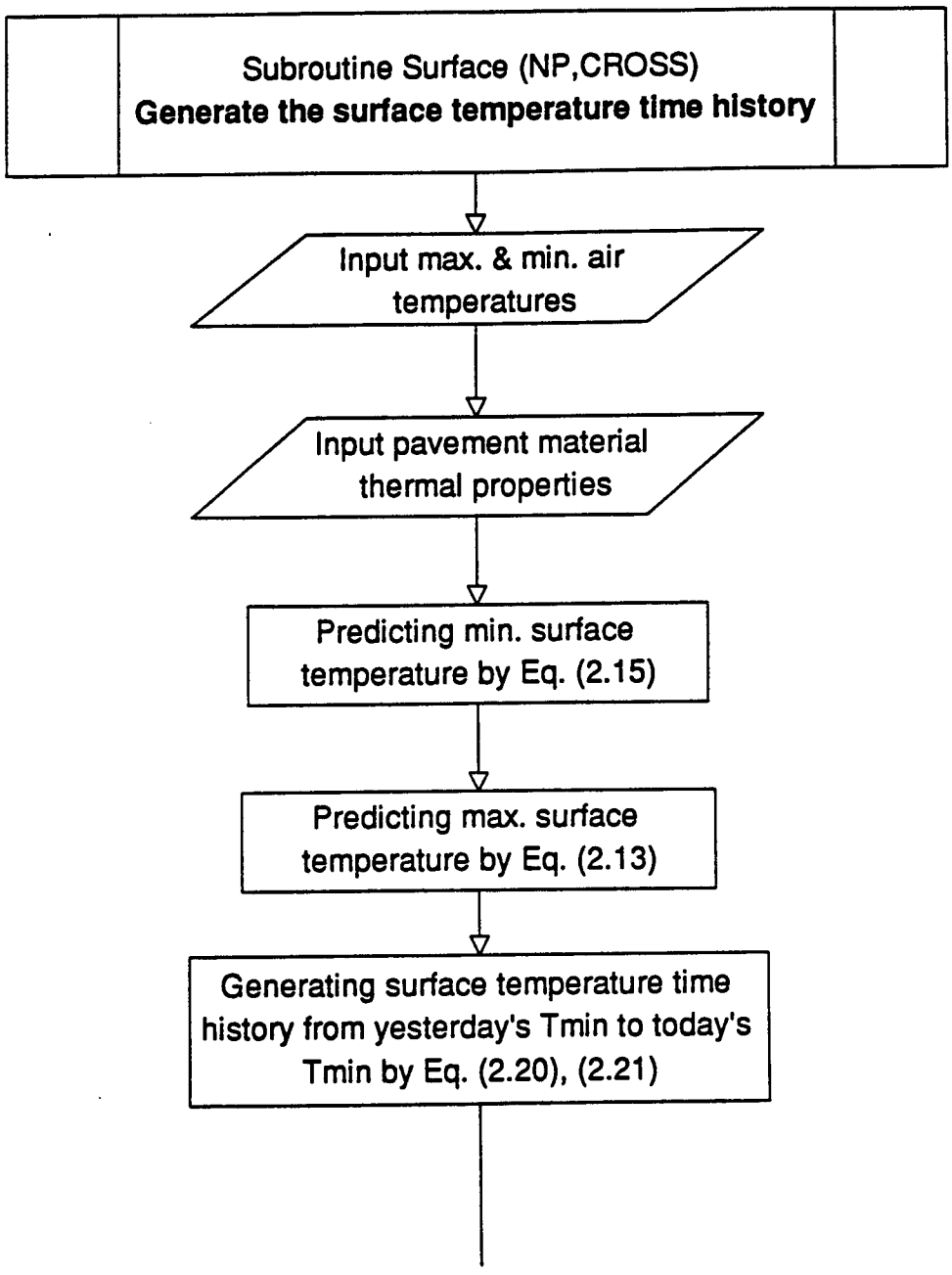

Figure II.6 Flow chart of the pavement surface temperature prediction procedure.

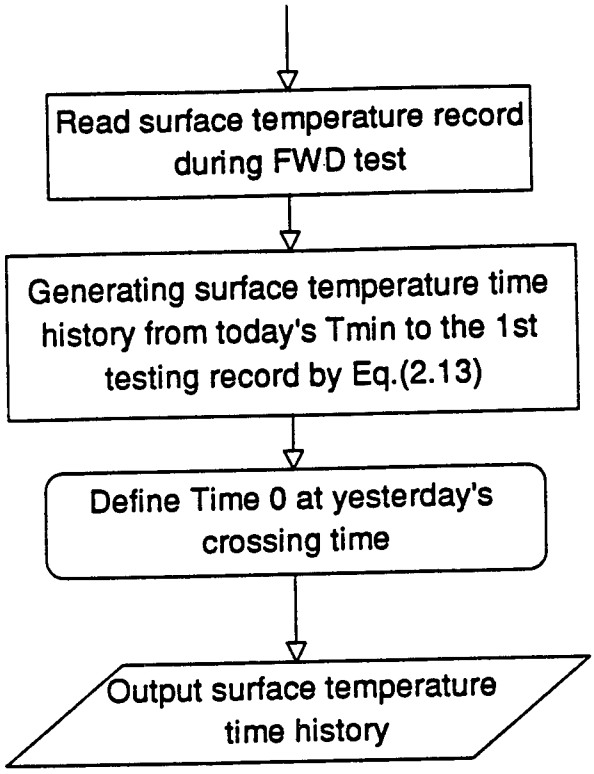

Figure II.6 Continue

The first step is to predict the surface maximum and minimum temperatures using Equations (II.13) and (II.15). These equations require prior knowledge of temperature difference between the surface and at depth x at the peaks. As starting values, 8°C and 2°C can be assumed for the day and the night, respectively. As the second step, a surface temperature time history is modeled by a modified sine-wave function as described earlier. The D-1 day's maximum surface temperature and this morning's minimum surface temperature were obtained from the first step and used to expand the normalized sine function. The value of this curve at D-1 day's crossing time is defined as the initial temperature, T_0. The surface temperature time history begins from D-1 day's crossing time and connects with D day's field temperature records. In the third step, the temperature profile inside the pavement is calculated by using Equation (II.6). D-1 day's crossing time is the starting time (t=0), and the variable t in Equation (II.6) represents the time elapsed since the starting time. The time used in the prediction procedure is local standard time. The day light saving time must be converted to the standard time.

The three steps discussed above should be repeated until (T_x-T_s) value at depth x converges reasonably (say, within 5% error over the previously assumed value). PD.FOR is developed to perform above three steps automatically. In summary, the input data for the temperature prediction program are tabulated in Table II.3.

The zenith angle, z, used in Equation II.8 is shown in Figure II.7. The value of the zenith angle is a function of the season and latitude. In the course of a year, the sun appears to traverse the entire heavens. Its apparent path being termed the ecliptic. The plane of the ecliptic is inclined to that of the celestial equator by almost 23°27' (the "obliquity of the ecliptic"). The ecliptic and the equator are shown in Figure II.8, which represent the celestial sphere with the

Table II.3. Input data for the temperature prediction program

Parameter	Range	Default value
Temperature and weather data:		
Yesterday's maximum and minimum air temperature	Obtained from local newspaper	
Yesterday's weather If the test site in a shade	Cloudy or sunny Considered as cloudy	
Today's surface temperature time history	Measured during FWD tests	
Location:		
Latitude		35.5° in NC
Thickness of AC layer		
Material properties:		
Thermal diffusivity α	0.0035 - 0.0055 m^2/hr	0.0037 m^2/hr
Solar absorbtivity α_l	0.85 - 0.93	0.90
Emissivity ε	0.85 - 0.93	0.90
Thermal conductivity k	0.43 - 1.67 (Btu/hr*ft^2 *F°)	0.8 (Btu/hr*ft^2 *F°)
Transmission coefficient τ_a	0.62 for cloudy - 0.81 for clear	depend on weather
Coefficient for atmospheric radiation ε_a	0.53 - 0.72 during day 0.61 - 0.83 during night	0.70 in day 0.81 in night
Surface heat transfer coefficient h_c	3.0 - 4.0 during day 1.4 - 2.5 during night (Btu/hr*ft^2 *F°)	3.5 during day 1.5 during night (Btu/hr*ft^2 *F°)

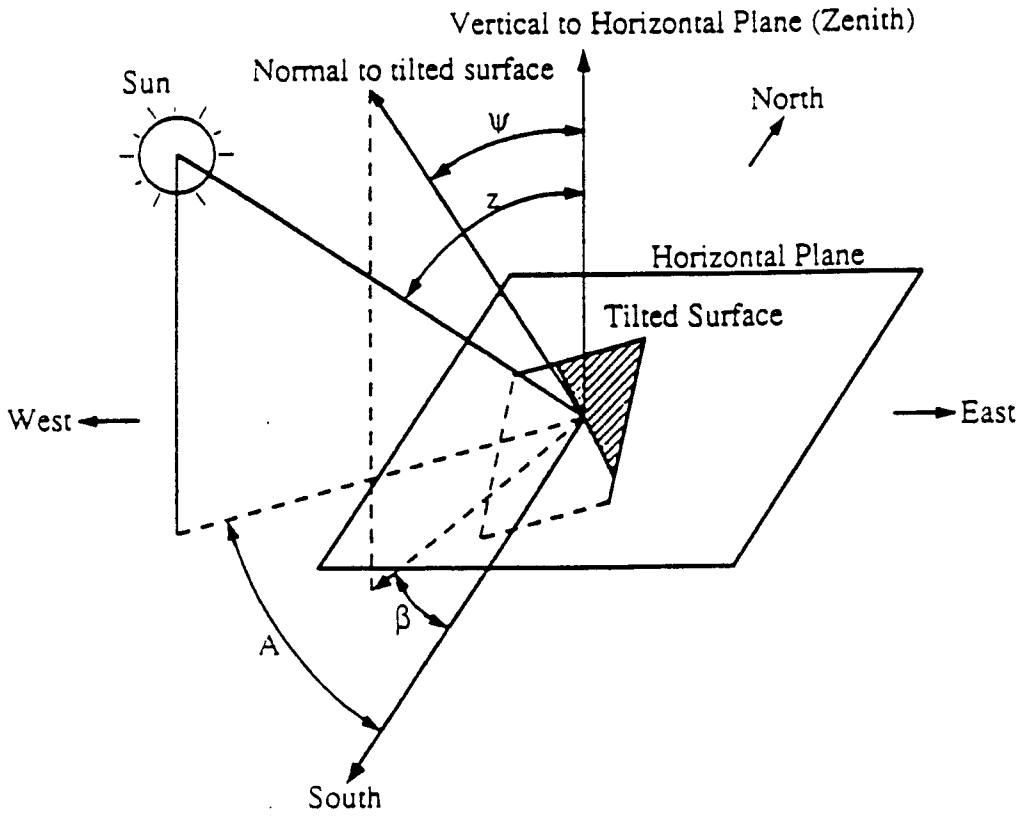

Figure II.7 Definition of solar and surface angles (Solaimanian and Kennedy, 1993).

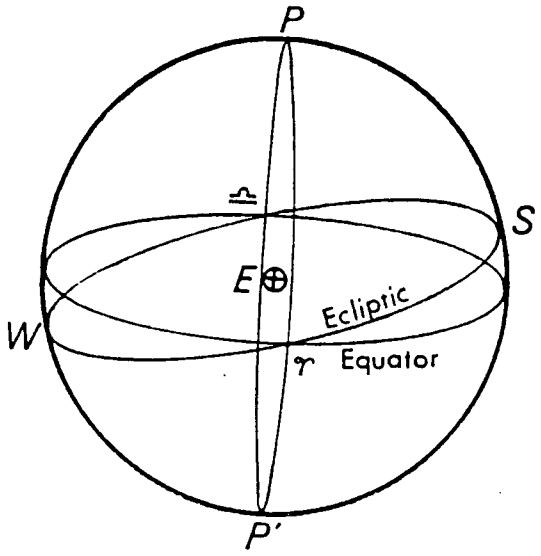

Figure II.8 Plane of the ecliptic and the celestial equator.

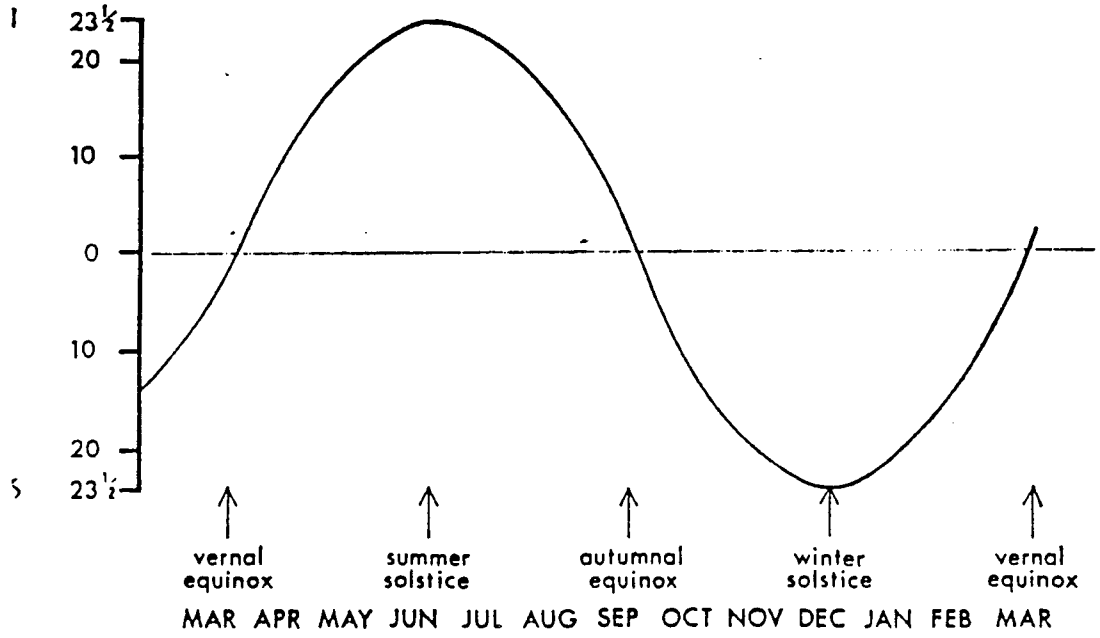

Figure II.9 Declination angle between the ecliptic plane and the celestial equator.

earth at the center. The difference between them in declination is provided in Figure II.9. The zenith angle can be approximately estimated by:

$$z = latitude - declination\ angle \quad \text{(II.28)}$$

Equation II.28 can be used in any latitude and any season. Solaimanian and Kennedy (1993) suggested that at noon sun time and in the region with latitude larger than 25°, z ≅ latitude - 20° from May to August, as shown in Figure II.10. More accurately method in calculating the zenith angle can be found in astronomy books.

II.5. Verification of New Temperature Prediction Procedure

In order to validate the proposed temperature prediction procedure, the predicted temperatures in the pavement are compared with those measured from the test sites. Eight cases presented in the following represent the examples with different climatic regions, different AC layer thicknesses, and different weather patterns in different seasons.

Case 1

The test site in Durham County is located in the piedmont region of North Carolina. The AC layer thickness is 250 mm (10 inches). As shown in Figure II.11, the FWD test began at 8:30 am and finished at 4:30 pm on August 14,1995. D-1 day's maximum air temperature and D day's morning minimum air temperature are obtained from local newspapers.

The predicted surface temperatures are generally in a good agreement with the measured data. The field weather record indicates that it was cloudy during the noon time of D-1 day. Transmission coefficient, τ_a, was selected to be 0.65. Equation II.13 predicted reasonable

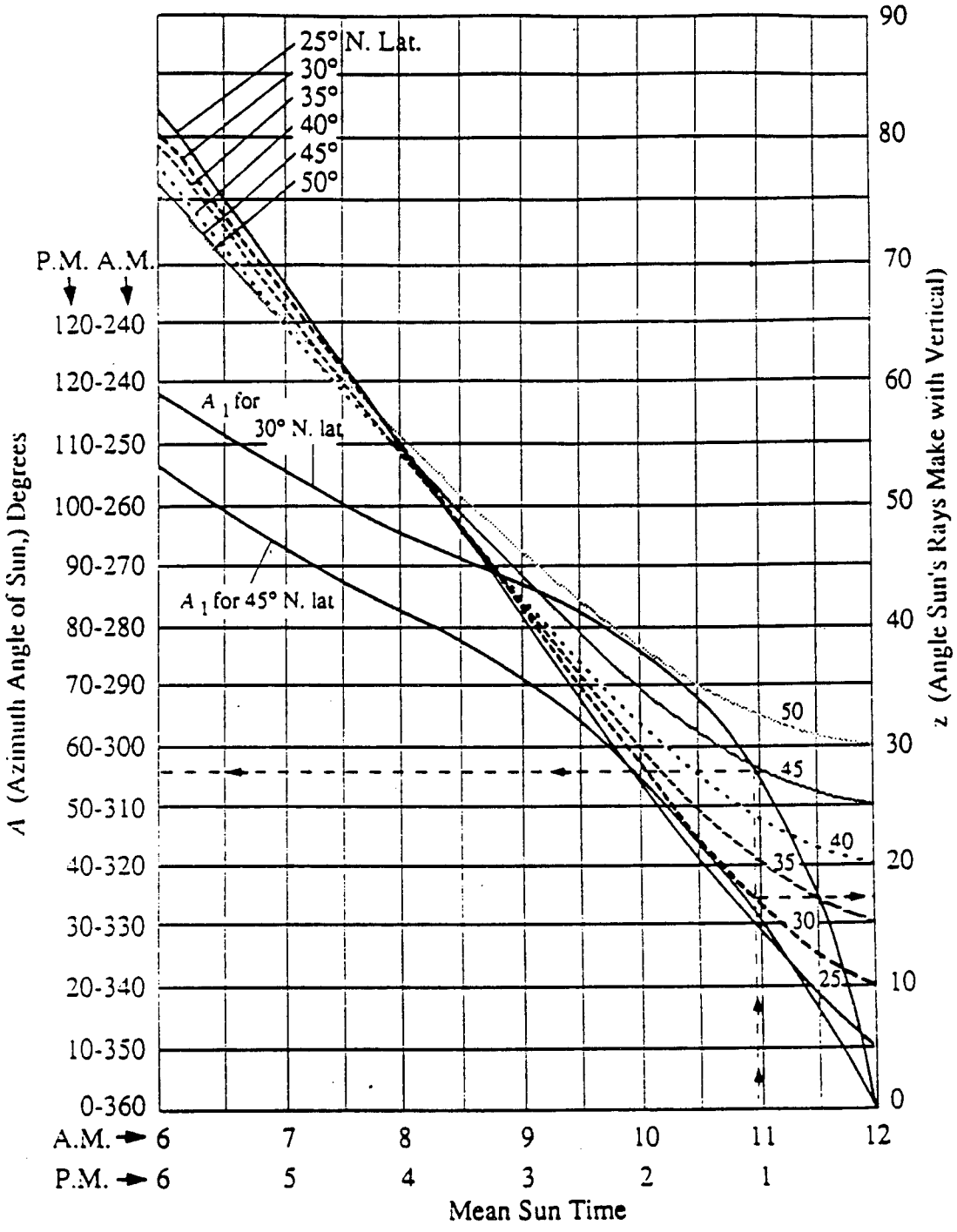

Figure II.10 Zenith angles for the period from May to August in Northern latitudes (Solaimanian and Kennedy, 1993).

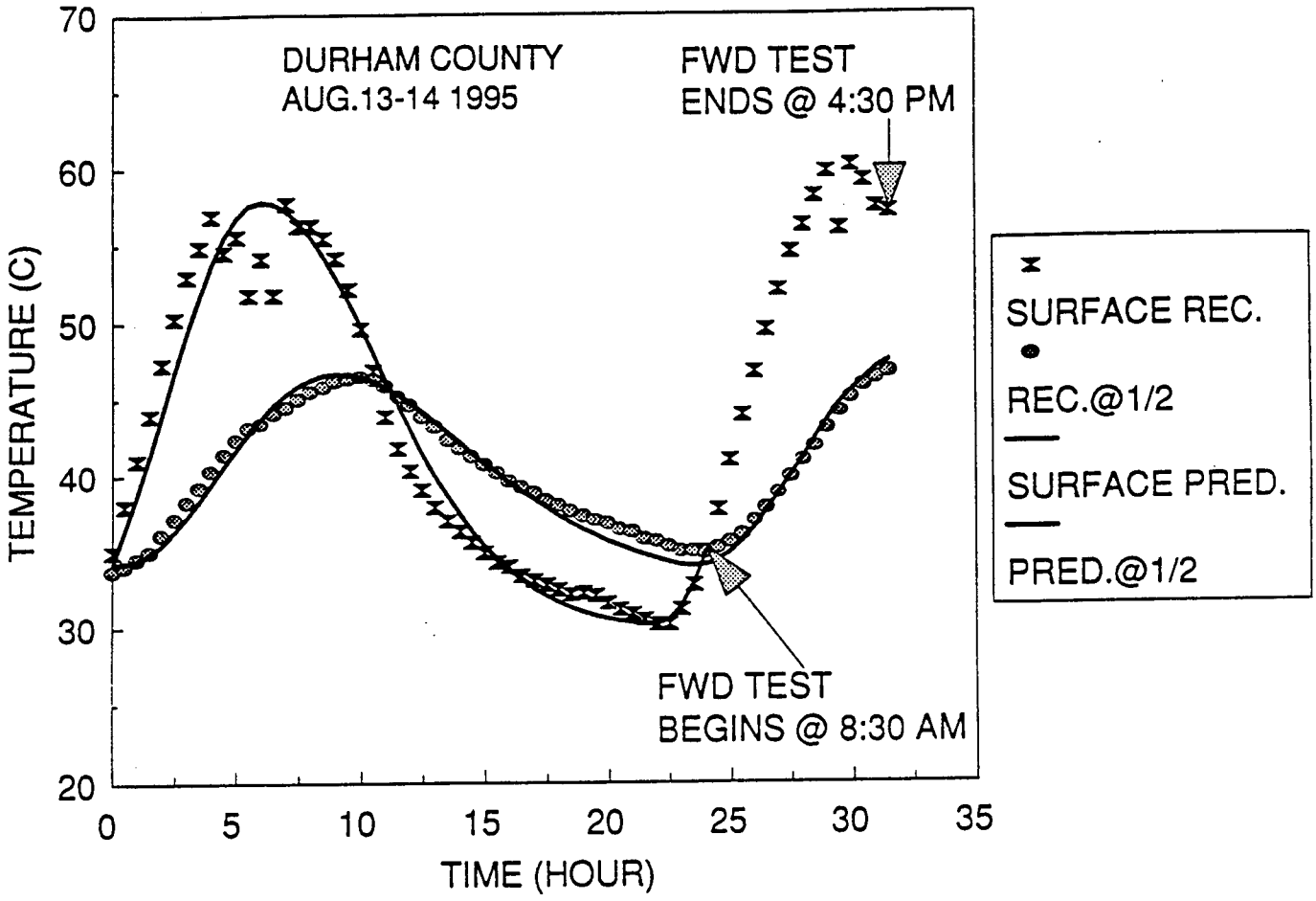

Figure II.11 Comparison between the predicted and the measured pavement temperatures (Durham County, August 13 and 14, 1995).

maximum surface temperature. During the night, heat transfer coefficient, h_c, was reduced to 1.44, and the prediction by Equation II.15 was satisfactory.

The accuracy of the prediction of the mid-depth temperature was also very good. This agreement suggests that the values used for the material properties and other parameters in the heat conduction equation are reasonable.

The sensitivity analysis was performed for the temperature at the crossing time (T_0) using the Durham data. T_0 values that are 5°C above and below the estimated crossing temperature were intentionally used for the prediction. The value of 5°C was found to be the worst error found from our data base. The results are displayed in Figure II.12. It can be observed that the incorrect T_0 inputs affect the prediction of D-1 day's surface temperatures significantly, but the effect is diminished as time elapses. As a matter of fact, the errors in predicting D day's mid-depth temperatures are within 2 °C.

Case 2

The test section in Pitt County is located in the eastern coastal region. The thickness of the AC layer is 114 mm (4.5 inches). Similar to Case 1, the pavement surface temperatures were measured during FWD tests on May 19, 1996. The weather was clear both D day and D-1 day. Transmission coefficient, τ_a, was selected to be 0.81. The predicted mid-depth temperature agrees with filed measurements quite well (Figure II.13).

Case 3

The test site used in this case is located in Wilkes County in the western mountain region. The AC layer is 240 mm (9.5 inches) thick. It was very cloudy during FWD tests on August 23, 1995, and clear D-1 day. The test location was shaded during afternoon. The transmission

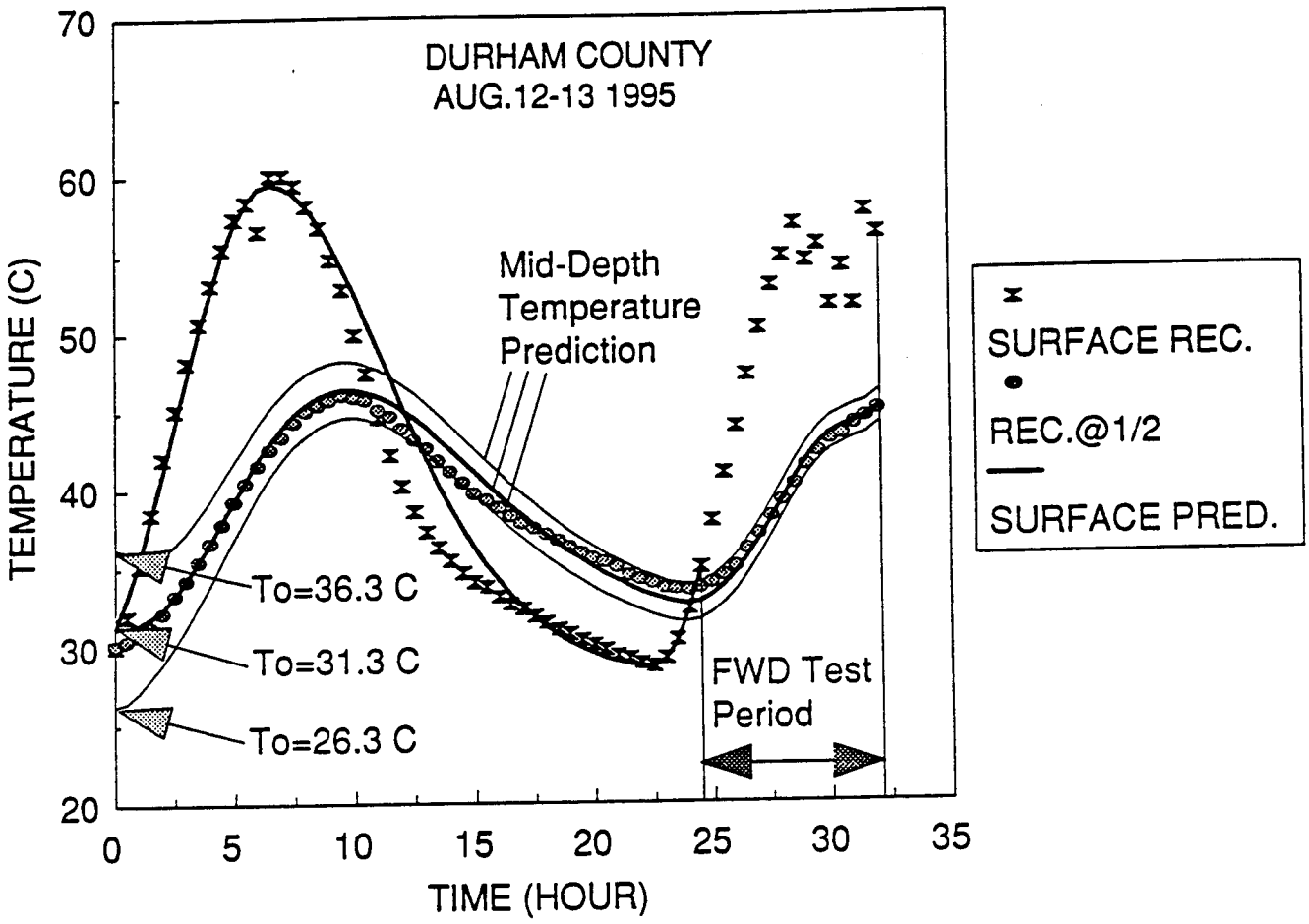

Figure II.12 Sensitivity analysis on the values of crossing temperature (Durham County, August 12 and 13, 1995).

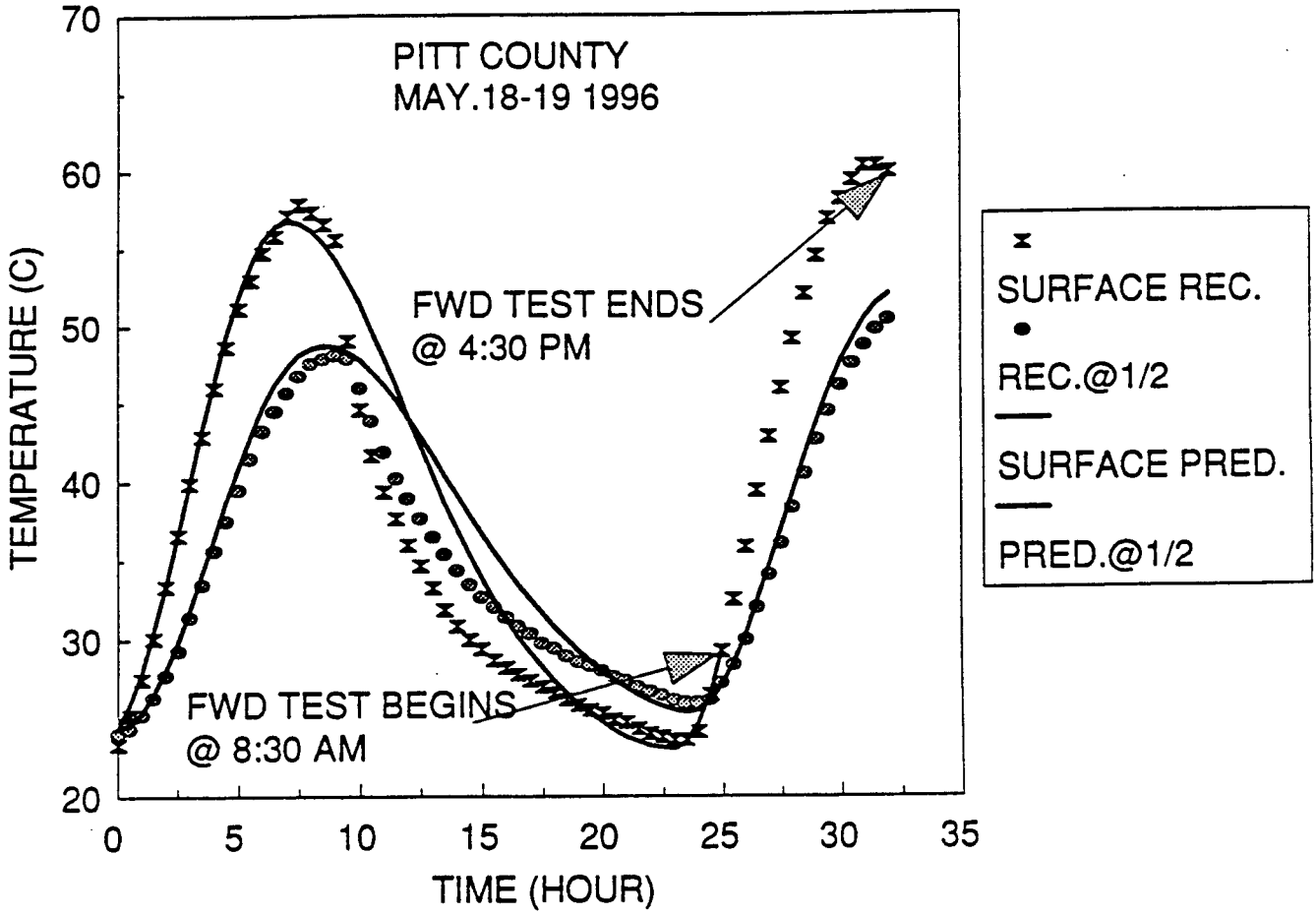

Figure II.13 Comparison between the predicted and the measured pavement temperatures (Pitt County, May 18 and 19, 1996).

coefficient was selected to be 0.62 due to shade. Although some discrepancies can be observed from D-1 day's surface temperature prediction, the predicted mid-depth temperature still agrees well with the field measurements (Figure II.14).

Case 4

The test site was in Pitt county, the same location as in Case 2. The pavement surface temperatures were measured during FWD tests on February 13, 1996. The weather on the testing day was clear, but partly cloudy on D-1 day. The D-1 day's maximum air temperature was 12.8 °C, and D day's morning minimum air temperature was -7.6 °C. The transmission coefficient was selected to be 0.75 due to partly cloudy weather. During winter time, the zenith angle is larger than that during summer. From Figure II.9, the zenith angle, z, was obtained to be 48 degrees. The comparison between the predicted temperature profile and the recorded profile is presented in Figure II.15. The model predicts the mid-depth temperature reasonably well during the FWD test period, although there exist large discrepancies between the predicted temperature and the recorded values during D-1 day's afternoon and evening times. It has been observed from our analysis that a good prediction result of D day's temperature profile can be obtained when D-1 day's maximum surface temperature and D day's minimum surface temperature are well estimated.

Case 5

The test site used in this case is located in Carteret County in the eastern region. The AC layer is 229 mm (9.0 inches) thick. There was no weather report during FWD tests on February 23, 1996 and D-1 day. We guessed thatD-1 day was cloudy, because D-1 day's maximum air temperature was much lower than D day's value. The transmission coefficient was selected to be

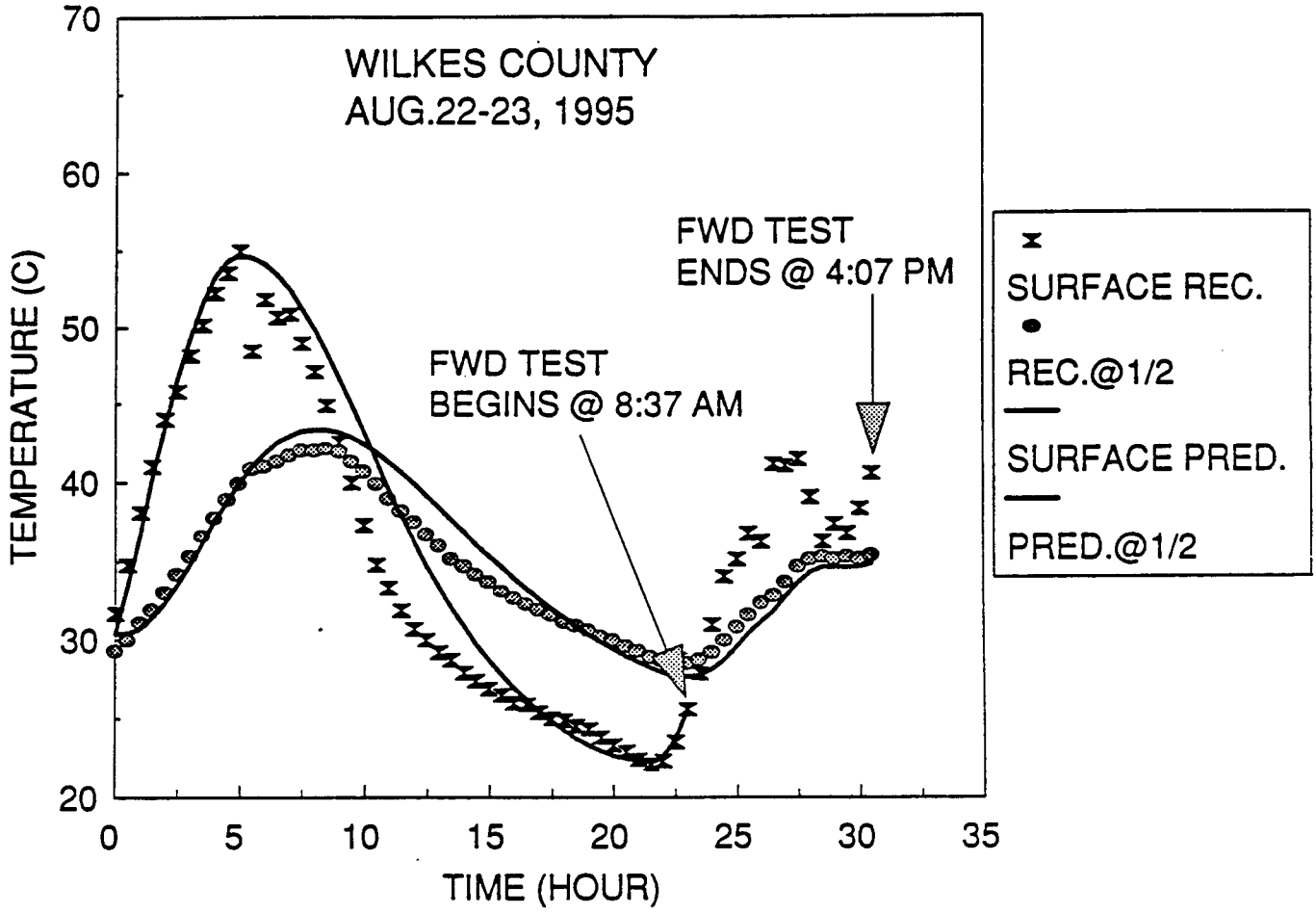

Figure II.14 Comparison between the predicted and the measured pavement temperatures (Wilkes County, August 22 and 23, 1995).

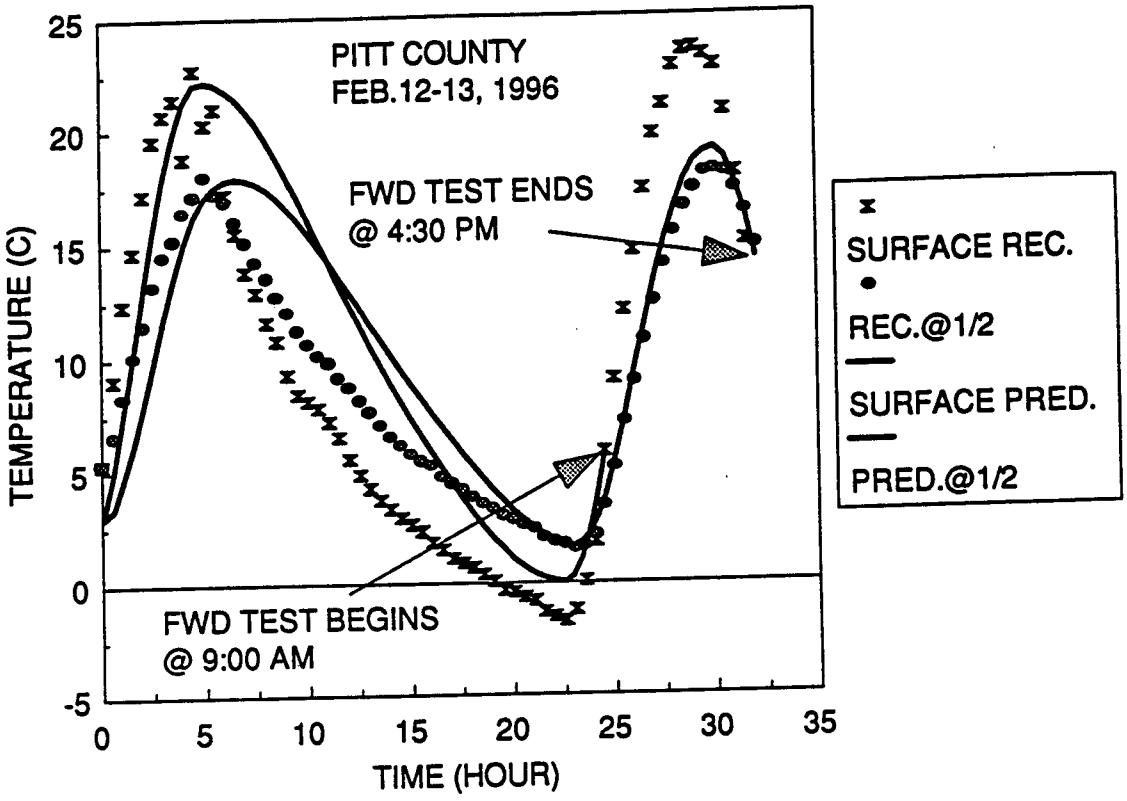

Figure II.15 Comparison between the predicted and the measured pavement temperatures (Pitt County, February 12 and 13, 1996).

0.62. The thermal diffusivity, α, was equal to 0.35 m^2/hr. As shown in Figure II.16, the differences between the predicted mid-depth temperature and the recorded mid-depth temperature during FWD tests are within about 1 °C. The recorded temperature history indicates that the D-1 day's crossing time is much earlier due to the weather condition than the average crossing time used in the prediction procedure. The D-1 day's crossing temperature utilized in the prediction is 3°C higher than the recorded value. However, D day's mid-depth temperatures are predicted reasonably well.

Case 6

The same test site as in Case 5 was tested on April 5, 1996. The weather in the FWD testing day was cloudy and clear D-1 day. The transmission coefficient was selected to be 0.81. The zenith angle was 25 degree during early April. The predicted results are plotted in Figure II.17.

Case 7

The test site used in this case is located in New Hanover County in the eastern region. The AC layer is 305 mm (12.0 inches) thick. It was clear during FWD tests on November 18, 1995 and D-1 day. The transmission coefficient was selected to be 0.81 due to the clear weather. The zenith angle in mid-November is 56.5 degrees. Although D day's minimum air temperature is below freezing point, the predicted minimum surface temperature agrees the measured temperature very well. The comparison between the predicted AC layer temperature and measured values is made in Figure II.18.

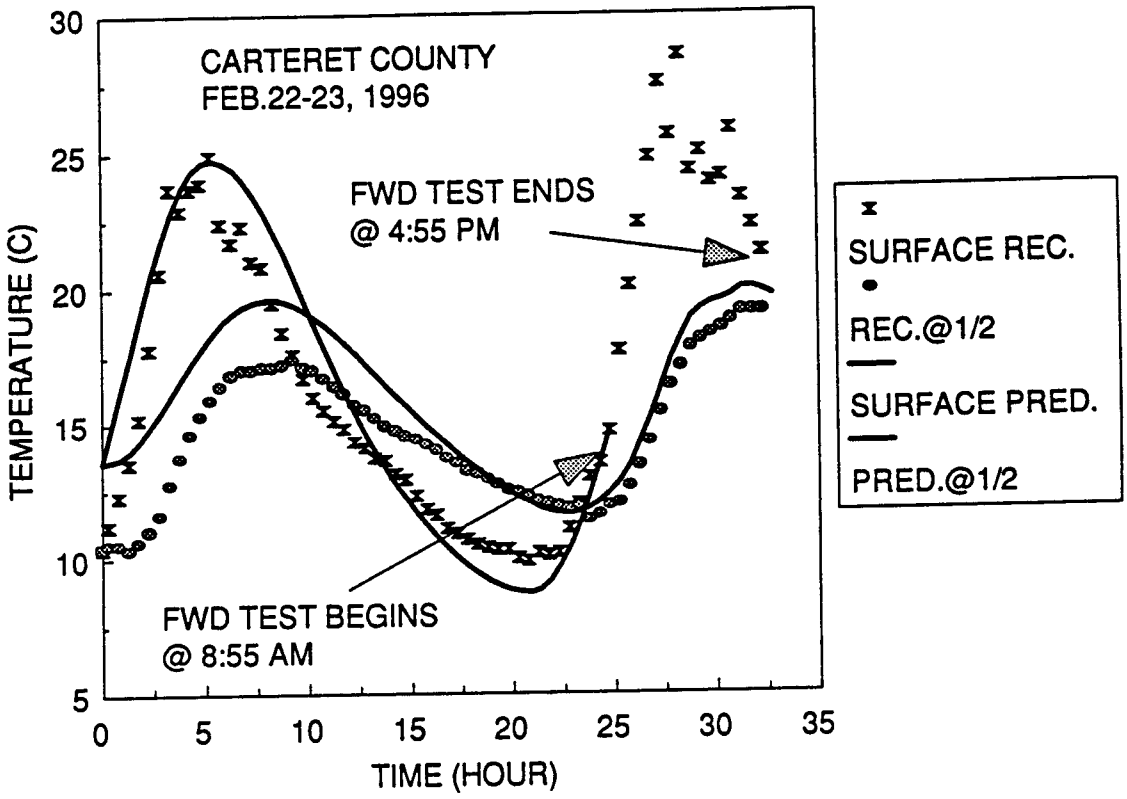

Figure II.16 Comparison between the predicted and the measured pavement temperatures (Carteret County, February 22 and 23, 1996).

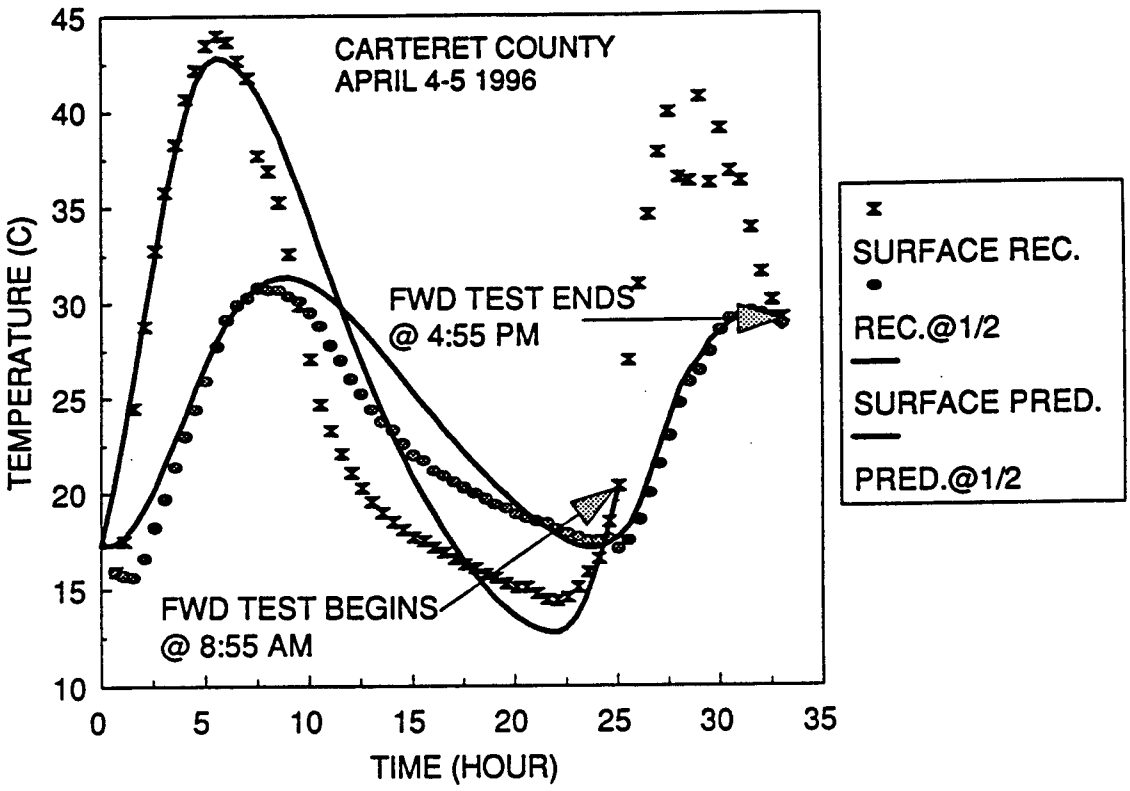

Figure II.17 Comparison between the predicted and the measured pavement temperatures (Carteret County, April 4 and 5, 1996).

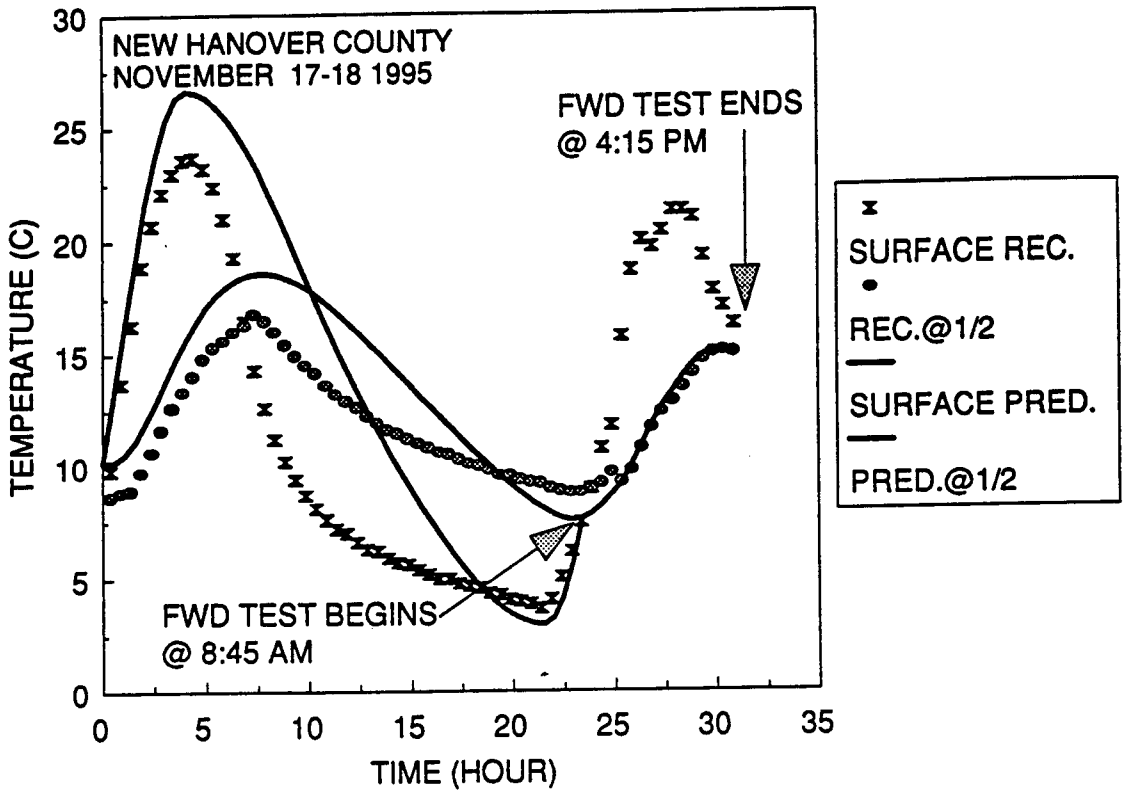

Figure II.18 Comparison between the predicted and the measured pavement temperatures (New Hanover, November 17 and 18, 1996).

Case 8

The test site used in this case is located in Polk County in the western mountain region. The AC layer is 165 mm (6.5 inches) thick. It was clear during FWD tests on April 3, 1996 and D-1 day. The transmission coefficient was selected to be 0.81 due to clear day. The thermal diffusivity, α, was equal to 0.40 m^2/hr. The zenith angle in early April is 25 degrees. The predicted mid-depth temperature agrees well with the field measurements (Figure II.19).

Since the proposed temperature prediction procedure is based on fundamental principles of heat transfer, it is site independent and can be applied to other states with a minimal amount of temperature data collection. All the heat transfer parameters used in the model are the values suggested by Solaimanian and Kennedy (1993) except the thermal diffusivity (α) value from Yoder and Witczak (1975), the surface coefficient of heat transfer (h_c), and the coefficient for atmospheric radiation (τ_a) for night time. The value for h_c at night was calculated from the empirical formula suggested by Solaimanian and Kennedy, and the night time value for τ_a is determined by trying different values until the predicted and the measured minimum surface temperatures match. All the cases presented above used the same values for the heat transfer parameters unless stated for specific reasons.

There are some limitations in the proposed procedure. If it was raining or snowing during D-1 day or early in D day's morning, the maximum or the minimum surface temperatures can not be predicted accurately because the presence of moisture on pavement surface changes the heat flow mechanisms that Equation (II.7) is based on. Although inaccurate prediction of the minimum surface temperature in D day's morning affects the prediction accuracy more

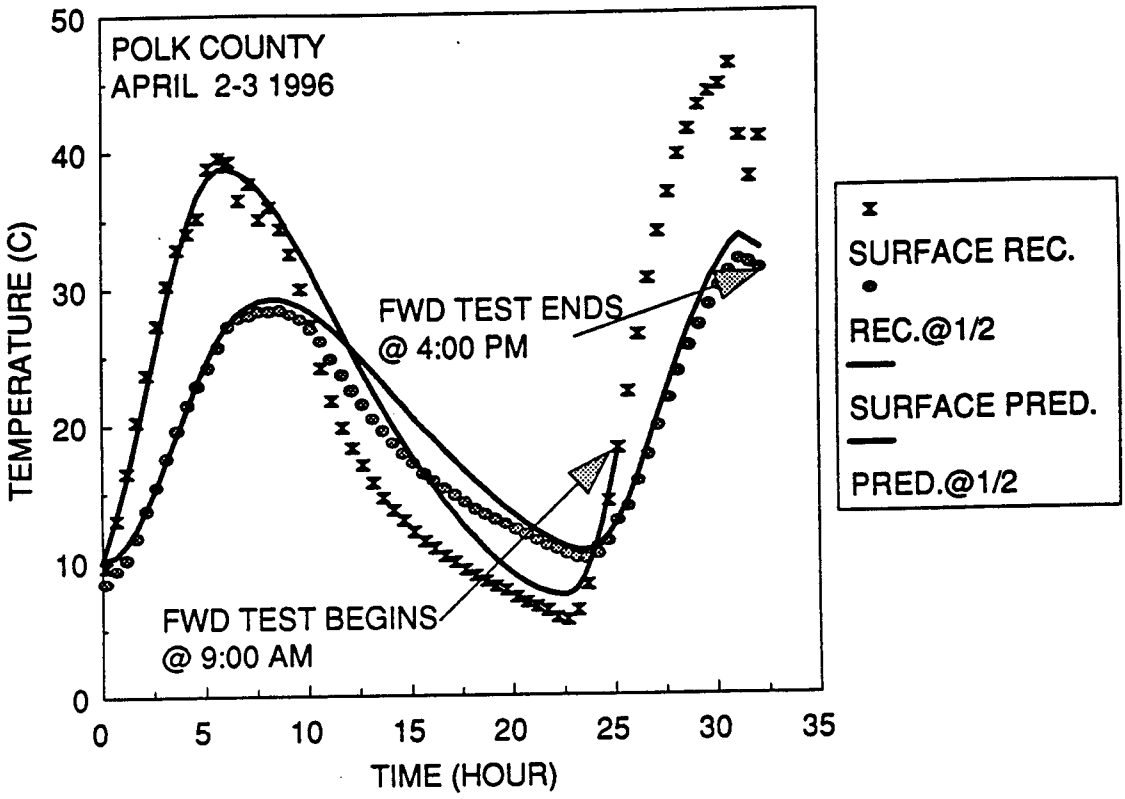

Figure II.19 Comparison between the predicted and the measured pavement temperatures (Polk County, April 2 and 3, 1996).

significantly, it is not our major concern because FWD testing is not usually conducted if there is moisture on the pavement surface due to safety reasons. Since the heat conduction theory inside the pavement is still valid, one may adjust the relationship between air and surface temperatures to obtain a more realistic surface temperature history for rainy or snowy days.

II.6. Conclusions

A simplified prediction procedure for AC layer depth temperatures is presented in this section. This method is based on fundamental principles of heat transfer and uses the surface temperature history since the morning of D-1 day to predict the AC layer mid-depth temperature at the time of FWD testing on D day. The surface temperature history is determined using the D-1 day's maximum air temperature, the minimum air temperature of D day's morning, and cloud conditions of D-1 day. The case studies using measured temperatures from pavement sections in different climatic regions of North Carolina and AC layer thicknesses under different weather patterns and seasons demonstrate that the proposed method can accurately predict the AC layer mid-depth temperature with input requirements practical enough to be accepted for NCDOT's routine deflection analysis. The application of this model to other states or climatic regions needs to be evaluated; however, the fundamental nature of the model will provide more general applicability than empirical models can if the calibration of the model parameters can be done with local temperature measurements.

PART III. TEMPERATURE CORRECTION OF MODULI AND DEFLECTIONS

III.1. Introduction

Due to urgent needs of developing a realistic temperature correction procedure, many researchers have developed temperature correction models (e.g., Ullidtz 1987, Johnson and Baus 1992, Baltzer and Jansen 1994, Kim et al. 1995, 1995a). The majority of these models are based on statistical analysis of field measurements. These models work effectively for pavements with similar mixture properties and pavement profiles to those on which the model was established. These empirical models often fail to effectively correct moduli and deflections for certain types of mixtures and pavement profiles.

It is understood from a rheological point of view that the thermo-viscoelastic properties of the asphalt mixture are primarily responsible for temperature effects on backcalculated moduli and pavement deflections. It is well known that asphalt mixtures possess high viscoelasticity imparted by the asphalt binder. The mechanical properties of asphalt mixtures and the responses of asphalt pavement systems depend on both loading time and temperature. However, through the time-temperature superposition principle the effects of both time and temperature can be accounted for by a single variable called "reduced time". It has been observed that the time-temperature superposition principle applies to asphalt mixtures (Pagen 1965, Kim and Lee 1995).

Kim at al. (1995, 1995a) developed empirical models for temperature-modulus and temperature-deflection corrections based on field measurements from North Carolina. These models were simple in form but practical enough for routine implementation.

However, the models were based on a limited data base. Test sites were located in the central region of the state and thus only a limited number of mixture types and pavement structures were considered. Therefore, there has been a need to test these models against data from other regions within the state with different mixtures and/or pavement structures so that they may be re-calibrated or revised accordingly.

In this project, the temperature correction models developed from the 92/93 study were first tested to see if they effectively correct backcalculated AC moduli and FWD center peak deflections gathered from different regions of the state. Based on this evaluation results, the 92/93 empirical models were re-calibrated and revised for better correction capabilities. However, it was found that even though these empirical models are effective and reasonably accurate for most of the mixture types and pavement profiles, data from some pavements with certain mixture types and pavement profiles cannot be satisfactorily corrected with these models.

In order to overcome the shortcomings of the empirical models and to gain an enhanced understanding of the theoretical implications in temperature-modulus and temperature-deflection corrections, an in-depth study was initiated and new analytical modulus and deflection correction procedures were developed within the framework of the linear viscoelasticity theory and the time-temperature superposition principle. The new procedures explicitly account for the thermo-rheological properties of the mixture and the structural design of the pavement section under consideration.

III.2. Theoretical Background

In order to provide a basis for theoretical treatment of temperature correction issues and for development of analytical models described in later sections, a brief review of the theory of linear viscoelasticity and the time-temperature superposition principle is given.

III.2.1. Linear viscoelasticity

For linear viscoelastic materials or structures, the input-response relationship can be expressed in convolution integral as follows (Schapery 1974):

$$R(t) = \int_0^t R_H(t-\tau)\frac{dI(\tau)}{d\tau}d\tau \qquad \text{(III.1)}$$

where R(t) is the response, I(t) is the input, and R = I = 0 for t < 0. The function $R_H(t)$ in (III.1) is commonly referred to as the *unit response function* as it signifies the response of the system to the unit step input; i.e., from (III.1)

$$R(t) = R_H(t) \quad for \quad I(t) = H(t) \qquad \text{(III.2)}$$

where H(t) is the Heaviside step function with H(t) = 1 for t > 0 and H(t) = 0 for t < 0. For example, in the case of controlled-strain test where preselected strain history is applied to a specimen, the input is the strain, the response is the stress, and the unit response function is the relaxation modulus. For controlled-stress tests, the input is stress, the response is the strain, and the unit response function is the creep compliance.

The convolution integral (III.1) applies not only to the stress-strain relations of linear viscoelastic materials but also to the structural analysis of linear viscoelastic systems, and is often called the *Boltzmann superposition integral.* In the stress-strain

relationship, $R_H(t)$ is a function of material properties only, but in a structural analysis problem $R_H(t)$ is a function of both material and geometrical parameters of the system. For instance, the uniaxial stress-strain relation for linear viscoelastic materials (such as asphalt mixtures) can be expressed by

$$\sigma(t) = \int_0^t E(t-\tau)\frac{d\varepsilon(\tau)}{d\tau}d\tau \qquad \text{(III.3)}$$

or

$$\varepsilon(t) = \int_0^t D(t-\tau)\frac{d\sigma(\tau)}{d\tau}d\tau \qquad \text{(III.4)}$$

where E(t) and D(t) are the uniaxial relaxation modulus and the creep compliance, respectively. Eqautions (III.3) and (III.4) imply that the modulus and the compliance are not simply the reciprocal of each other. In fact, it can be shown that they are related by the following equation (e.g., Ferry 1980):

$$1 = \int_0^t E(t-\tau)\frac{dD(\tau)}{d\tau}d\tau \qquad \text{(III.5)}$$

for $t>0$.

To illustrate a structural analysis problem that can be represented by (III.1), the surface deflection of a pavement system subjected to surface loading (e.g., FWD loading) can be considered,

$$w(t) = \int_0^t w_H(t-\tau)\frac{dq(\tau)}{d\tau}d\tau \qquad \text{(III.6)}$$

where w(t) is the deflection at time t at a particular position of the pavement surface, q(t) is the applied load, and $w_H(t)$ is the *unit deflection function* that is defined as the deflection of the system under the unit step loading, $q(\tau) = H(\tau)$.

III.2.2. Time-temperature superposition

In general, the mechanical properties of viscoelastic materials depend not only on loading time but also on temperature. Especially some of the mechanical properties of amorphous polymers have a strong dependence upon temperature. There exists a special class of viscoelastic materials whose temperature dependence of mechanical properties is amenable to analytical description. This class of materials is referred to as being *thermorheologically simple.* The simplifying feature of the thermorheologically simple materials is that, when the unit response function (e.g., creep compliance or relaxation modulus) curve measured at different constant temperatures are all plotted against time on the logarithmic scale, the curves can be superposed so as to form a single curve (called a *master curve*) corresponding to an arbitrary fixed temperature (called a *reference temperature*) by means of horizontal translations only. Examples of the master curve are shown in Figure III.3.1.

This feature has a very significant consequence in that the dependence of the material property upon both time and temperature can be represented by dependence upon a single variable called *reduced time*, and the feature is often referred to as *time-temperature superposition* or *reduced-time method.* In mathematical notation, e.g., for the uniaxial relaxation modulus,

$$E(t,T) = E_M(\xi) \tag{III.7}$$

where $E_M(\xi)$ is the master relaxation modulus corresponding to a reference temperature (T_R), and for constant temperatures,

$$\xi = \frac{t}{a_T} \tag{III.8}$$

where ξ and a_T are the reduced time and the *time-temperature shift factor*, respectively. The a_T is a temperature dependent material function which reflects the influence of temperature on internal viscosity of the material. It is determined by the horizontal distance between the master curve and any one of the isothermal curves in a logarithmic time scale.

For temperatures above the glass transition temperature of the material, the shift factor a_T for a thermorheologically simple material is usually expressed in the following form:

$$\log a_T = -\frac{c_1(T - T_R)}{c_2 + T - T_R} \tag{III.9}$$

where c_1, c_2, and T_R are constants. Equation (III.9) is commonly referred to as *WLF equation* (Williams, Landel, Ferry 1955).

Now, the input-response relations of a thermorheologically simple linear viscoelastic medium can be expressed, from (III.1) , as follows:

$$R(t) = \int_0^t R_H(\xi - \xi') \frac{dI(\tau)}{d\tau} d\tau \tag{III.10}$$

where

$$\xi' = \int_0^\tau \frac{1}{a_T} d\tau' \tag{III.11}$$

and $\xi = \xi'|_{\tau=t}$. The variable τ' in (III.11) is the dummy variable of integration and a_T is a function of temperature as represented by (III.9) . The temperature varies with time in

general, i.e., $a_T = a_T(T(t))$, and for constant temperatures (isothermal conditions), (III.11) reduces to (III.8) .

The significance of (III.10) is that the same unit response function determined at a constant temperature can be used to calculate the responses at other constant temperatures or under general transient temperatures simply by replacing the physical time with the reduced time which accounts for the effects of both time and temperature.

III.2.3. Analysis of layered viscoelastic system

In order to determine the deflections of a pavement system, an analysis of layered viscoelastic system needs to be performed. An analytical method of temperature-deflection corrections introduced later requires forward deflection calculations of a given pavement system subjected to FWD loading at different temperatures. An analysis of a viscoelastic system usually requires and utilizes the solutions to the corresponding elastic system based on an elastic-viscoelastic correspondence relationship. Therefore, for an analysis of a viscoelastic multi-layered system (typically simulating a flexible pavement system), an adequate understanding of the analysis method of the corresponding elastic multi-layered system is essential.

An in-depth theoretical background and detailed procedure for the analysis of a layered viscoelastic system subjected to a transient surface load at different temperatures is given in Appendix B.

III.3. Laboratory Creep Tests on Field Cores

Information on the thermomechanical properties of the asphalt mixture which was used in constructing the pavement section under consideration is essential in analytical correction of moduli or deflections. This information may be obtained from different sources and test methods. Laboratory mechanical tests on field cores or lab-fabricated specimens can be carried out to obtain this information. A field core retrieved from three test sites (each representing east, central, and west region of the state) was tested to obtain creep curves at different temperatures, from which the master creep curve and the time-temperature shift factor of the mixture was obtained.

A 100-mm (4-inch) diameter AC core was retrieved from each of the three test sites; New Hanover (eastern), Durham (central), and Wilkes (western). These cores were subjected to laboratory creep tests at different temperatures in order to determine the creep compliance of the mixture as a function of time and temperature. These pavements are full-depth AC pavements and the thicknesses of the AC layers are 305 (New Hanover), 254 (Durham), and 242 mm (Wilkes), respectively. The creep compliances obtained at different temperatures and the master creep curve at the room temperature of 25 °C are given in Figures III.3.1(a)-(c) for each of the three sites considered.

The master curve was generated by overlapping the isothermal curves according to the time-temperature superposition principle. The master creep curves were then converted, based on (III.5), to the master relaxation curves shown in Figure III.3.2. The time-temperature shift factors a_T are given in Figure III.3.3. It can be seen from Figure III.3.2 that the viscoelastic characteristics of mixes at three sites are quite different in

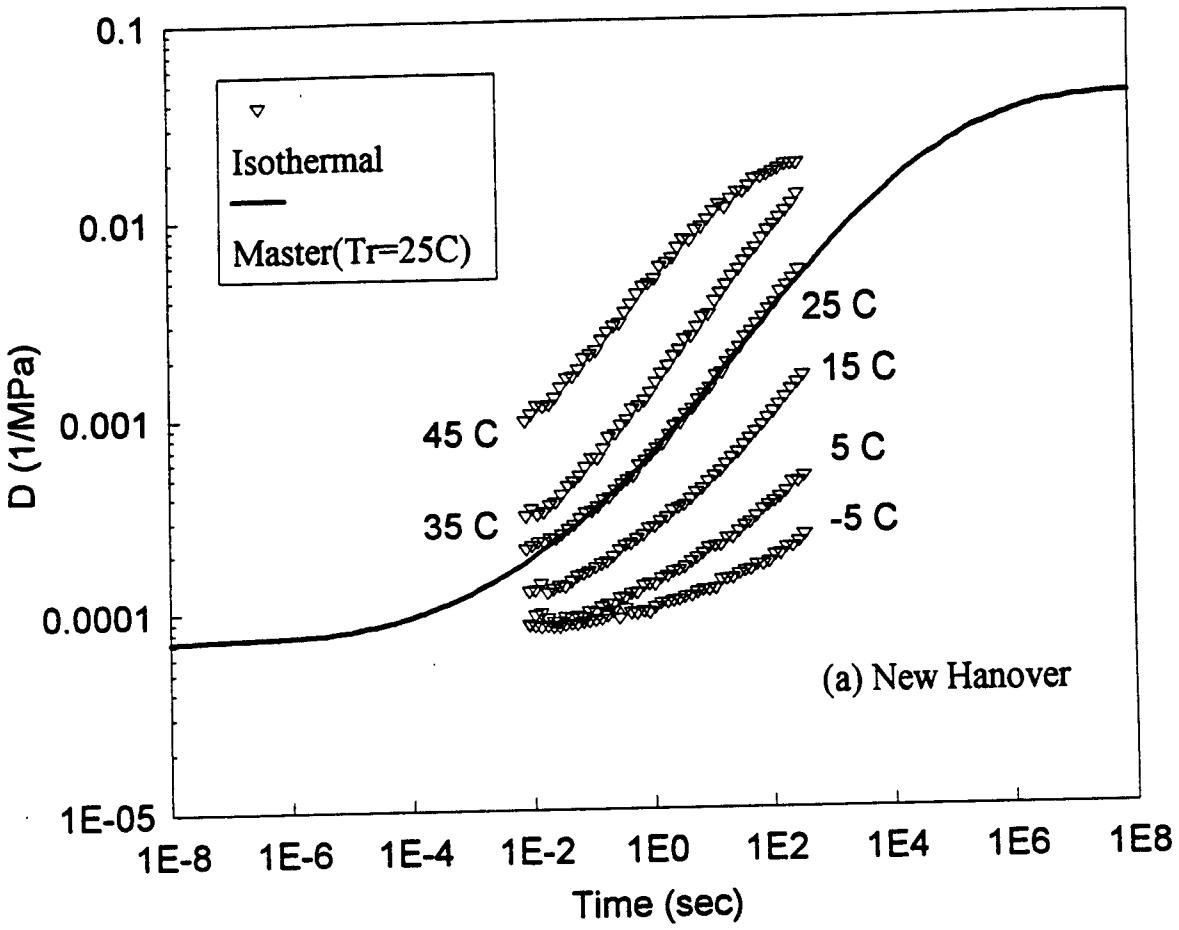

Figure III.3.1. Isothermal and master creep compliances of the asphalt mixtures from three test sites; (a) New Hanover.

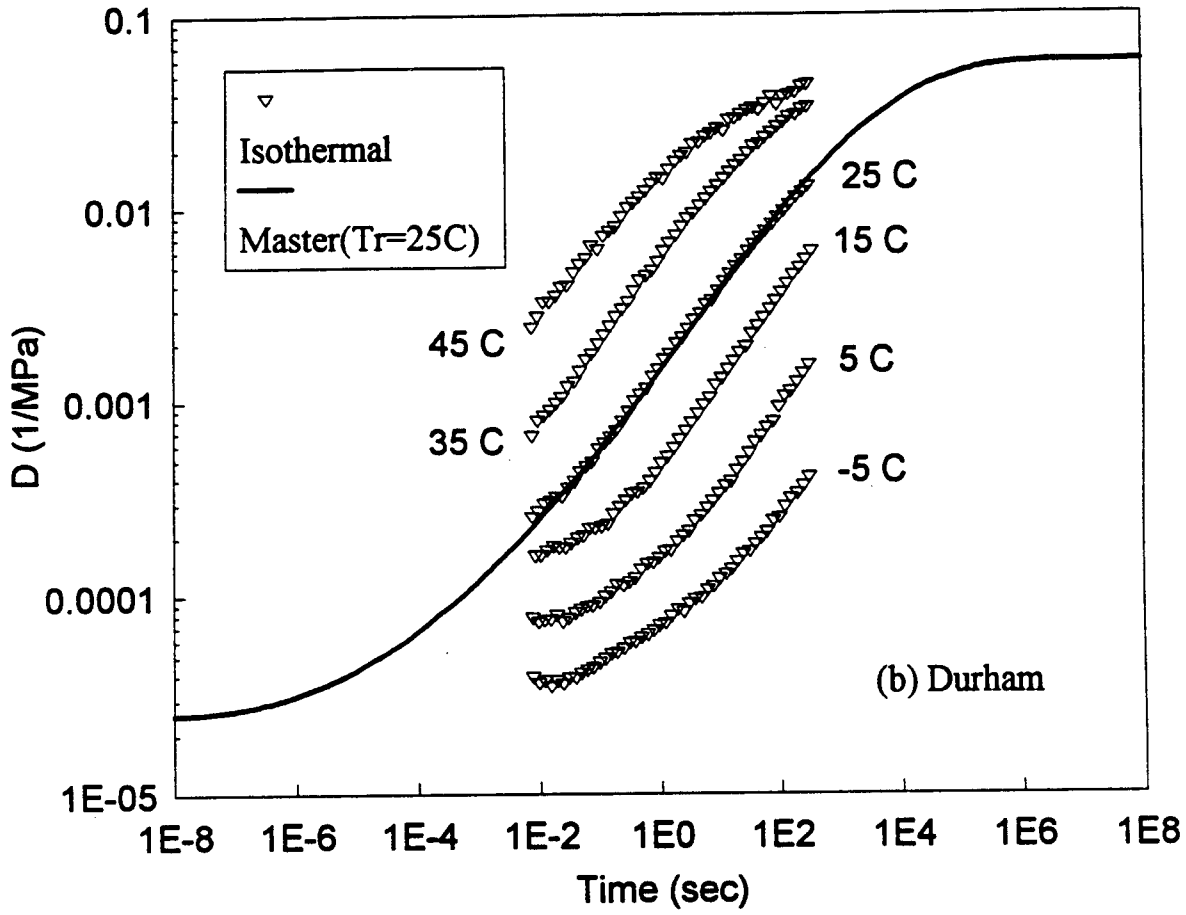

Figure III.3.1. (Continued); (b) Durham.

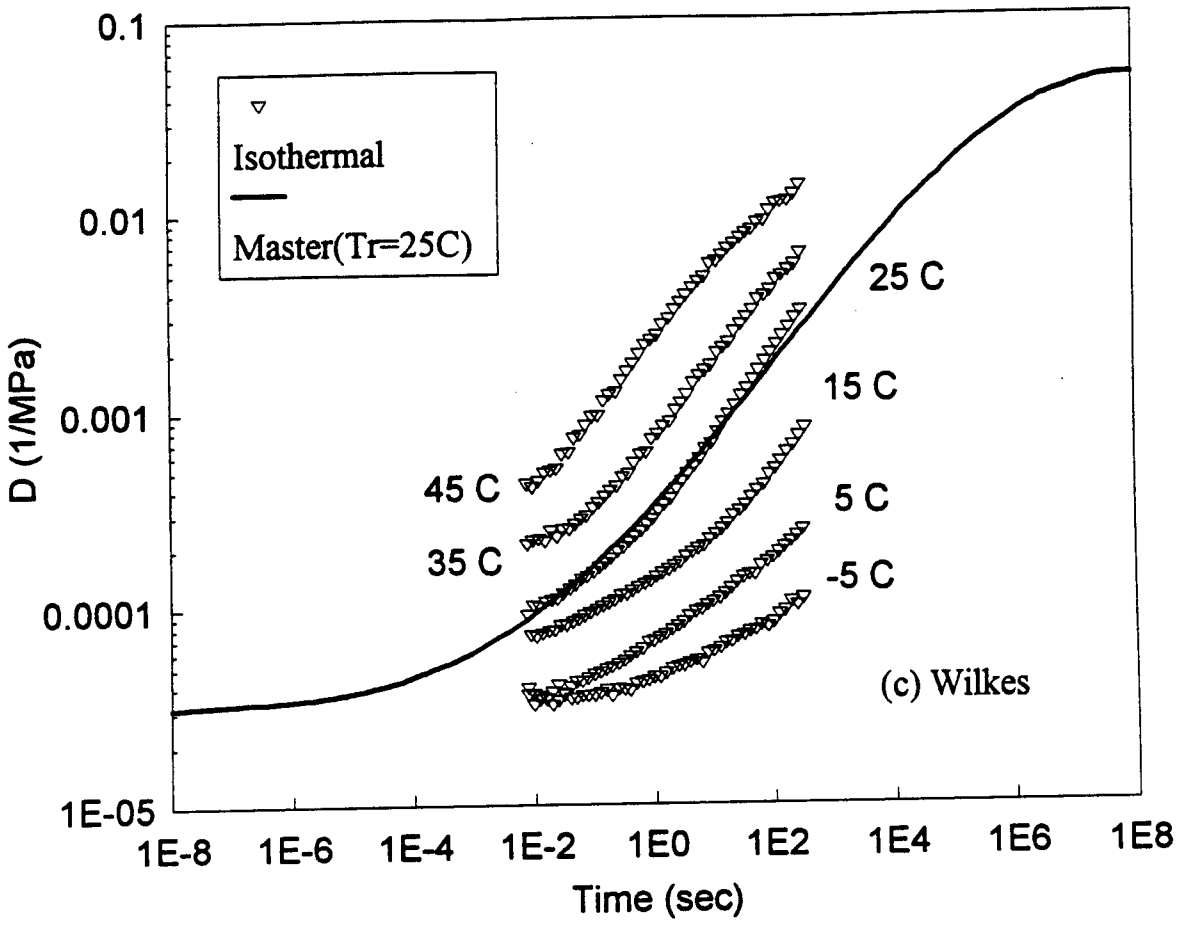

Figure III.3.1. (Continued); (c) Wilkes.

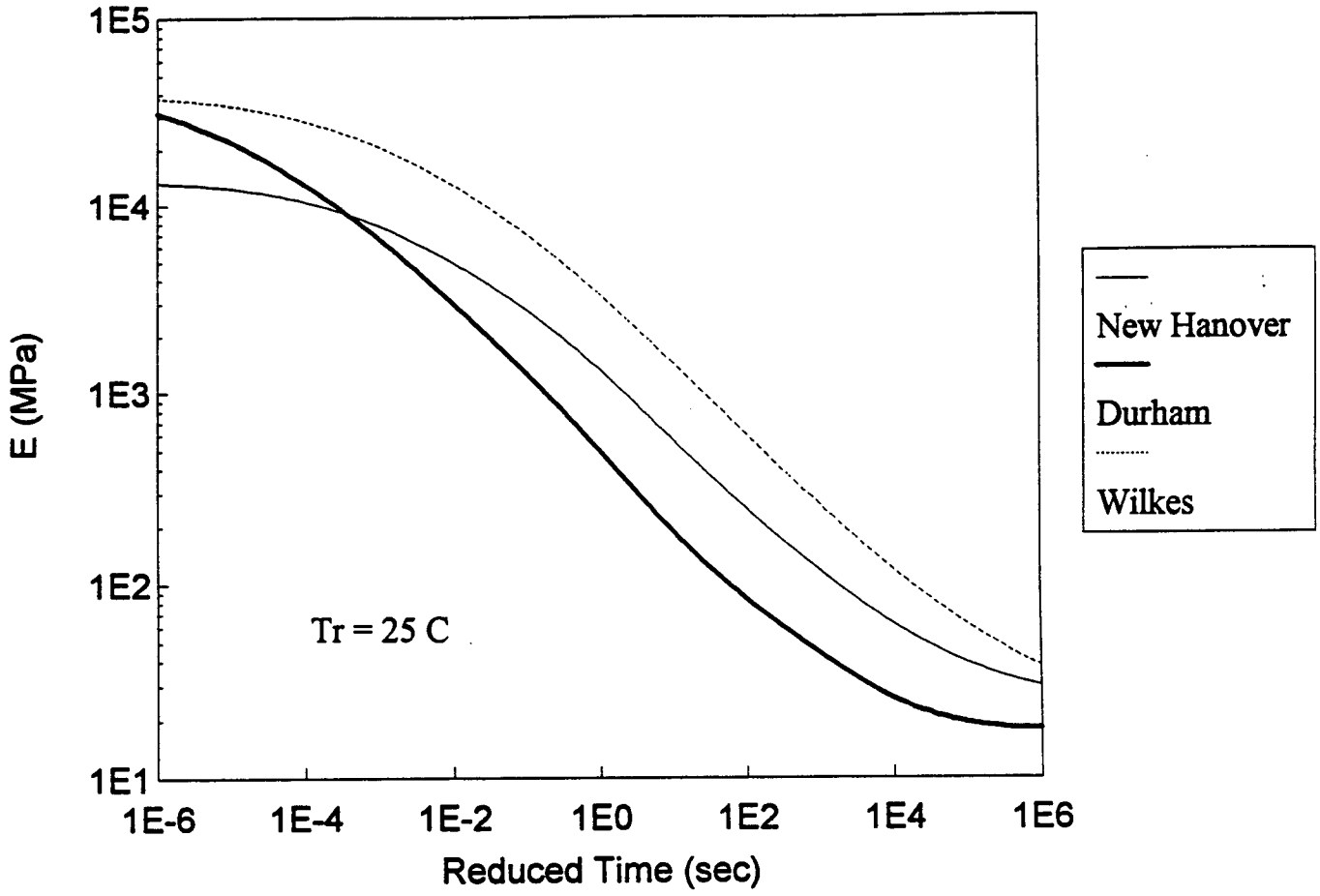

Figure III.3.2. Master relaxation moduli
of the asphalt mixtures from three test sites.

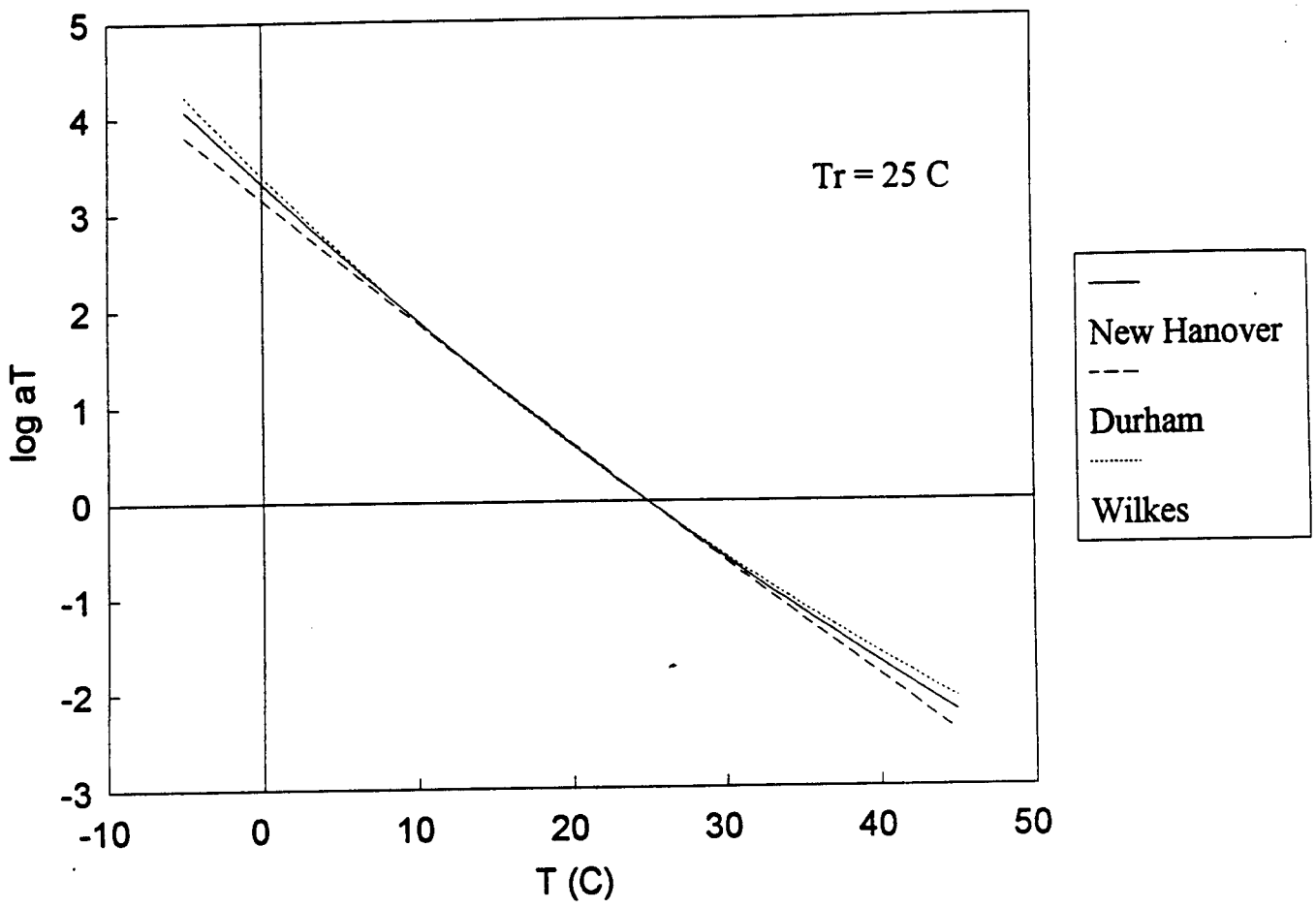

Figure III.3.3. Time-temperature shift factors of the asphalt mixtures from three test sites.

magnitude and time-dependency. The mix from Wilkes site exhibits greater moduli values while that from Durham site shows higher viscoelasticity (or time-dependency).

The shift factors of all three mixes exhibit roughly a descending linear relationship with the mix temperature on the semi-log scale (Figure III.3.3). It is believed that shift factor is primarily dependent upon rheological characteristics of the asphalt binder used whereas the relaxation modulus is affected both by binder properties and mixture properties (e.g., asphalt content). Therefore, the mix-to-mix variation in modulus is expected to be greater than that of shift factor because variation of the mixture properties is more significant than that of the binder properties in a typical case.

An analytical expression of the relaxation function may be obtained by fitting an appropriate mathematical representation, such as the one given below (often referred to as the *Prony series* representation), to the known relaxation data:

$$E(t) = E_{\infty} + \sum_{i=1}^{N} E_i e^{-t/\rho_i} \qquad \text{(III.12)}$$

where E_∞, E_i, and ρ_i are all constants. The quantity E_∞ in (III.12) is the long-time equilibrium modulus, and ρ_i are the relaxation times. Different versions of power-law representations are often used to describe the relaxation or creep behavior of many polymeric materials including asphalt binders and asphalt mixtures. However, even though the power-law representations have many advantages associated with their simplicity, in some cases they fail to adequately describe the creep or relaxation curves over a long range (or many decades) of time. Also in some computational procedures, using the Prony series representation is more efficient than using a power-law representation.

III.4. Temperature Correction of Backcalculated AC Moduli

III.4.1. General

To find the modulus corrected to a reference temperature (20°C is adopted in this study), the modulus backcalculated from a deflection basin is normally multiplied by a factor, i.e.,

$$E_{T_0} = \lambda_E E_T \tag{III.13}$$

where E_{T0} is the modulus corrected to temperature T_0, and E_T is the backcalculated modulus of the asphalt mixture at temperature T. Therefore, the temperature-modulus correction factor λ_E can be defined by

$$\lambda_E = \frac{E_{T_0}}{E_T}. \tag{III.14}$$

In order to find the characteristics of the temperature-dependence of AC modulus, the modulus is plotted against the AC effective temperature (temperature at the mid-depth of the AC layer) on the semi-log scale as shown in Figures III.4.1(a)-(d). Figures III.4.1(a), (b), and (c) show the AC moduli backcalculated from FWD deflection basins measured within the east, central, and west regions of North Carolina, respectively. Three different sites were selected in east and west regions, and five different sites are considered for central region. Four of the central region sites are the ones used in the 92/93 project of which data are all incorporated in the current study. FWD deflection basins under the 9 kip load were used. Modulus data from all three regions are combined and shown in Figure III.4.1(d). The moduli and temperature data used in Figures III.4.1(a)-(d) are given in Appendix C.

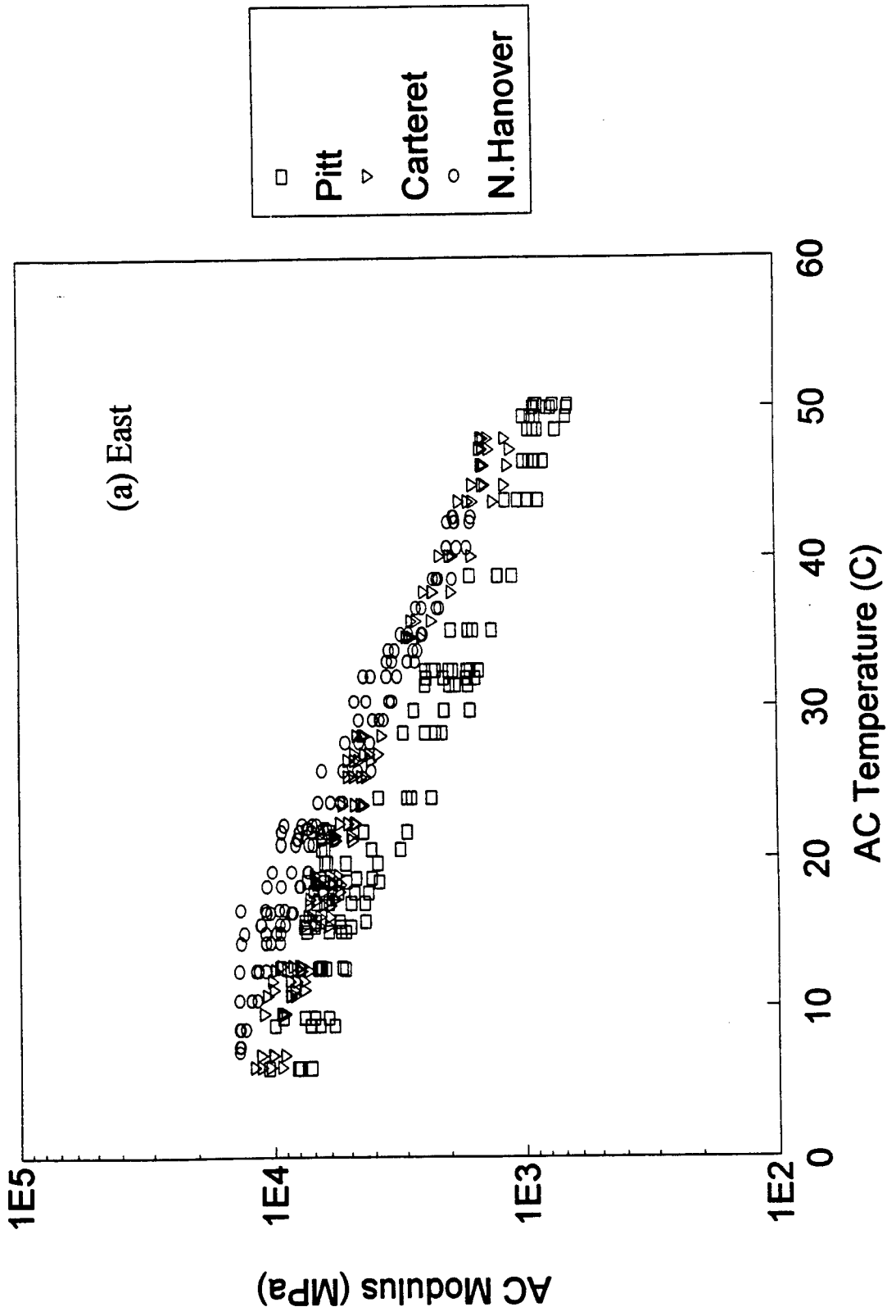

Figure III.4.1. Variation of backcalculated AC modulus with temperature; (a) east region.

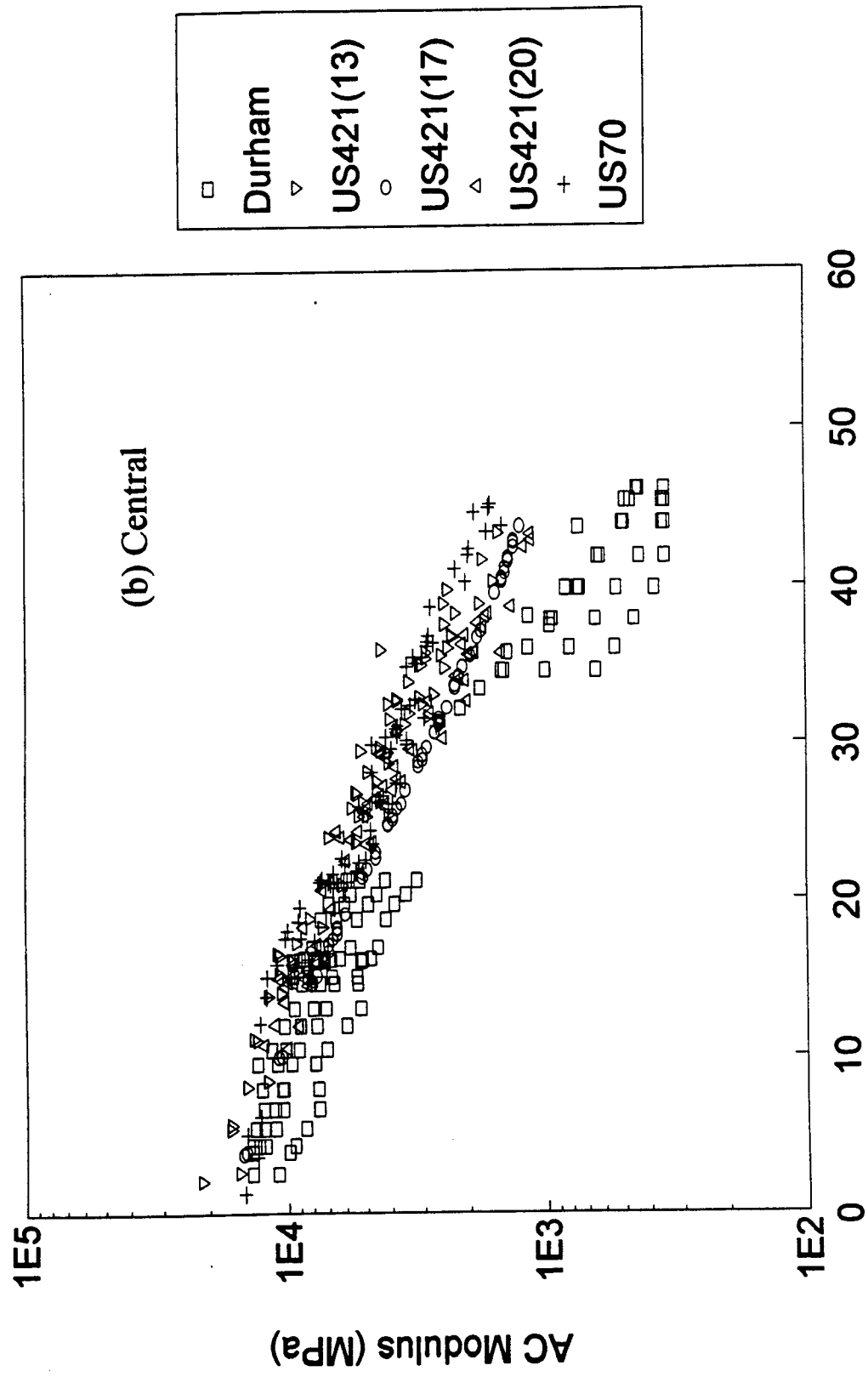

Figure III.4.1. (Continued); (b) central region.

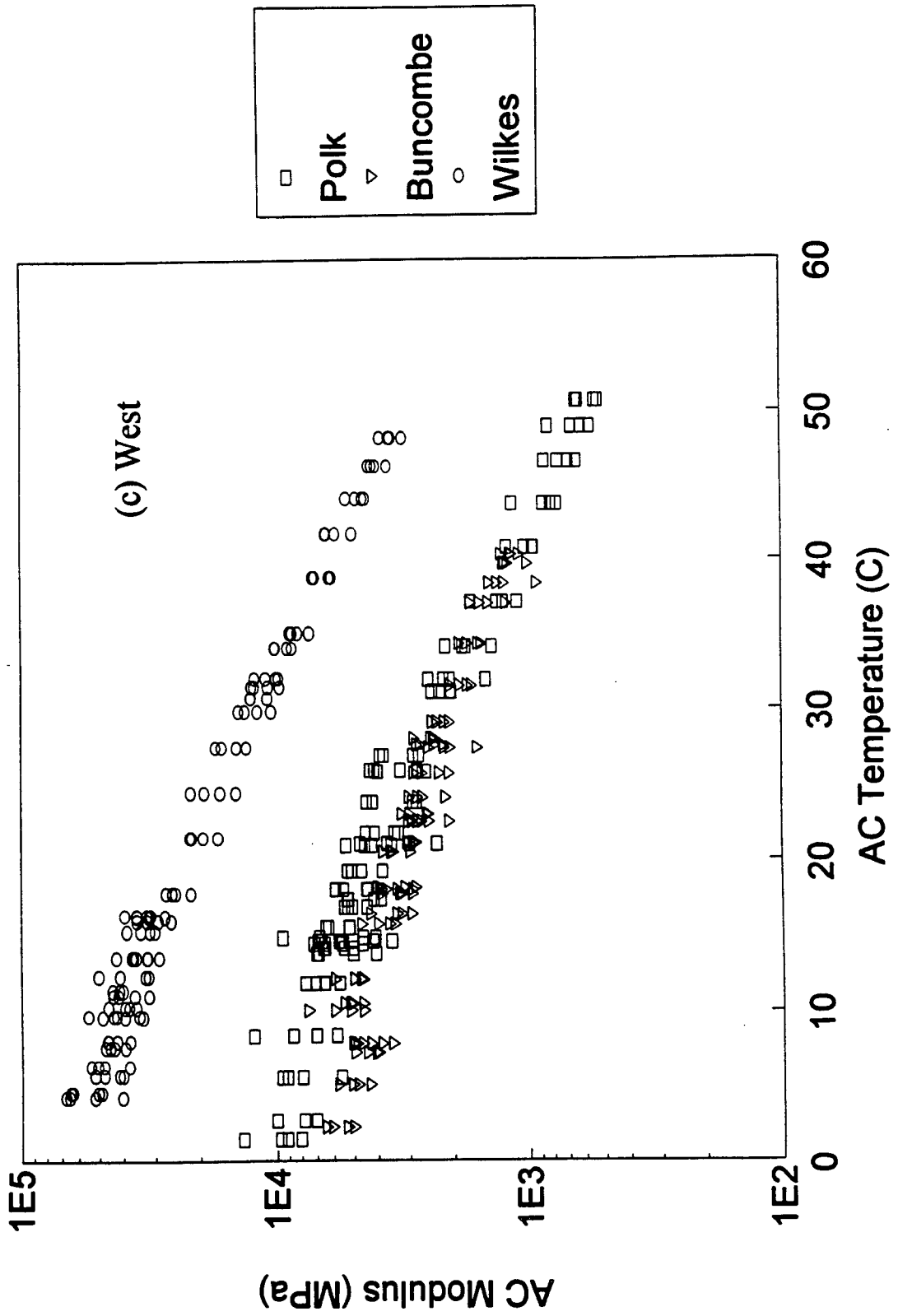

Figure III.4.1. (Continued); (c) west region.

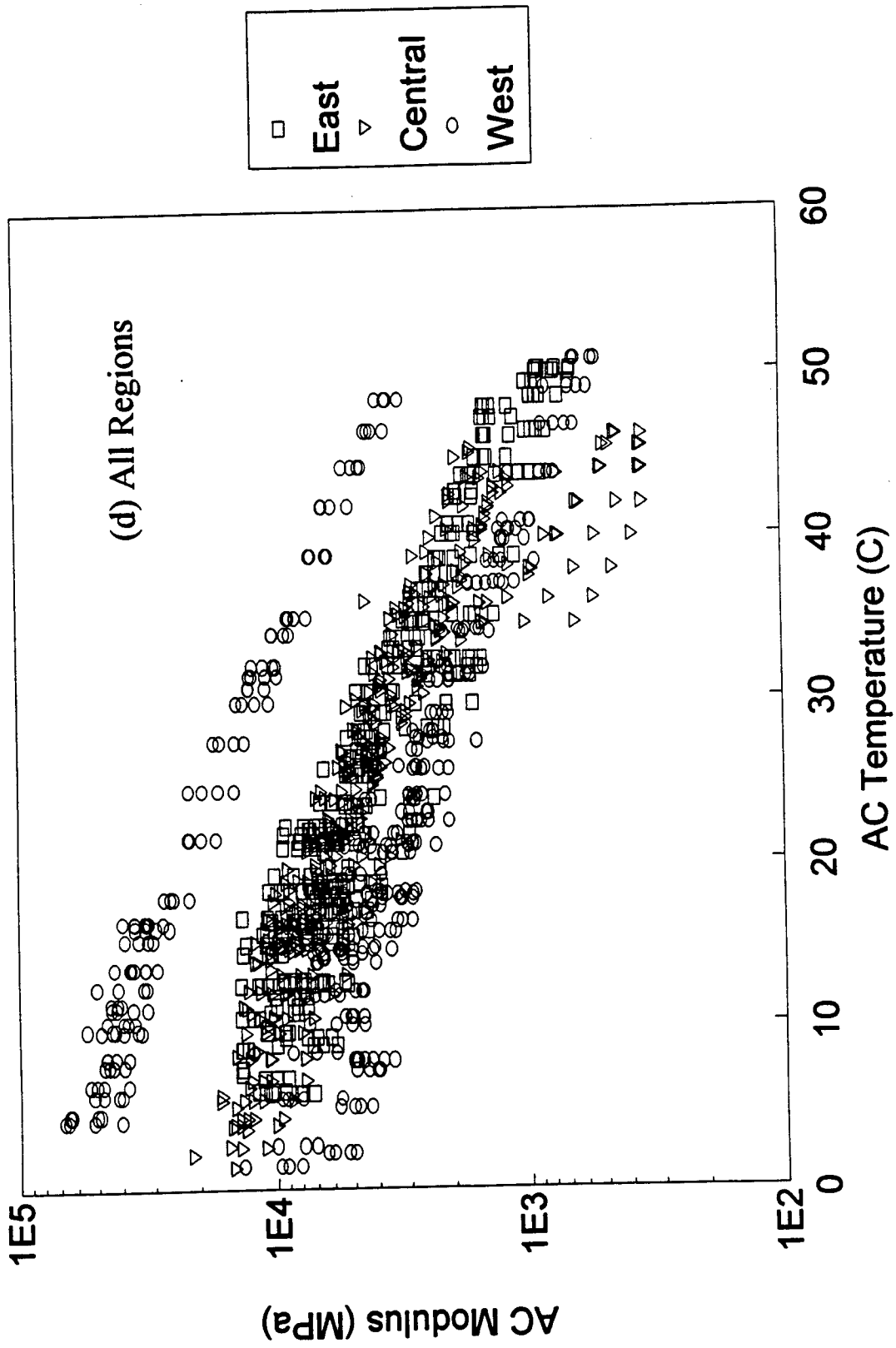

Figure III.4.1. (Continued); (d) all regions.

Overall, the trend can be characterized by a descending linear relationship between the log modulus (E) and the temperature. The degree of the temperature-dependence, which can be indicated by the slope of the straight line, varies from site to site (or, more specifically, mixture to mixture). Figure III.4.2 shows a typical linear fit and the slope (m-value) between log E and T measured at Pitt county site. The slopes of the linear fit of log E versus T relationship, denoted by m's, were computed for each site, region, and for the entire state, and are given in Table III.4.2.

When one idealizes the modulus-temperature relationship by a linear relationship between log E and T, it can be shown that the correction factor defined by (III.14) can be expressed directly in terms of the slope, m. Let us take the following linear form of log E versus T relationship:

$$\log E = a - mT \qquad \text{(III.15)}$$

where a is the intercept of the log E axis and $-m$ is the slope in the log E versus T plot. Rewriting (III.15),

$$E = 10^{a-mT}. \qquad \text{(III.16)}$$

Substituting (III.16) into (III.14), one finally obtains the correction factor in terms of m as follows:

$$\lambda_E = 10^{m(T-T_0)}. \qquad \text{(III.17)}$$

No particular correlation was found to exist between the m-values and the AC layer thicknesses (Figure III.4.3), which can be expected because m-values are material-dependent factors and should not be affected by the layer geometry of the pavement system under consideration.

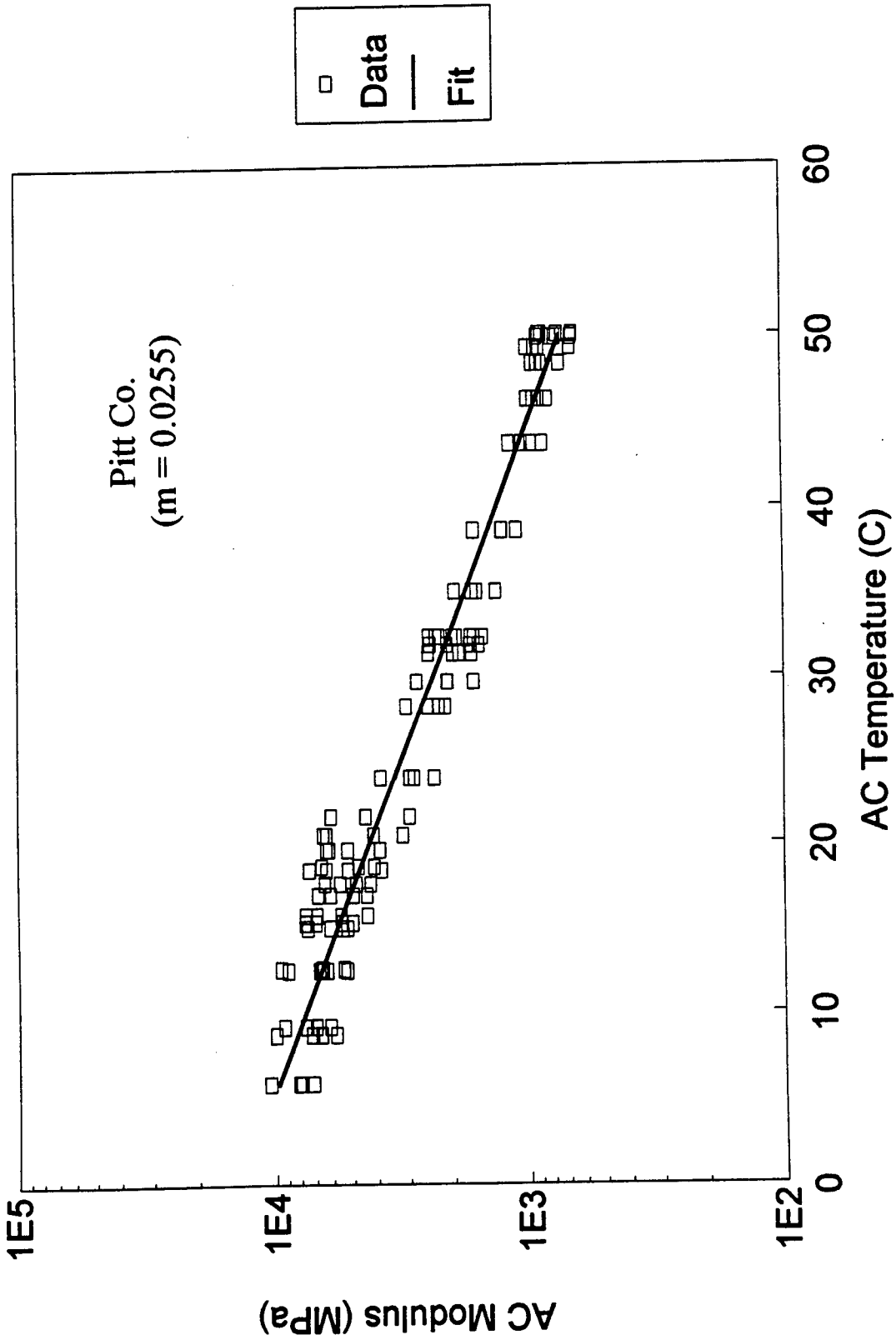

Figure III.4.2. A typical linear regression and the negative slope (m-value) of the linear fit of log E versus T data (on Pitt site).

Table III.4.2 The negative slope (m-value) of the linear fit of log E versus T for each site, region, and the state

Sites (AC Thickness, mm)	m - values	Regions	m - values	Statewide m - value	92/93Model m - value
Pitt (115)	0.0255	East	0.0251	0.0262	0.0275
Carteret (229)	0.0224				
New Hanover (305)	0.0273				
Durham (254)	0.0374	Central	0.0297		
US421-13 (191)	0.0265				
US421-17 (89)	0.0280				
US421-20 (229)	0.0320				
US70 (140)	0.0244				
Polk (166)	0.0258	West	0.0237		
Buncombe (203)	0.0183				
Wilkes (242)	0.0271				

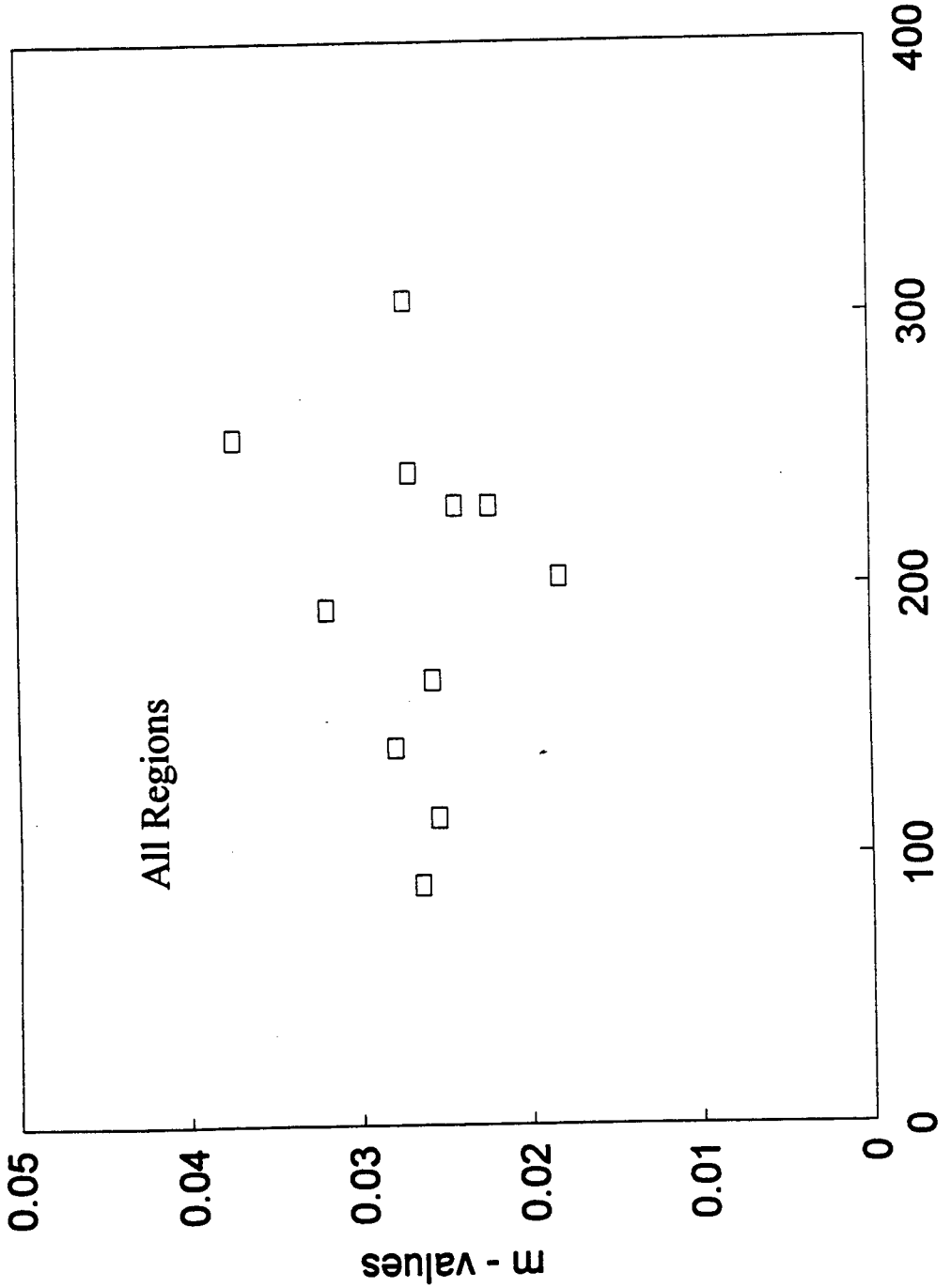

Figure III.4.3. The negative slope (m-values) of the linear fit of log E versus T data for all regions.

Several methods have been proposed for correction of backcalculated AC moduli to a reference temperature. Johnson and Baus (1992) recommended the following formula which is based on Lytton et al. (1990) who took an approximation from the Asphalt Institute (1982):

$$\lambda_E = 10^{-0.0002175(70^{1.886} - T^{1.886})} \qquad \text{(III.18)}$$

where T are in °F. Ullidtz (1987) developed a model based on backcalculated moduli from the AASHO Road Test deflection data. His correction model is given by

$$\lambda_E = \frac{1}{3.177 - 1.673 \log T} \qquad \text{(III.19)}$$

for T >1 °C. Baltzer and Jansen (1994) developed a correction model based on statistical analysis of backcalculated moduli and measured AC temperatures in the form of (III.17) with a reference temperature of 20°C. They proposed that m = 0.018 be used with the temperature at the one-third depth of AC layer selected as the effective AC temperature.

III.4.2. 92/93 Model - The Empirical Modulus-Correction Model Developed from the 92/93 Study

Kim et al. (1995, 1995a) developed a correction model that takes the form of (III.17) based on statistical analysis of backcalculated moduli and AC temperatures measured from the central region of North Carolina. They found that with m = 0.0275 the model best fits to the field data. Overall, the m-values for the central-region sites are greater than those for the east and west region sites, which indicates that the mixtures used in construction of pavements in the central region possess greater viscosity and are more susceptible to temperature changes.

The backcalculated moduli presented in Figures III.4.1(a)-(d) are corrected using the 92/93 model and are presented in Figures III.4.4(a)-(d), respectively. Overall, the corrections appear to be good except the Durham site within the central region. The moduli for Durham site are undercorrected by the model. This phenomenon is believed to be due to the exceptionally high viscosity of the mixture used in Durham site. Based on these observations, the model has been improved by considering the following approaches: (III.1) regionalize the model; i.e., find an m-value for use within each of the three regions of the state, (III.2) find a representative m-value for statewide use, and (III.3) develop an analytical correction procedure for each mixture type used. These three approaches are described in the next three subsections.

III.4.3. Regional Model - New Empirical Modulus-Correction Models Based on Regional Field Data

Assuming that similar mixture types are used in pavement construction within each region of the state, one can develop a regional empirical model based on the observation of the field data obtained from sites within that particular region. Again, utilizing the linear relationship between log E and T, one can adopt a modulus correction factor of the form (III.17). A proper m-value for each region is already given in Table III.4.2. The empirical models for each region as well as for the entire state in comparison with the 92/93 model are graphically shown in Figures III.4.5(a) and (b) on the semi-log and the linear scale, respectively.

The moduli were corrected according to (III.13) and (III.17) with respective m-value for all three regions and are presented in Figures III.4.6(a)-(d). The quality of

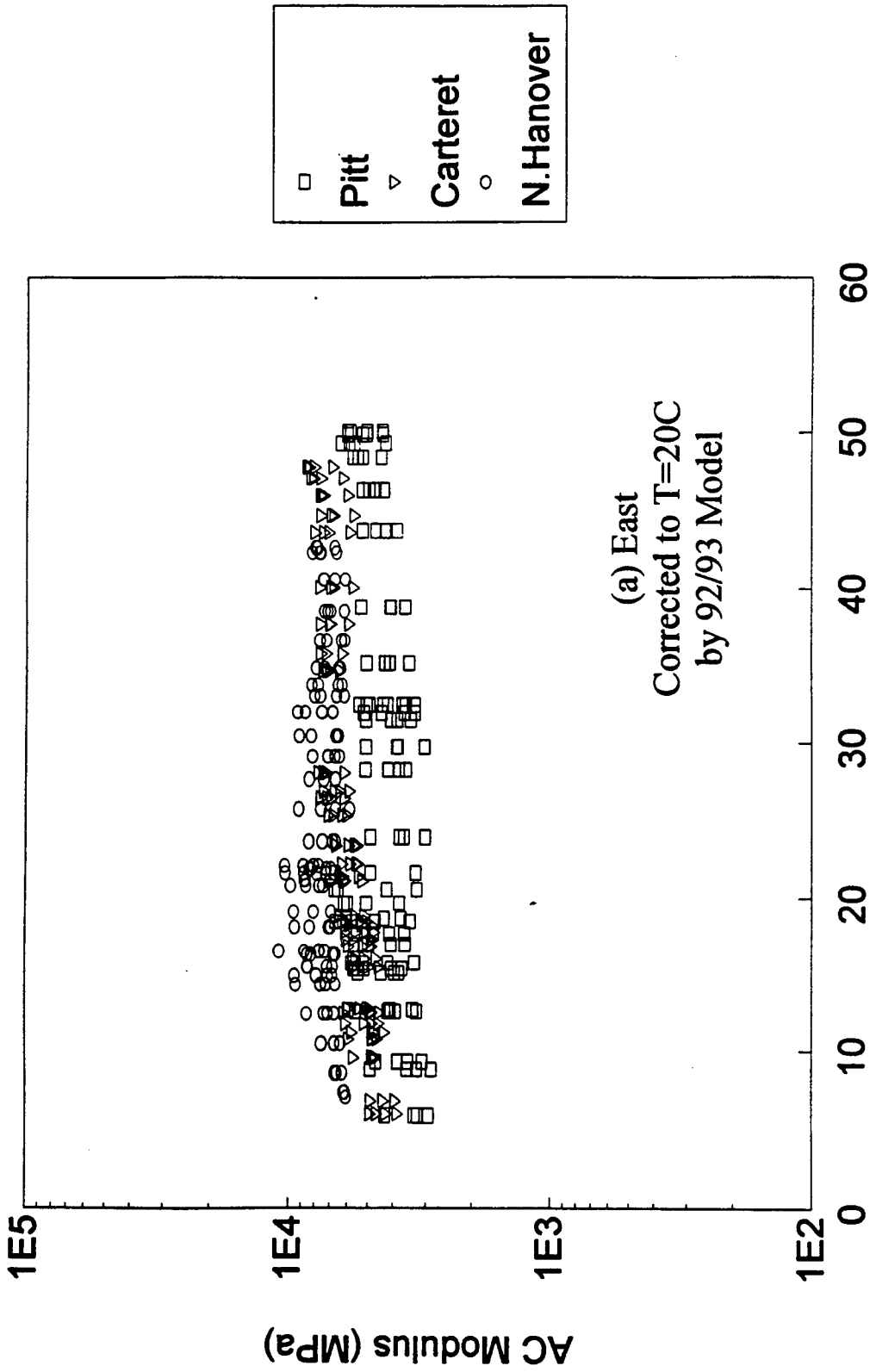

Figure III.4.4. Temperature-corrected AC moduli using the 92/93 empirical model; (a) east region.

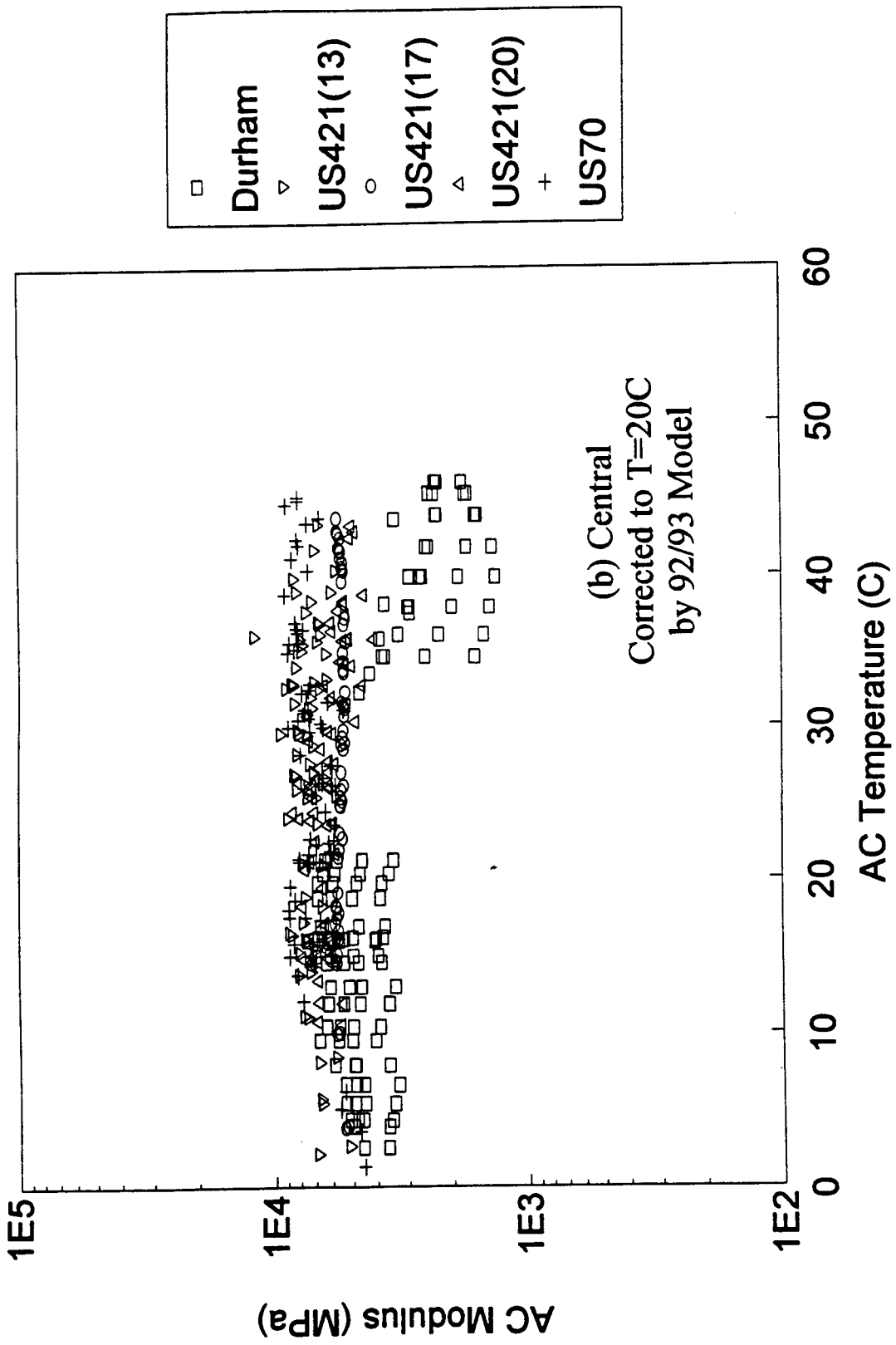

Figure III.4.4. (Continued); (b) central region.

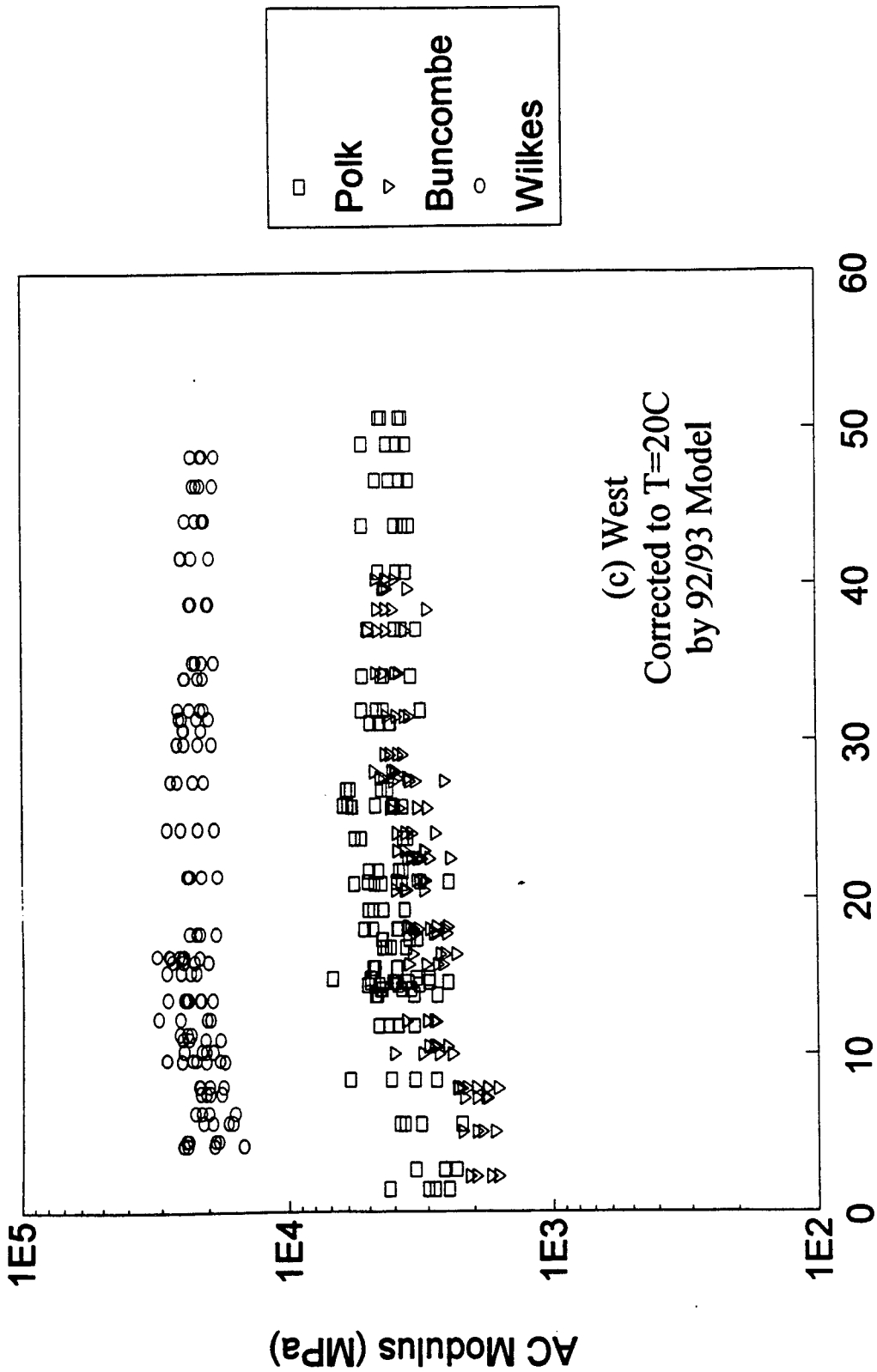

Figure III.4.4. (Continued); (c) west region.

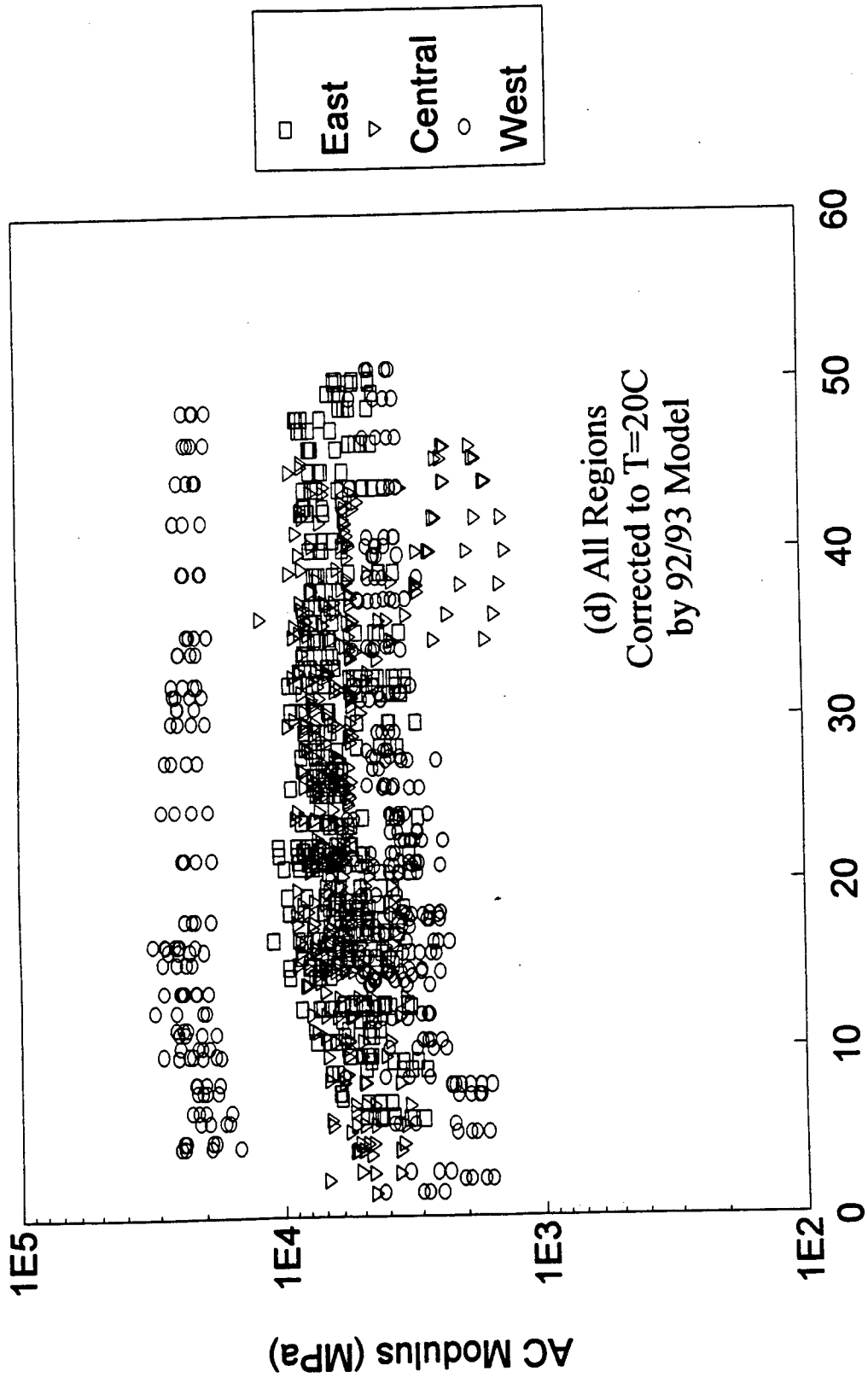

Figure III.4.4. (Continued); (d) all regions.

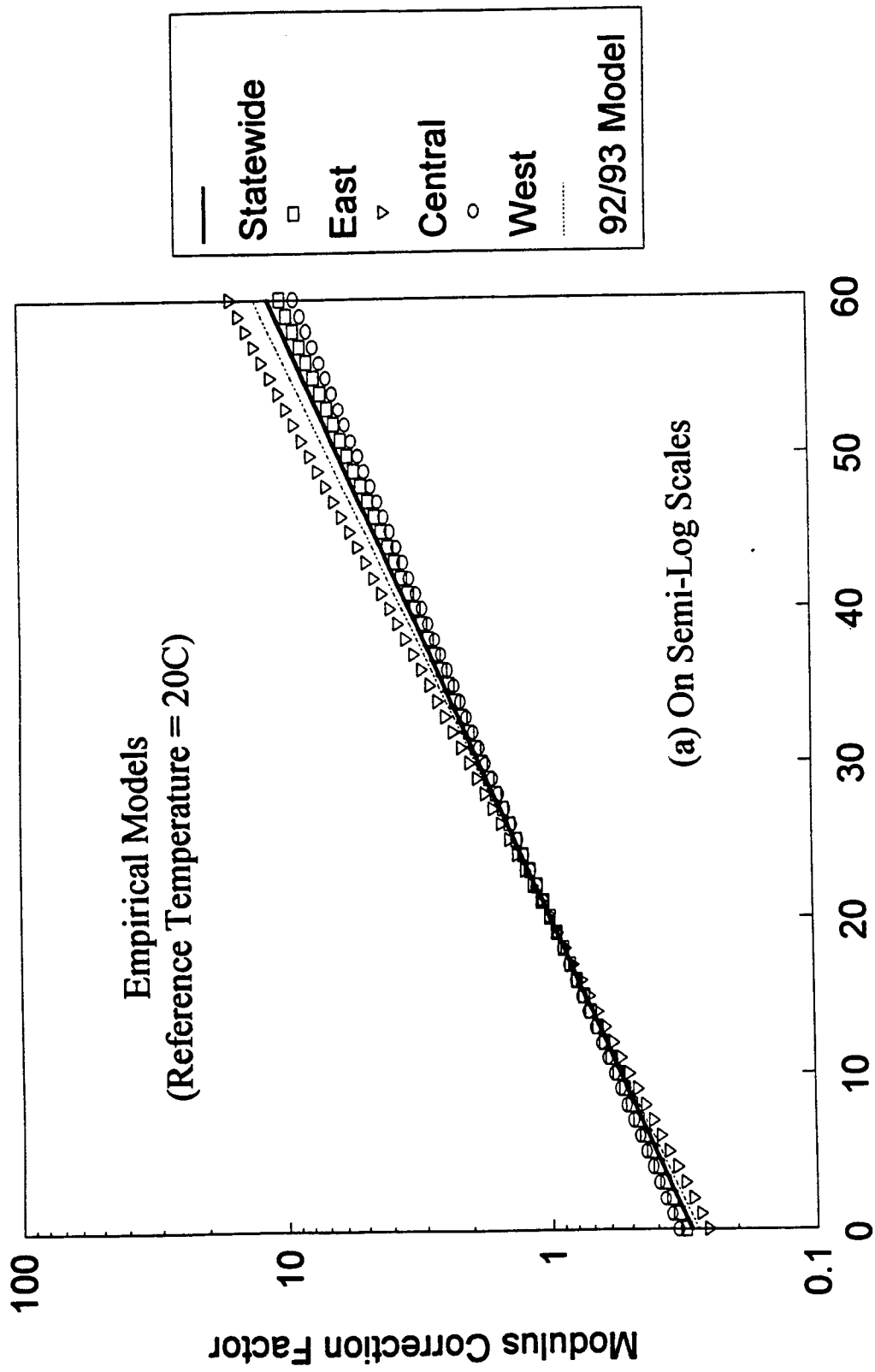

Figure III.4.5. The temperature correction factors for AC moduli from various empirical models; (a) on the semi-log scales.

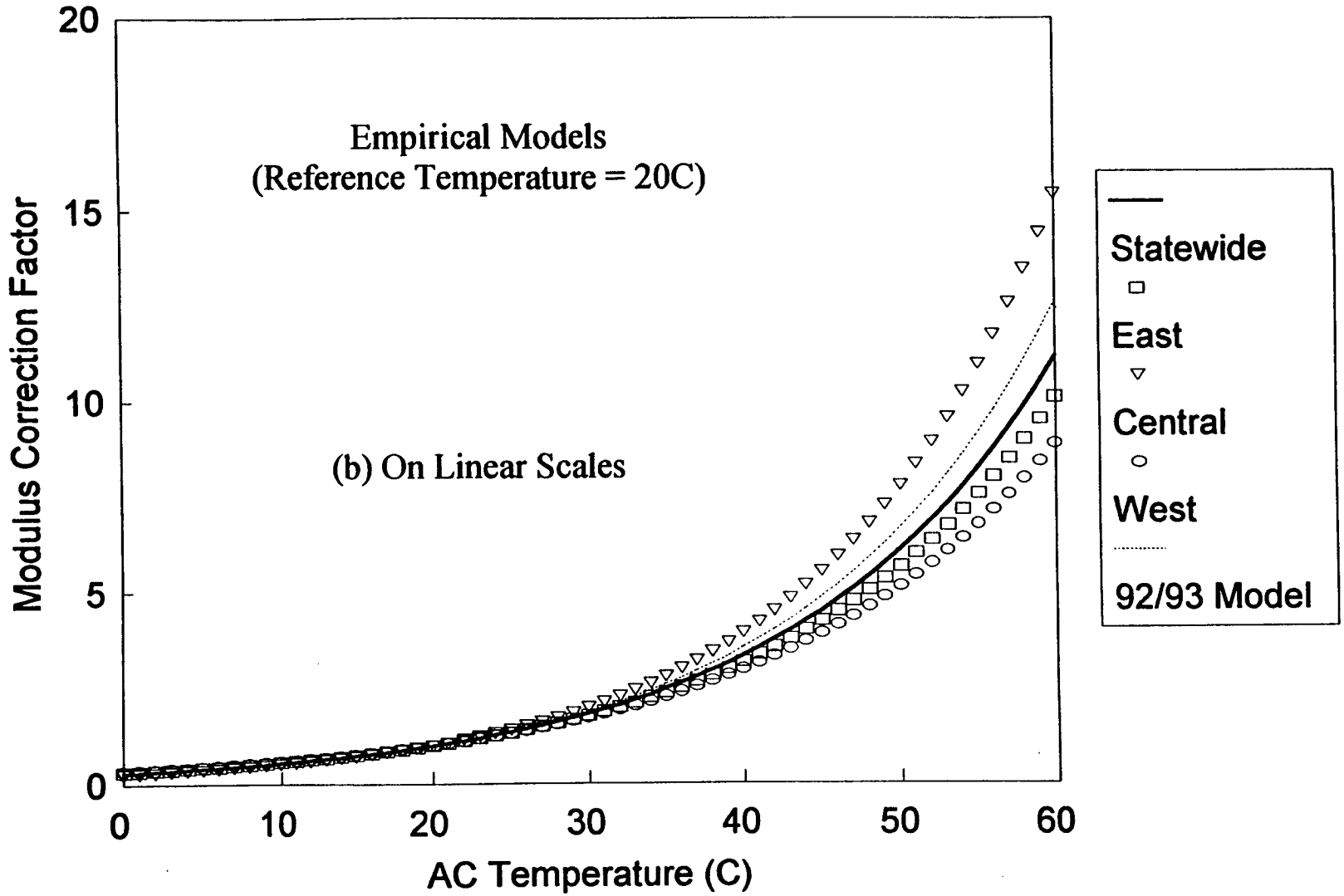

Figure III.4.5. (Continued); (b) on the linear scales.

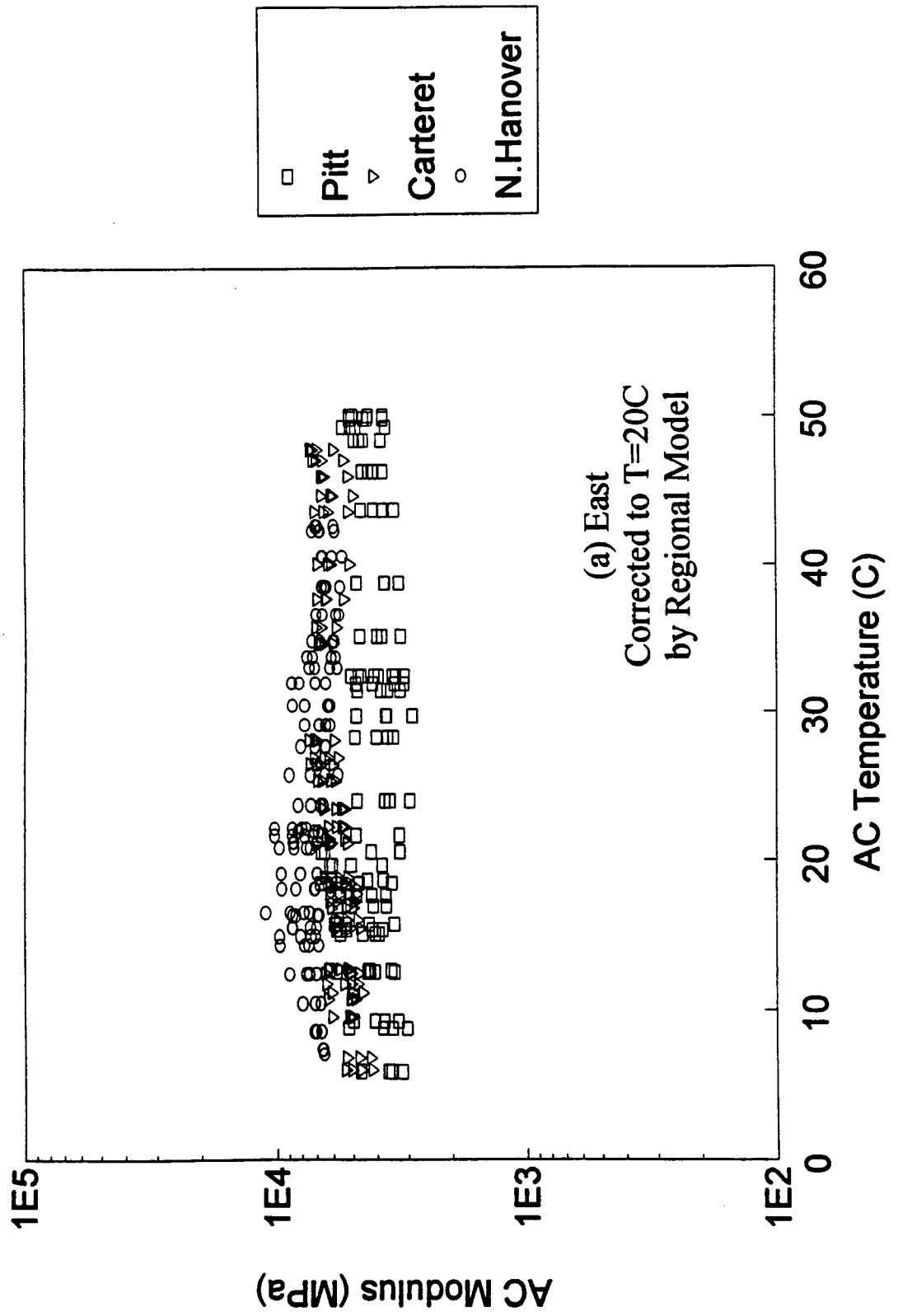

Figure III.4.6. Temperature-corrected AC moduli using the regional empirical models; (a) east region.

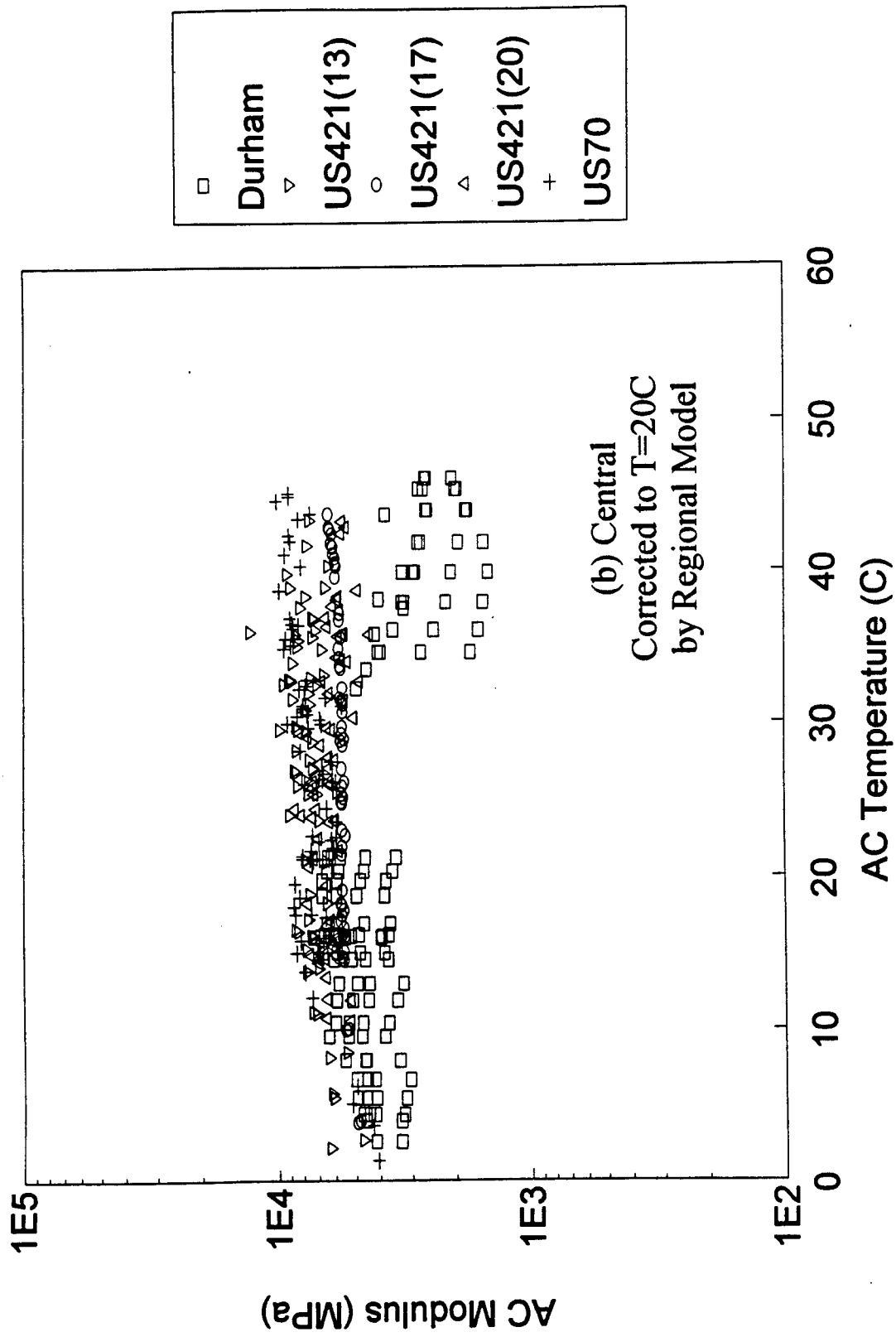

Figure III.4.6. (Continued); (b) central region.

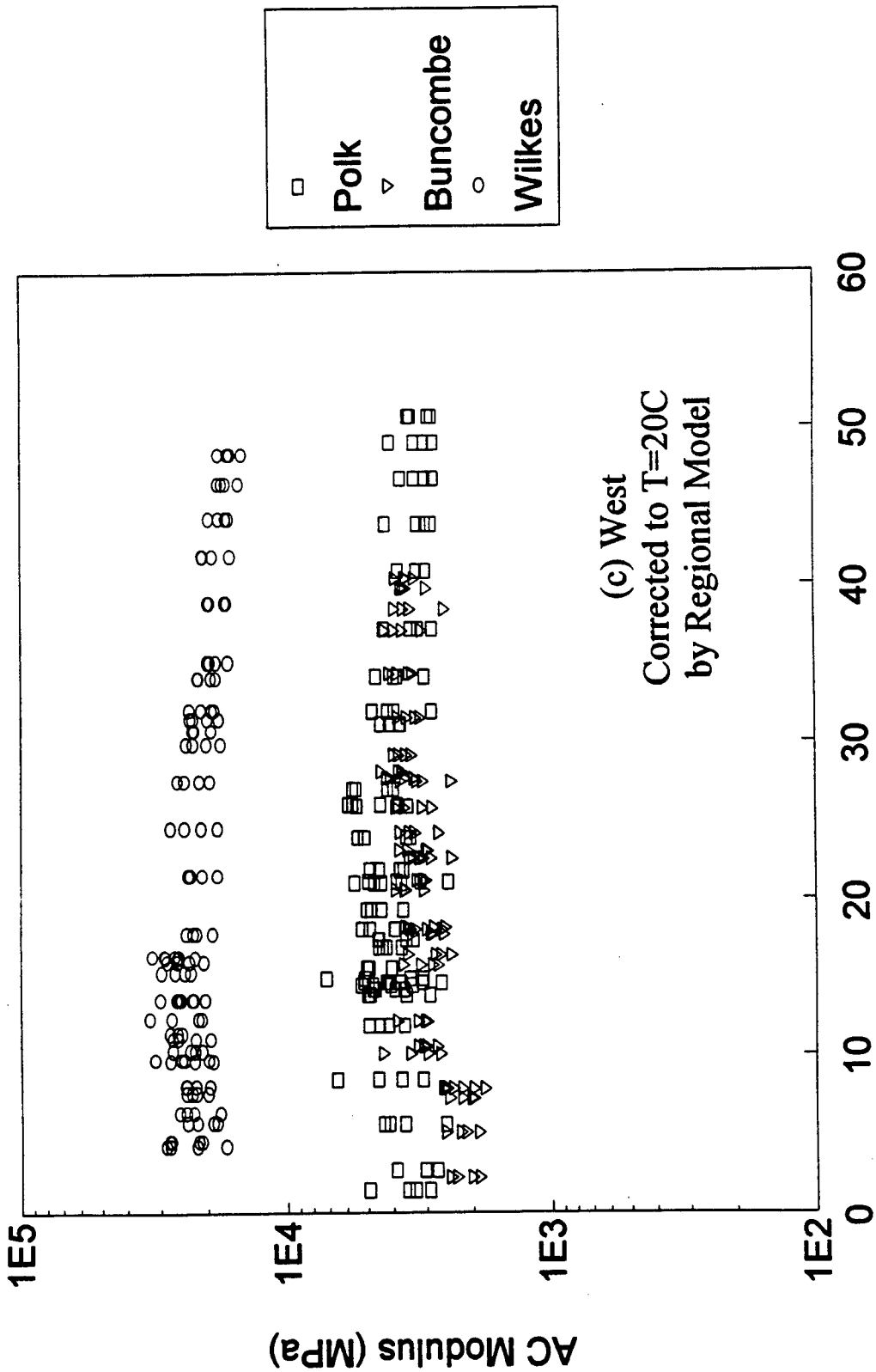

Figure III.4.6. (Continued); (c) west region.

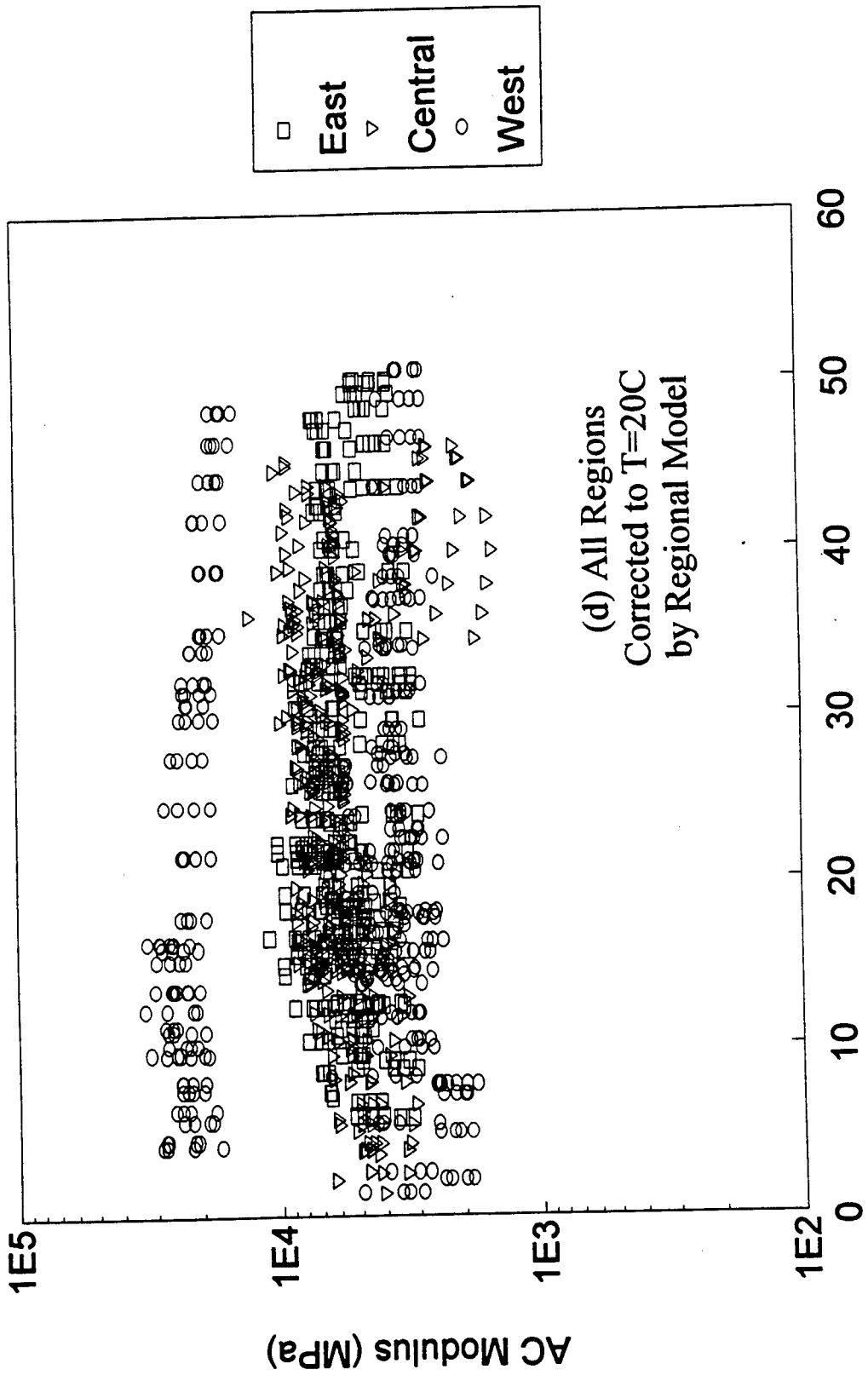

Figure III.4.6. (Continued); (d) all regions.

correction has improved for most of the sites in comparison with the 92/93 model. However, for Durham site, the regional model still falls short of complete correction. It is to be noted that the model for the central region to which Durham site belongs was based on the field data not only from Durham site but also from the four sites of the 92/93 study.

III.4.4. Statewide Model - A New Empirical Modulus-Correction Model Based on Statewide Field Data

A statewide empirical model is obtained based on the same procedure as that used in the 92/93 model and the forgoing regional models, except that a different m-value that can better represent the entire state is used. An m-value of 0.0262 as given in Table III.4.2 is adopted for the statewide model, and the resulting correction factor curve is shown in Figures III.4.5(a) and (b). It can be seen that the new statewide model is quite close to the 92/93 model. The moduli corrected by the new statewide model are given in Figures III.4.7(a)-(d).

III.4.5. Analytical Model - A New Analytical Modulus-Correction Model Based on Individual Mixture Properties

As has been indicated in the previous discussions, the empirical models apply well to most of the pavements as long as the pavement under consideration was constructed using one of the *common* mixtures. In other words, if the pavement to be evaluated is constructed out of mixtures with unusual thermo-mechanical properties, the temperature correction of the backcalculated moduli using an empirical model may not be good enough. However, if one knows the required thermo-mechanical properties of the

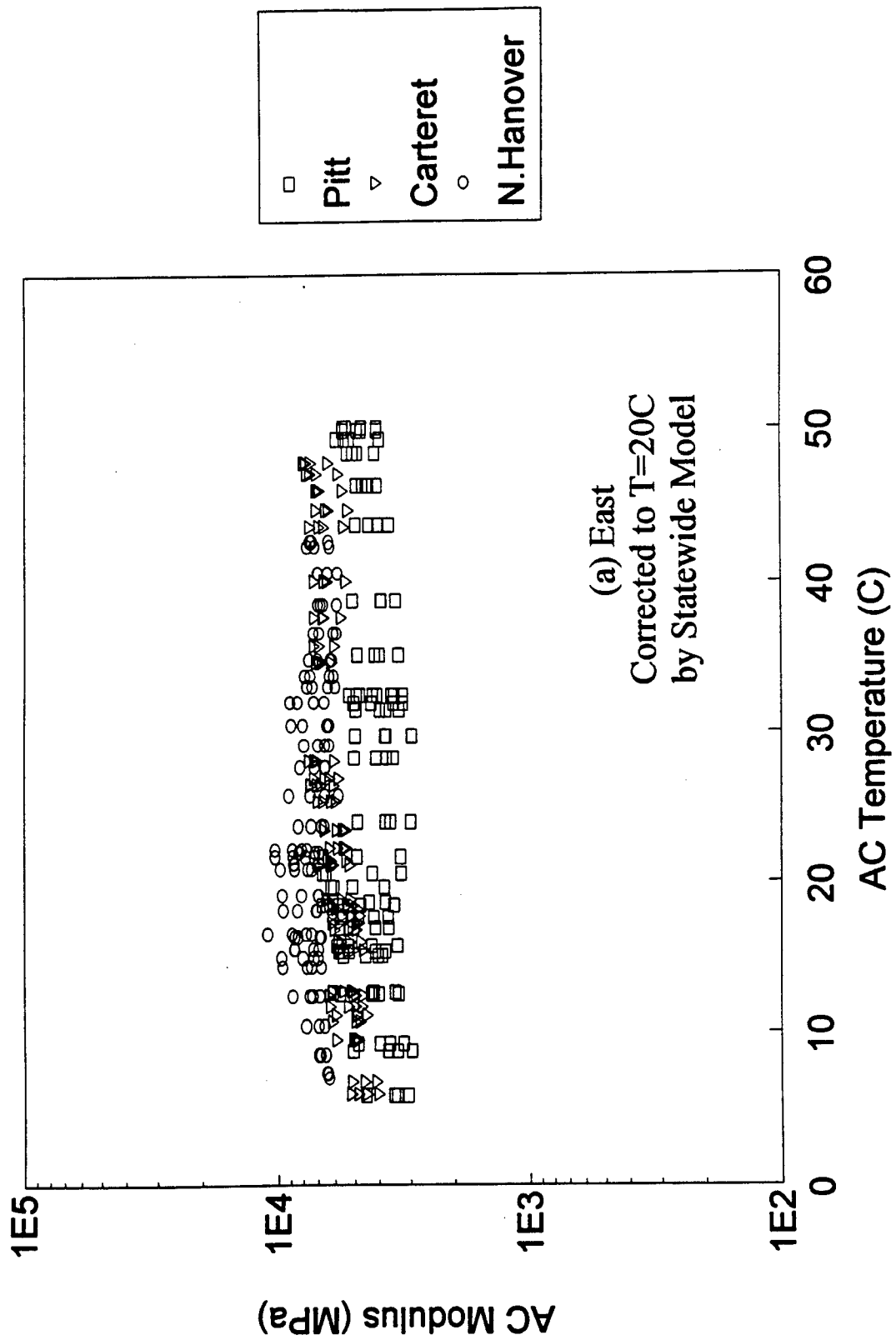

Figure III.4.7. Temperature-corrected AC moduli using the statewide empirical model; (a) east region.

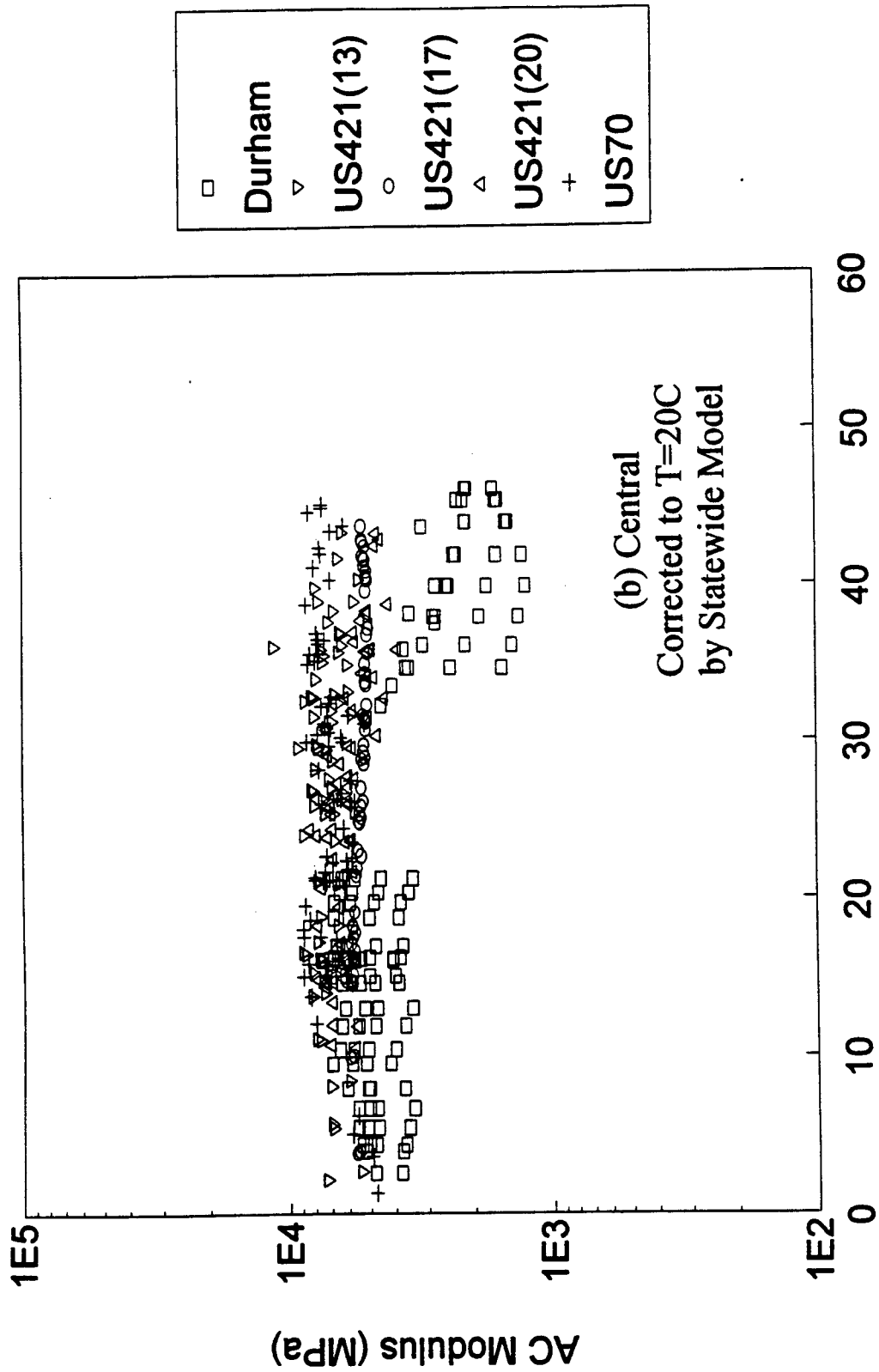

Figure III.4.7. (Continued); (b) central region.

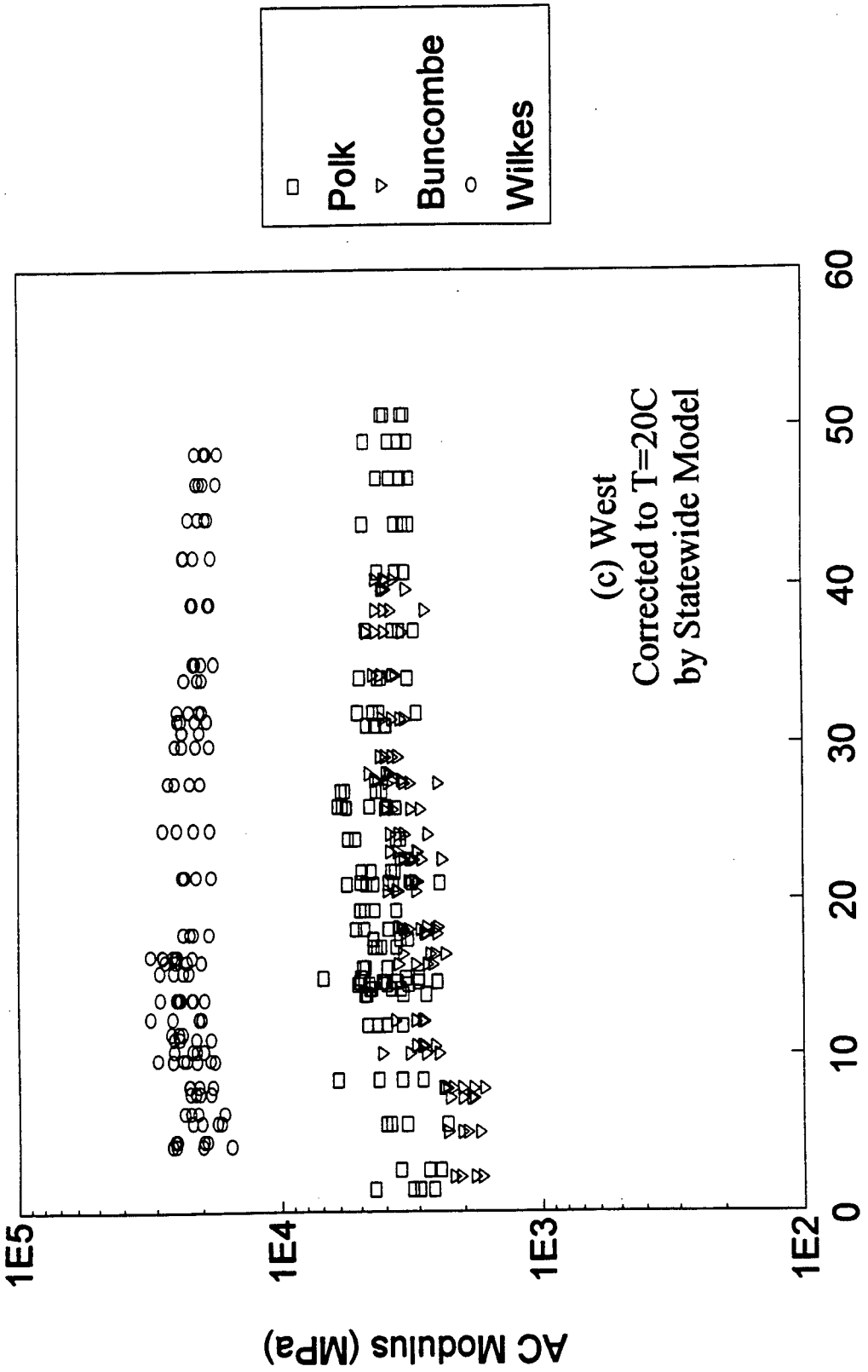

Figure III.4.7. (Continued); (c) west region.

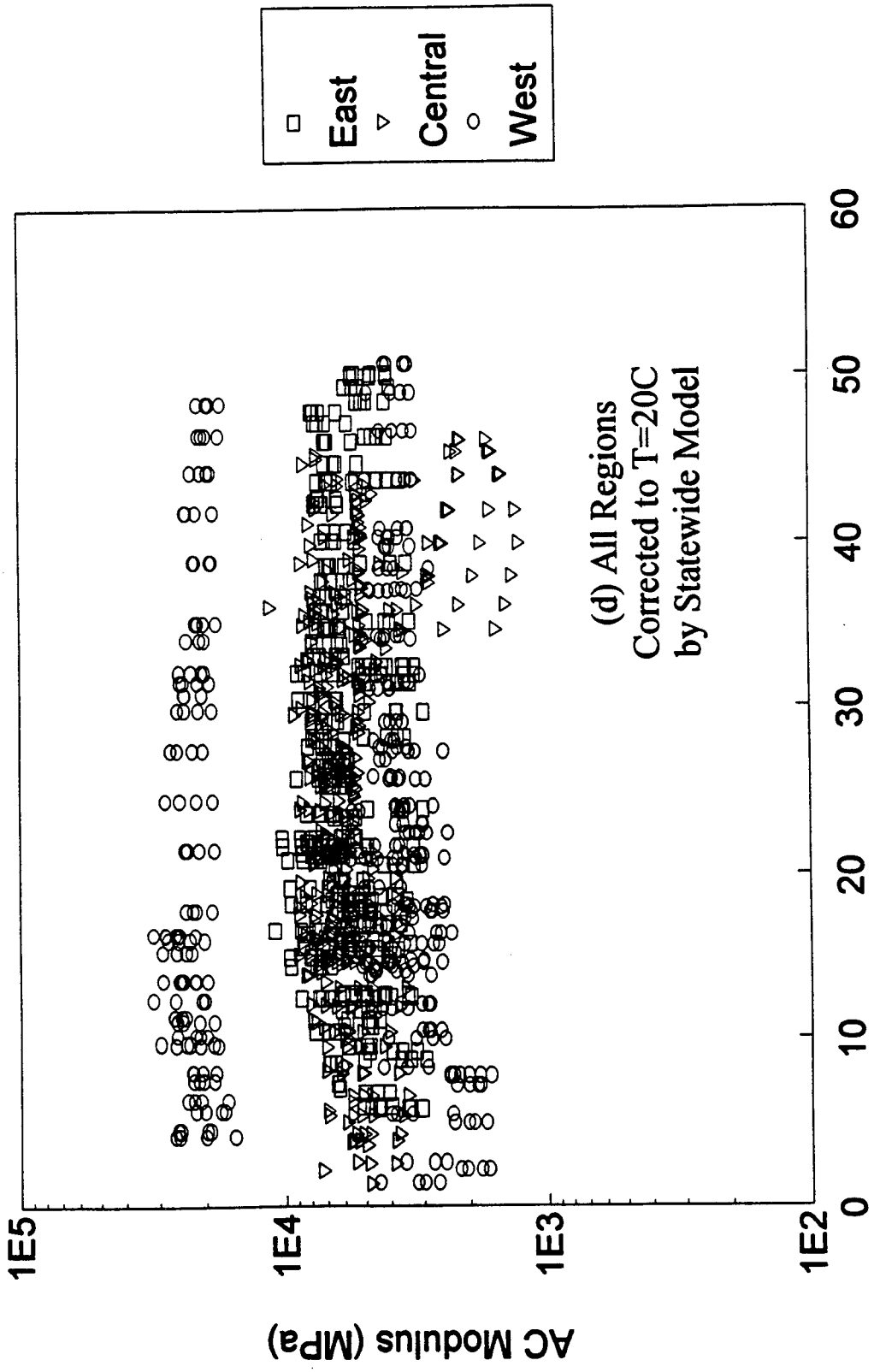

Figure III.4.7. (Continued); (d) all regions.

mixture, he can obtain a correction factor for that mixture type through a theoretical analysis.

When the relaxation modulus E(t) and the time-temperature shift factor $a_T(T)$ for the asphalt mixture under consideration are available (usually through laboratory tests on field cores or lab-fabricated specimens), one can define the theoretical correction factor consistent with (III.14) as follows:

$$\lambda_E = \frac{E(\xi_0)}{E(\xi)} \tag{III.20}$$

where the reduced times ξ_0 and ξ are defined, respectively, by

$$\xi_0 = \frac{t_1}{a_T(T_0)} \quad and \quad \xi = \frac{t_1}{a_T(T)} \tag{III.21}$$

in which t_1 is the loading duration that needs to be determined based on the characteristic of the loading pulse of the NDT equipment used, T_0 is the reference temperature, and T is the temperature under consideration. For most FWD devices, the overall loading pulse resembles the haversine curve with duration of approximately 0.03 second and the peak loading intensity occurs at about 0.015 second after the load is applied. Most backcalculation algorithms use the peak loading intensity and the corresponding peak deflections measured from a number of sensors as the pertinent data. Therefore, it is reasonable to take a loading time of 0.015 second (i.e., $t_1 = 0.015$).

The analytical correction factors given by (III.20) for the three test sites from which field cores were retrieved and tested are graphically shown in Figures III.4.8(a)-(c) in comparison with the empirical models discussed above. It is seen that the analytical model is not necessarily in a linear function of the temperature as in the empirical models.

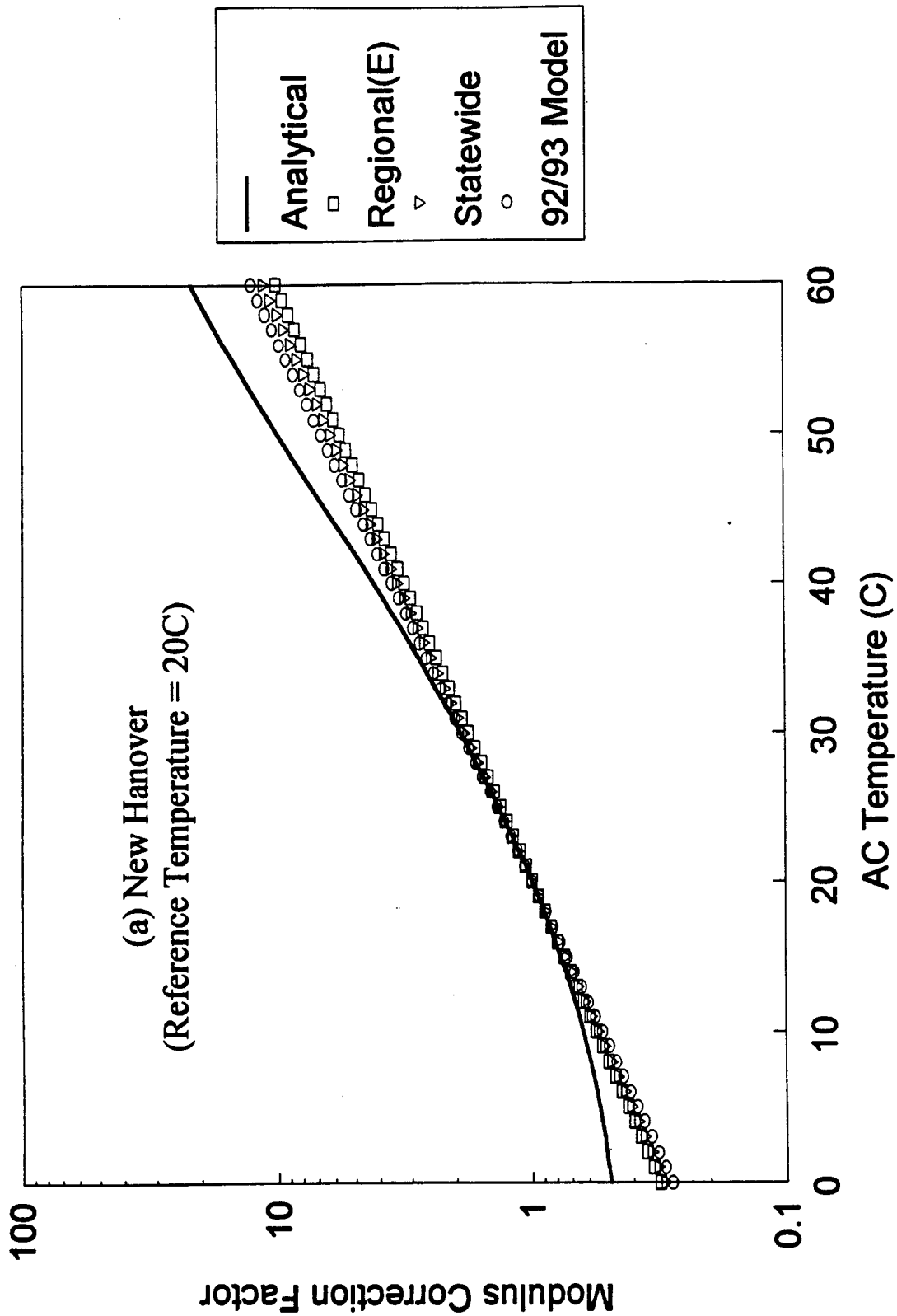

Figure III.4.8. The temperature correction factors for AC moduli from new analytical model in comparison with the empirical models; (a) New Hanover.

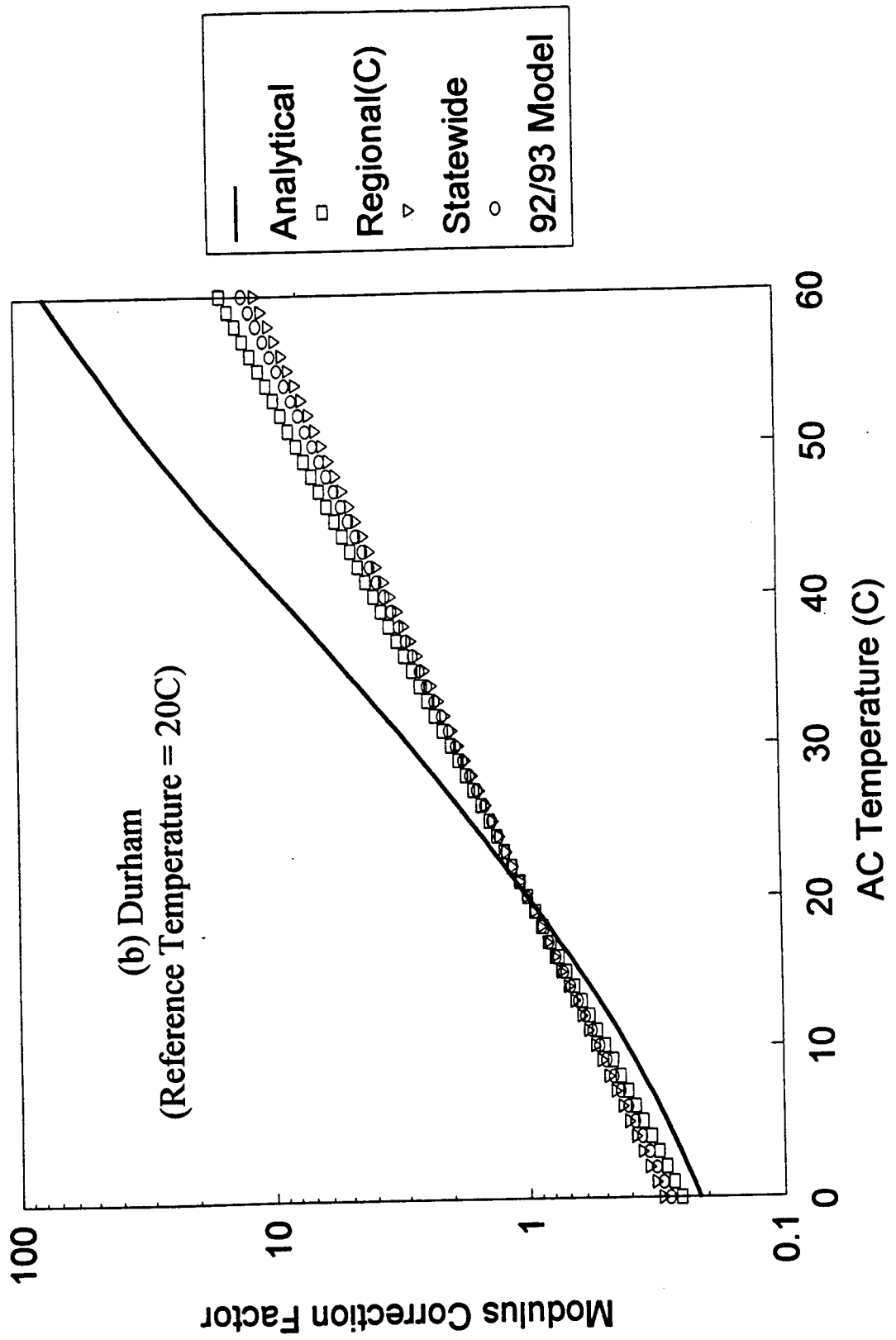

Figure III.4.8. (Continued); (b) Durham.

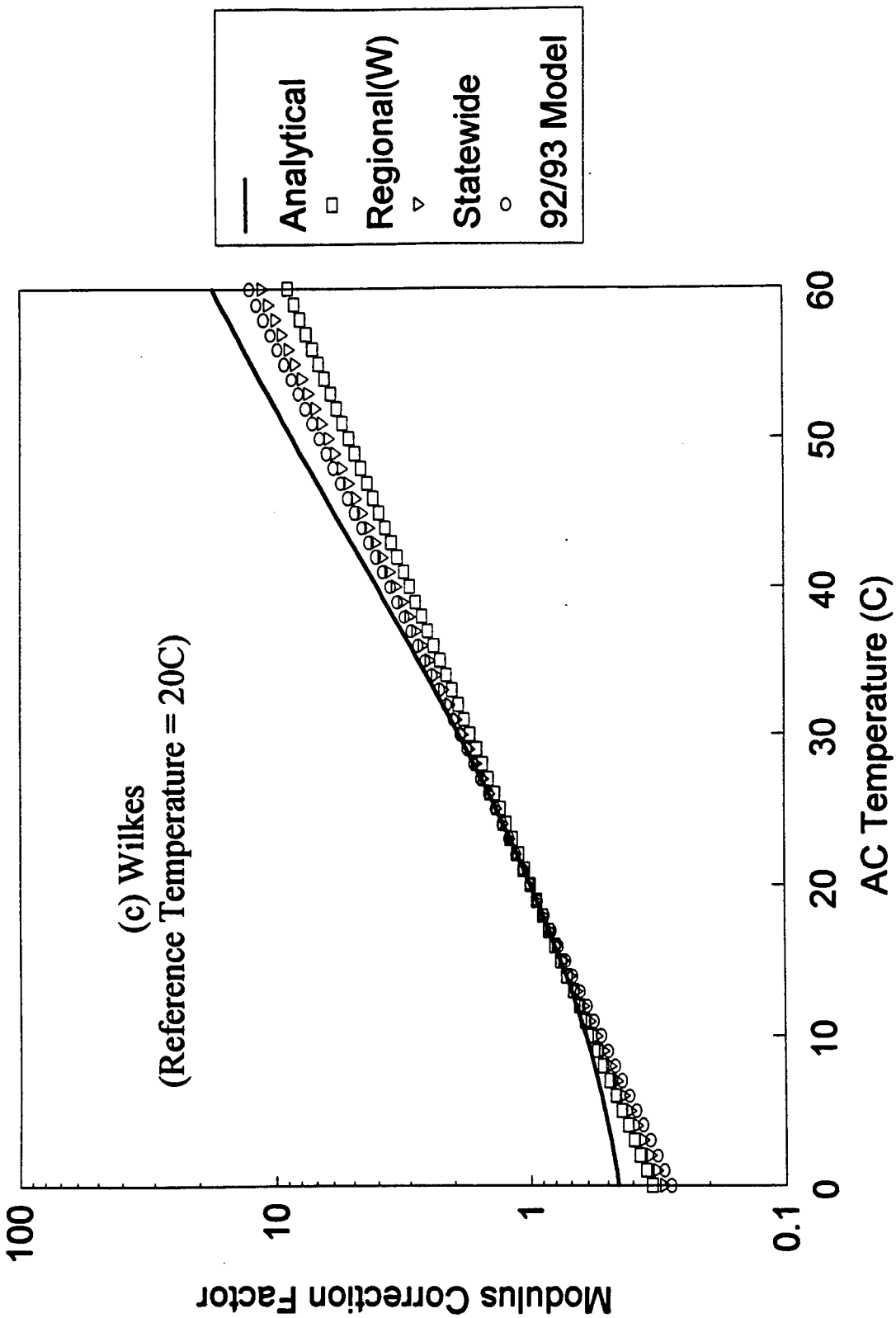

Figure III.4.8. (Continued); (c) Wilkes.

As can be expected, greatest deviation of the analytical model from the empirical models is observed in Durham site which has unusual mixture properties.

The moduli corrected by the analytical correction factors in comparison with the empirical models are presented in Figures III.4.9(a)-(c) for each site considered. In all three sites, the corrections were improved by using the analytical model. In order to compare the qualities of corrections between different models, the slope of the straight-line fit of log E(corrected) versus T data was computed for each model used (and indicated in Figure III.4.9(a)-(c)). The negative slopes indicate that the model undercorrects the moduli and the positive slopes for overcorrection; the perfectly ideal model will results in a slope of zero. It is seen that the analytical model does not correct the moduli perfectly. There are many possible factors that one may attribute this imperfect corrections to. The difference in state of stress of the core before and after it was retrieved from the field, the difference between the actual non-uniform temperature distribution within the field AC layer and the averaged uniform temperature of the core realized in the lab, and errors and limitations involved in laboratory testing may all contribute to these discrepancies. The theoretical assumptions and simplifications (e.g., linear elastic homogeneity assumptions and negligence of dynamic effects) associated with the backcalculation procedure should also be taken into account. However, despite these discrepancies between the field moduli and the lab data, one may determine the modulus correction factor using the lab data and apply them to correct the field moduli to the desired temperature because the correction factor depends on the *ratio* of the moduli at two different temperatures rather than the *magnitude* of moduli. Usually the lab and the field moduli curves exhibit the similar curve shape over the range of temperatures and the

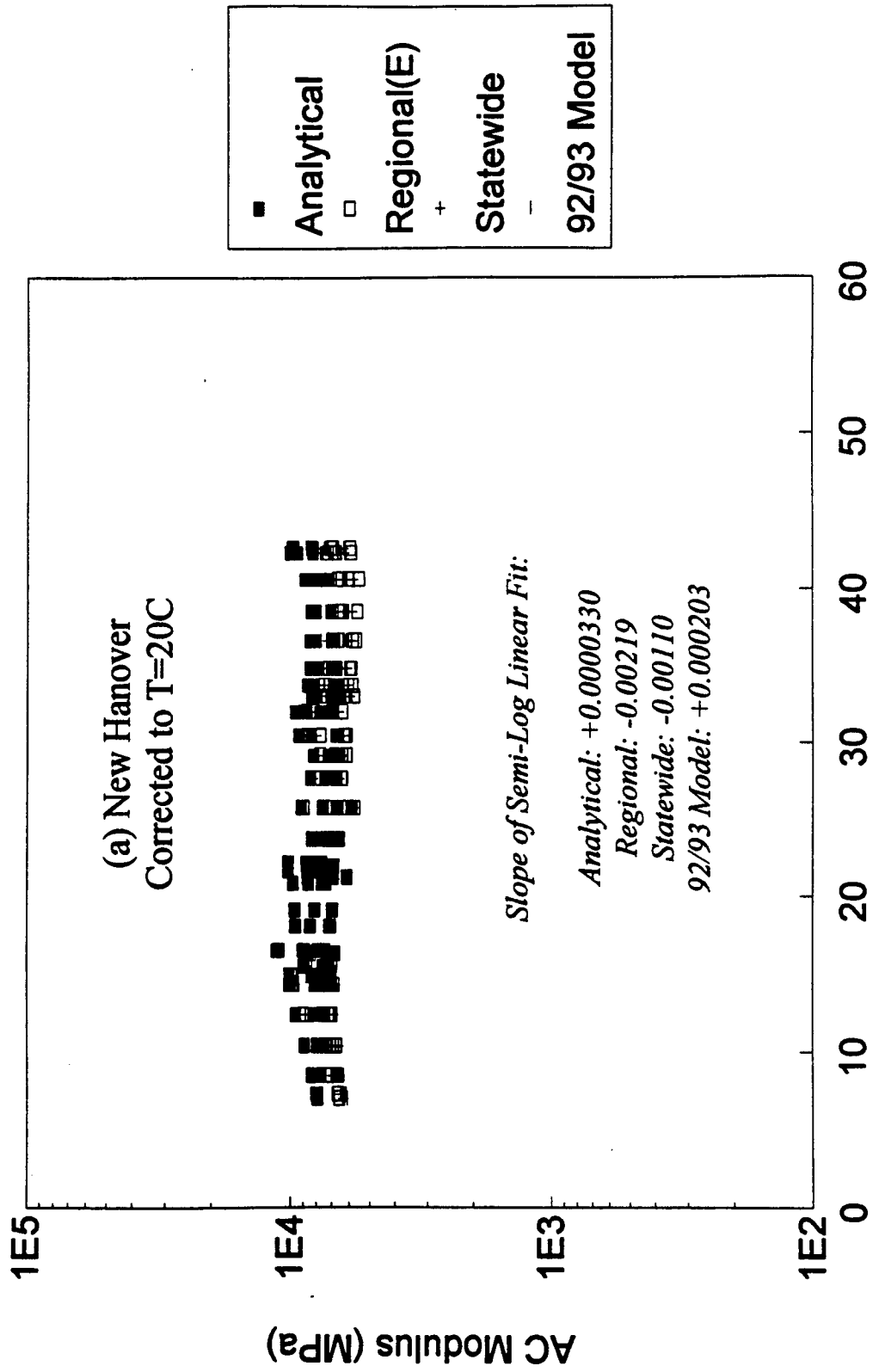

Figure III.4.9. Temperature-corrected AC moduli using new analytical model in comparison with the empirical models; (a) New Hanover.

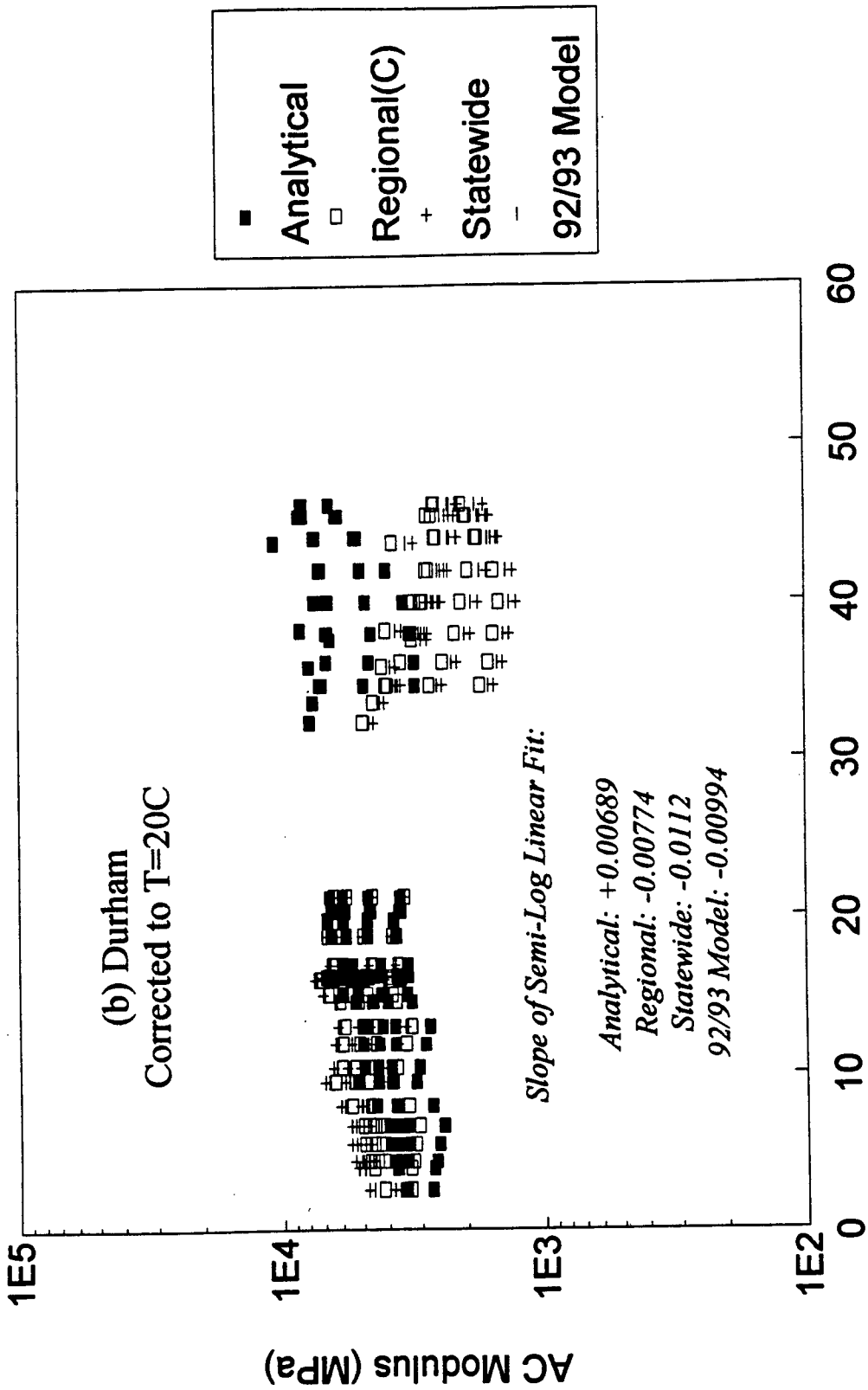

Figure III.4.9. (Continued); (b) Durham.

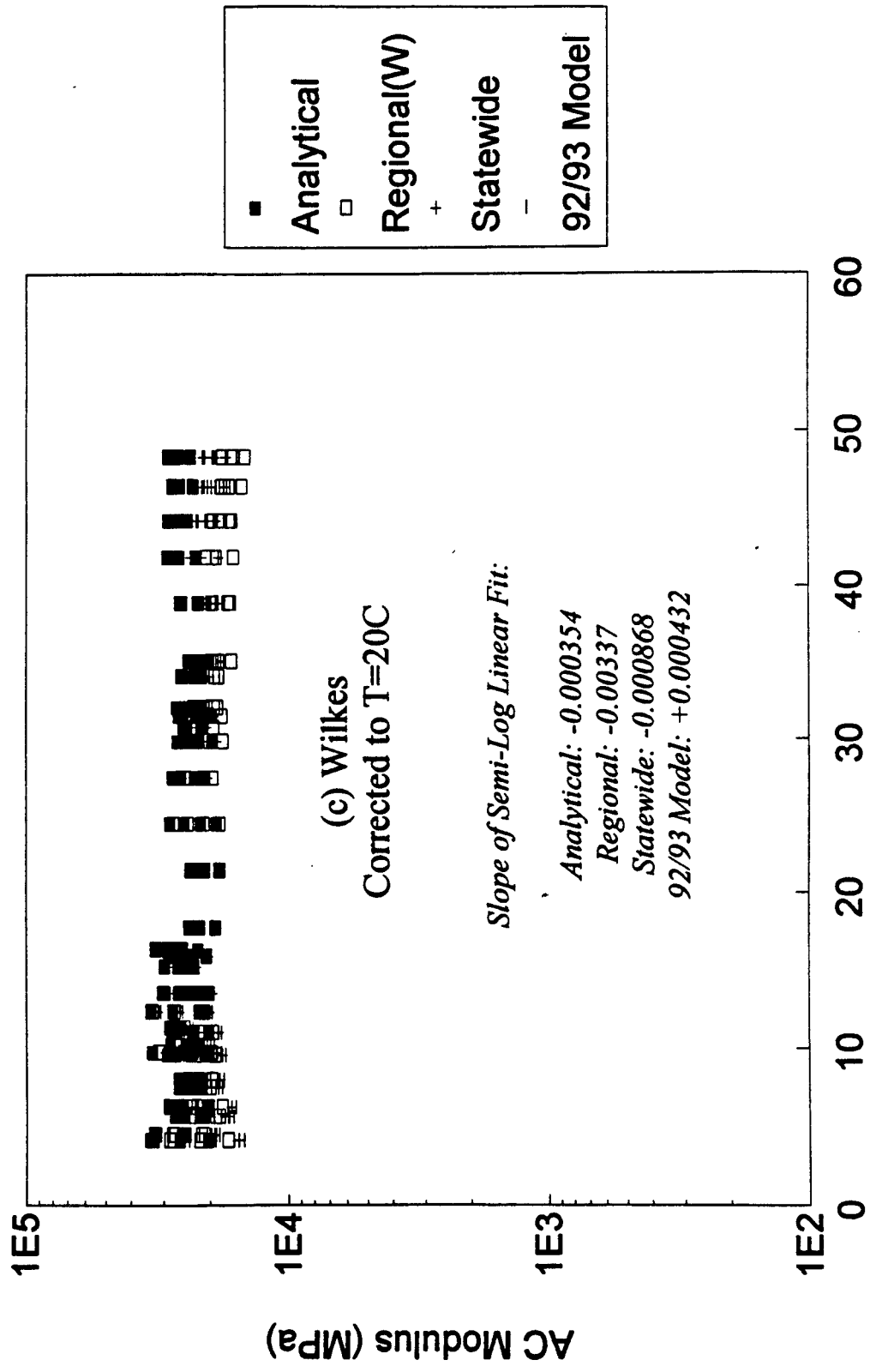

Figure III.4.9. (Continued); (c) Wilkes.

ratios of moduli at different levels of temperature are fairly close between the lab and the field situations.

III.5. Temperature Correction of FWD Center Peak Deflections

III.5.1. General

Deflection values corrected to a reference temperature (e.g., 20°C) can be obtained by multiplying appropriate factors to the deflections measured at an arbitrary temperature, i.e.,

$$w_{T_0} = \lambda_w w_T \tag{III.22}$$

where w_{T0} is the deflection corrected to temperature T_0 and w_T is the deflection at temperature T. Therefore, the temperature-deflection correction factor λ_w can be defined as

$$\lambda_w = \frac{w_{T_0}}{w_T} \tag{III.23}$$

In order to find the characteristics of the temperature-dependence of the deflection, the measured deflections are plotted against the AC effective temperature on the semi-log scale as shown in Figures III.5.1(a)-(d). Figures (a), (b), and (c) show the FWD center peak deflections measured within the east, central, and west regions of North Carolina, respectively. The deflection and temperature data used in Figures III.5.1(a)-(d) are presented in Appendix C.

Overall, the trend can be roughly characterized by a linear relationship between the log of deflection and the temperature. The degree of the temperature-dependence which is indicated by the slope of the straight line varies from site to site. Figure III.5.2

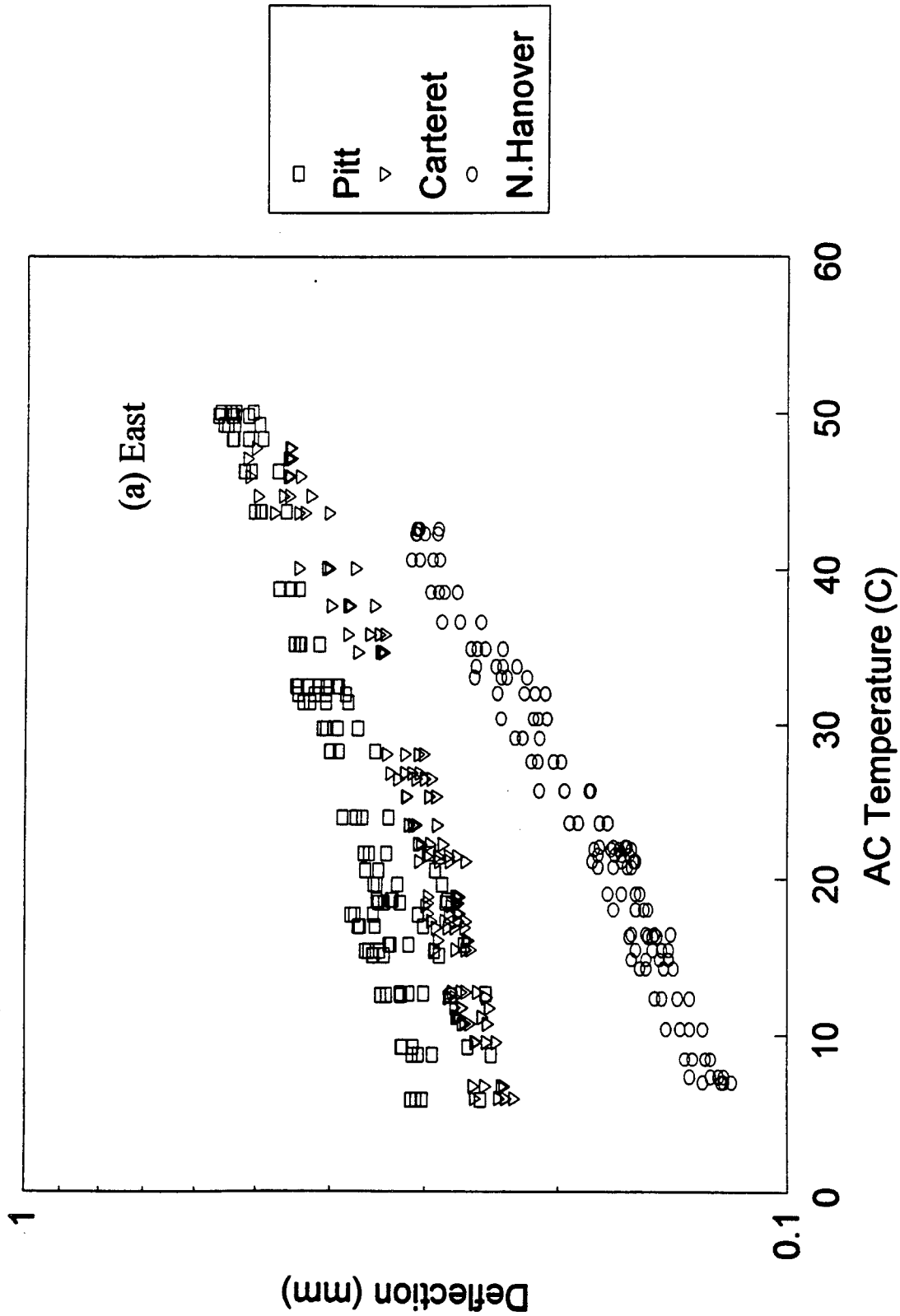

Figure III.5.1. Variation of center peak deflection with temperature; (a) east region.

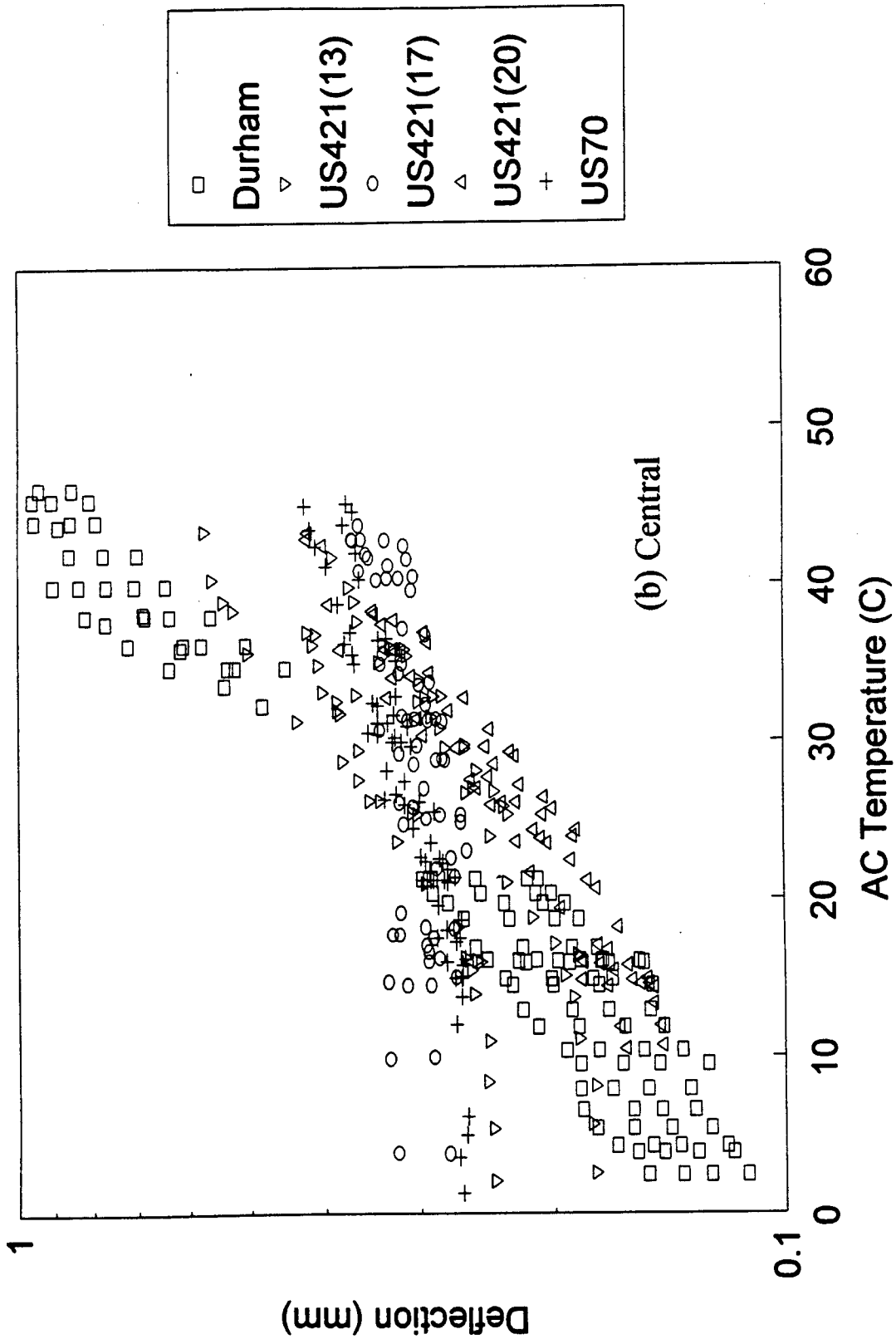

Figure III.5.1. (Continued); (b) central region.

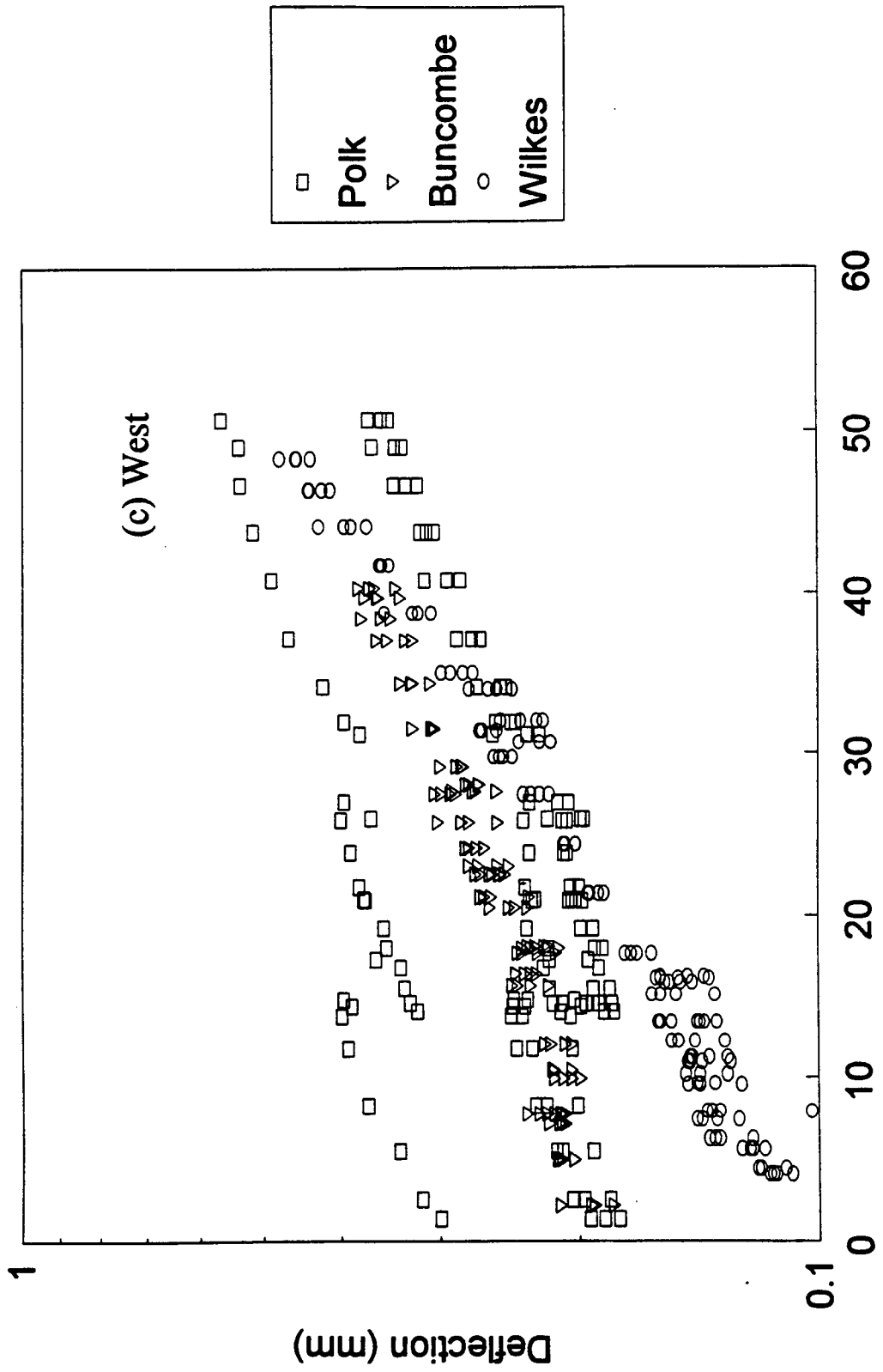

Figure III.5.1. (Continued); (c) west region.

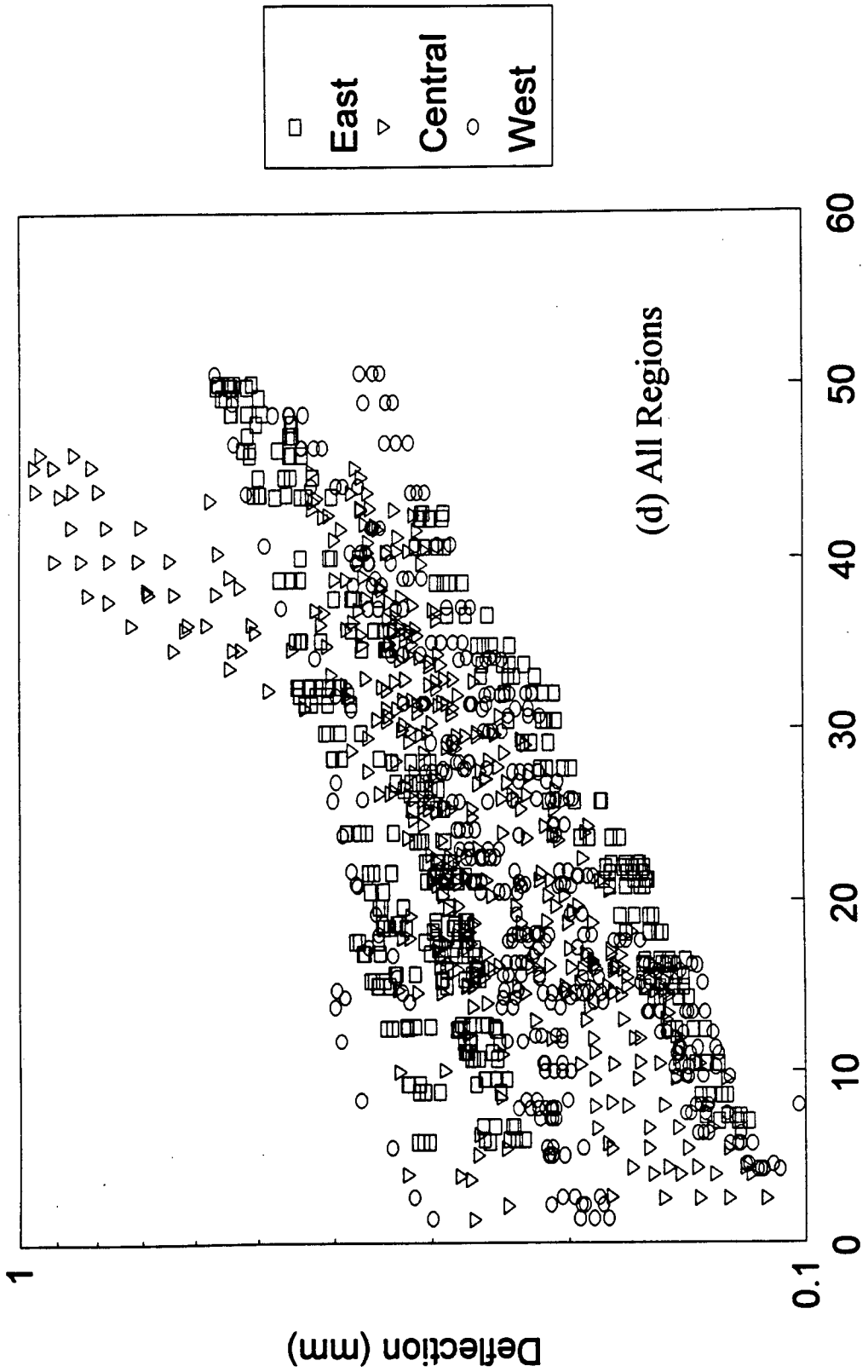

Figure III.5.1. (Continued); (d) all regions.

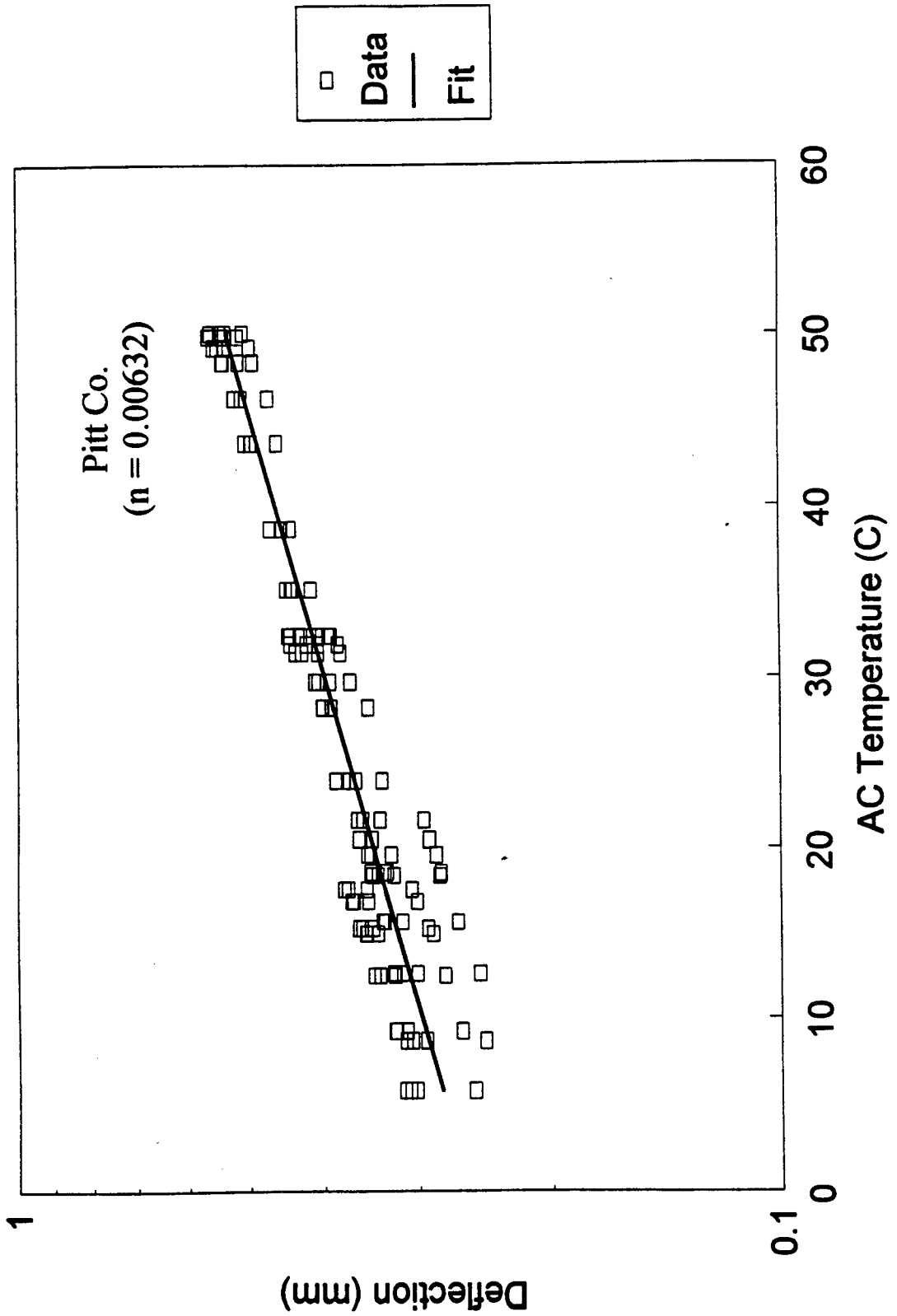

Figure III.5.2. A typical linear regression and the slope (n-value) of the linear fit of log w versus T data (on Pitt site).

shows a typical linear fit and the slope (n-value) between log w and T measured at Pitt county site. The slopes of the linear fit of log w versus T relationship, denoted by n's, were computed for each site and are given in Table III.5.1.

When one idealizes the deflection-temperature relationship by a linear relationship between log w and T, it can be shown that the correction factor defined by (III.23) can be expressed directly in terms of the slope of the straight line. Let us take the following linear form of log w versus T relationship:

$$\log w = b + nT \tag{III.24}$$

where b is the y-axis (log w axis) intercept and n is the slope in the log w versus T plot. Rewriting (III.24),

$$w = 10^{b+nT}. \tag{III.25}$$

Substituting (III.25) into (III.23), one finally obtains the correction factor in terms of n as follows:

$$\lambda_w = 10^{-n(T-T_0)}. \tag{III.26}$$

It was found that the n-value is an increasing function of the thickness of AC layer. In order to determine the analytical expression of this thickness-dependence of the n-values, they were plotted against the thickness in Figures III.5.3(a)-(d) for each site and for the entire state, respectively. Even though the correlation is relatively weak, it is clear that generally n-value increases with increasing thickness. The thickness dependence of n-value may be understood in that the surface deflection of a pavement system subjected to FWD loading at a given temperature depends not only on the properties of the asphalt mixture but also on the layer geometry of the pavement system as well as loading. Since it was difficult to find a particular functional form, a linear fit was made for each case and

Table III.5.1 The slope (n-value) of the linear fit of log w versus T for each site, and C-value (III.27) for each region and the state

Sites (AC Thickness, mm)	n - values	Regions	C - values	Statewide C - value
Pitt (115)	0.00632	East	3.61E-5	4.65E-5
Carteret (229)	0.00687			
New Hanover (305)	0.0112			
Durham (254)	0.0215	Central	5.80E-5	
US421-13 (191)	0.0100			
US421-17 (89)	0.00187			
US421-20 (229)	0.0142			
US70 (140)	0.00512			
Polk (166)	0.00519	West	4.32E-5	
Buncombe (203)	0.0724			
Wilkes (242)	0.0130			

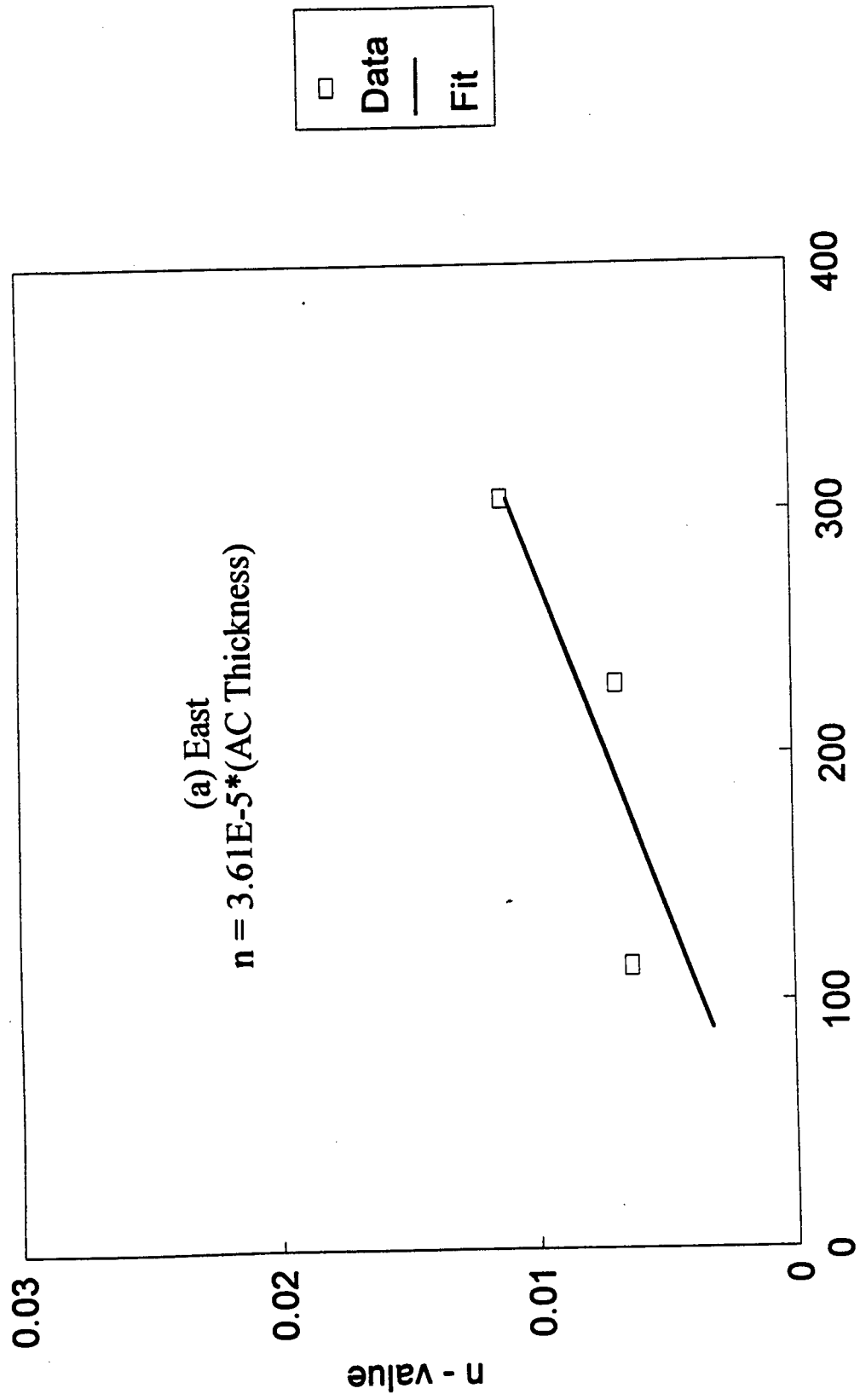

Figure III.5.3. The variation of n-value with AC layer thickness; (a) east region.

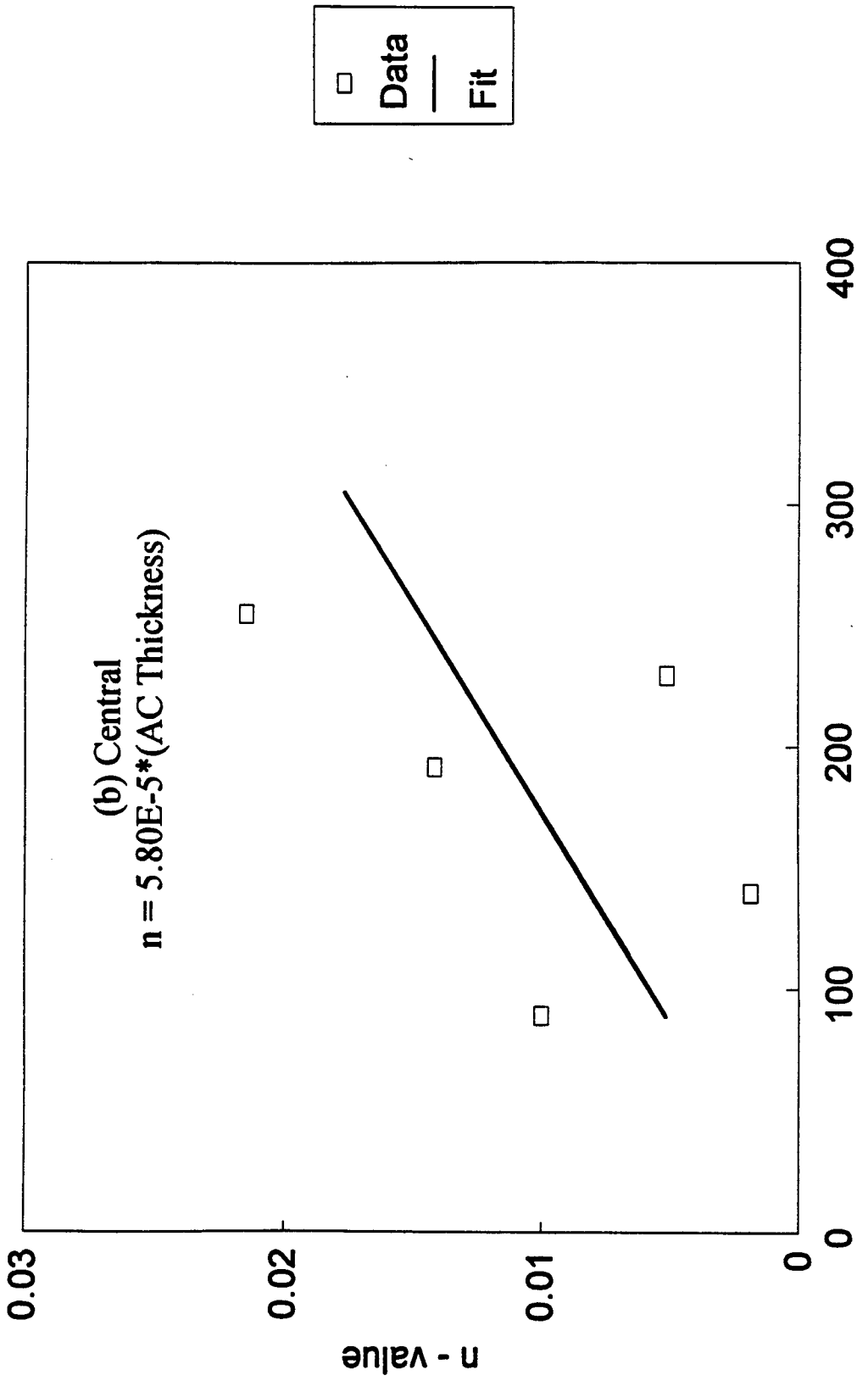

Figure III.5.3. (Continued); (b) central region.

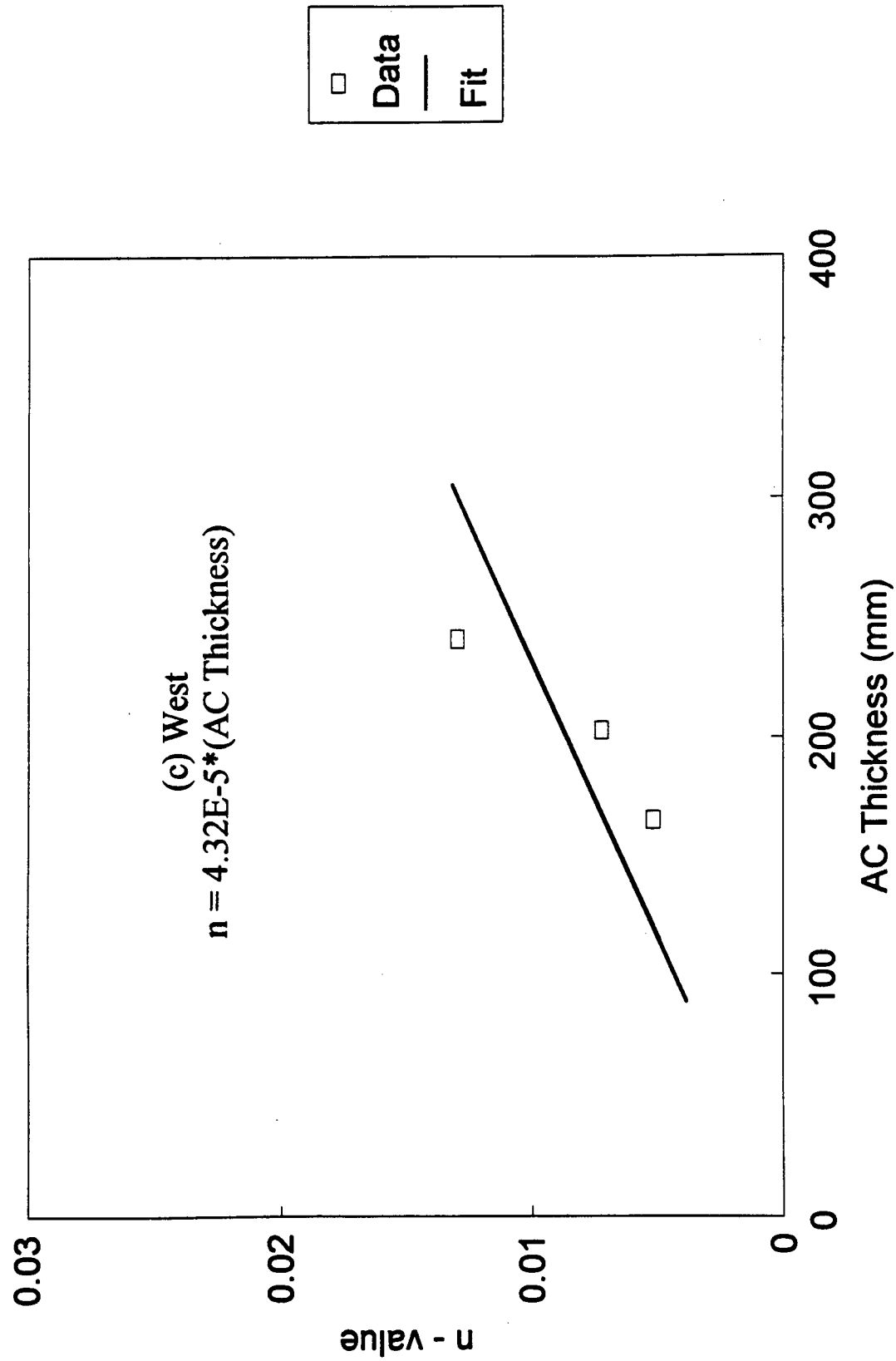

Figure III.5.3. (Continued); (c) west region.

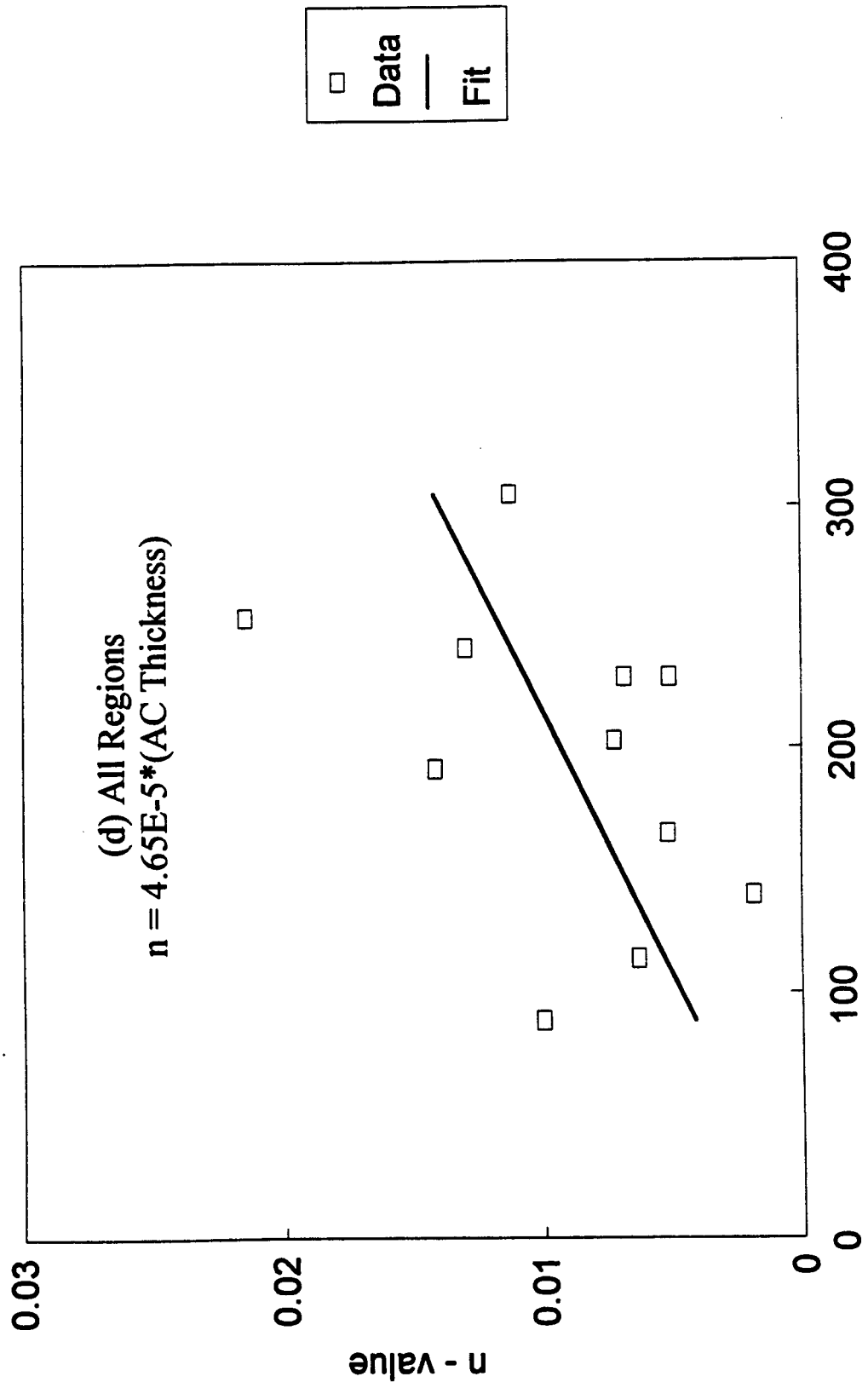

Figure III.5.3. (Continued); (d) all regions.

the coefficient thus obtained is indicated in each figure. Since, theoretically n should be zero for the zero thickness (absence of asphalt layer), the y-intercept of each line is set to zero. The slope in the n versus thickness curve will be denoted by C hereinafter, i.e., n will be expressed as

$$n = C h_{AC}. \tag{III.27}$$

where h_{AC} is the thickness of AC layer. Substituting (III.27) to (III.26), one obtains

$$\lambda_w = 10^{-C h_{AC} (T-T_0)}. \tag{III.28}$$

The C-values for each of the three regions and for the entire state are also summarized in Table III.5.1.

III.5.2. 92/93 Model - The Empirical Deflection-Correction Model Developed from the 92/93 Study

Kim et al. (1995, 1995a) proposed a deflection correction model based on the statistical analysis of measured deflections and temperatures in North Carolina. Their model takes the following form:

$$\lambda_w = 10^{-A (h_{AC})^B (T-20)} \tag{III.29}$$

where h_{AC} is the AC layer thickness in mm, T is the temperature in °C, and the constants A and B were given, respectively, to be 5.807E-6 and 1.4635 for wheel path, and 6.560E-6 and 1.4241 for lane center. It can be seen that with B = 1 and T_0 = 20, (III.29) reduces to (III.28).

The FWD center peak deflections presented in Figures III.5.1(a)-(d) are corrected using the 92/93 deflection correction model and are presented in Figures III.5.4(a)-(d).

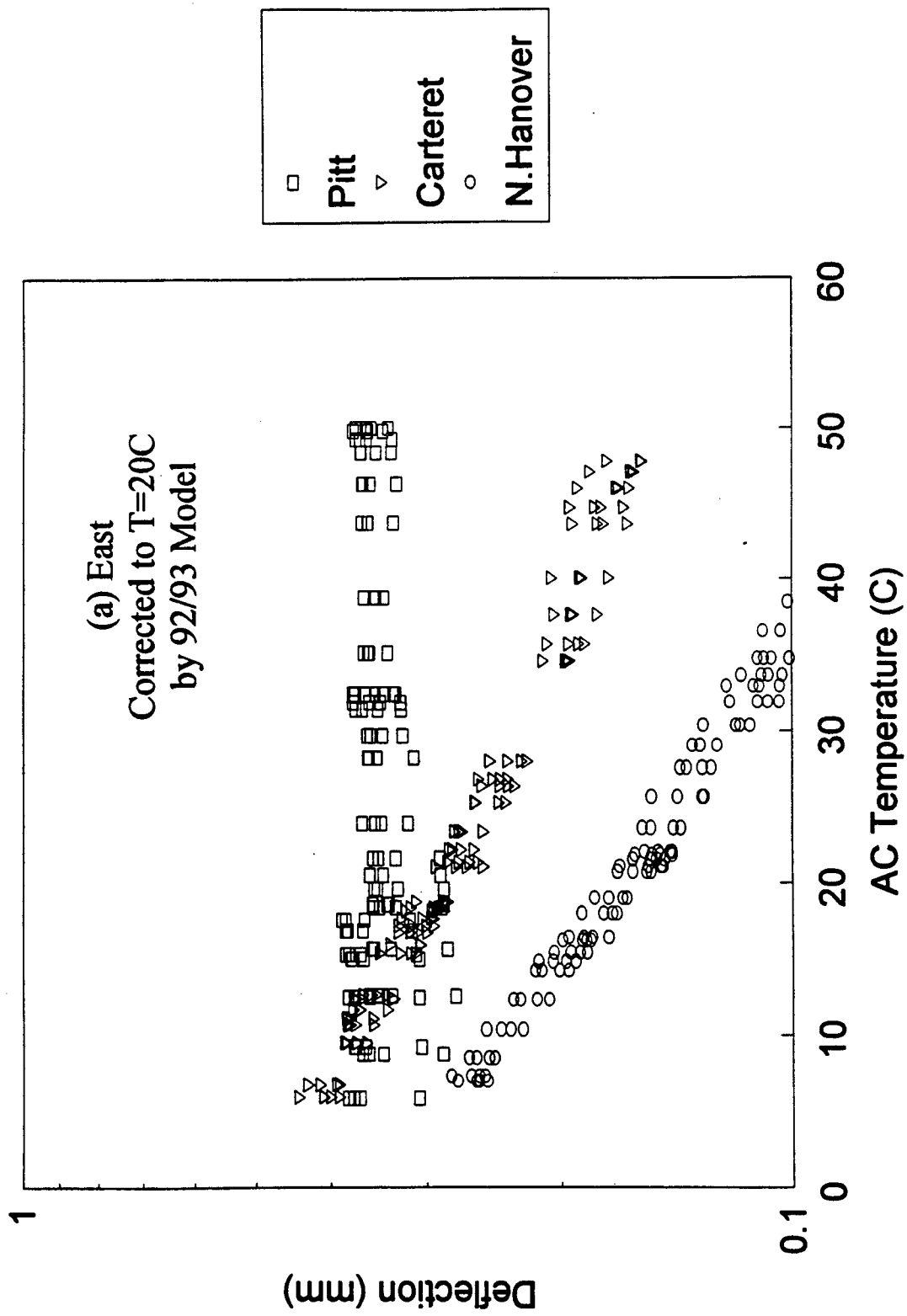

Figure III.5.4. Temperature-corrected deflections using the 92/93 empirical model; (a) east region.

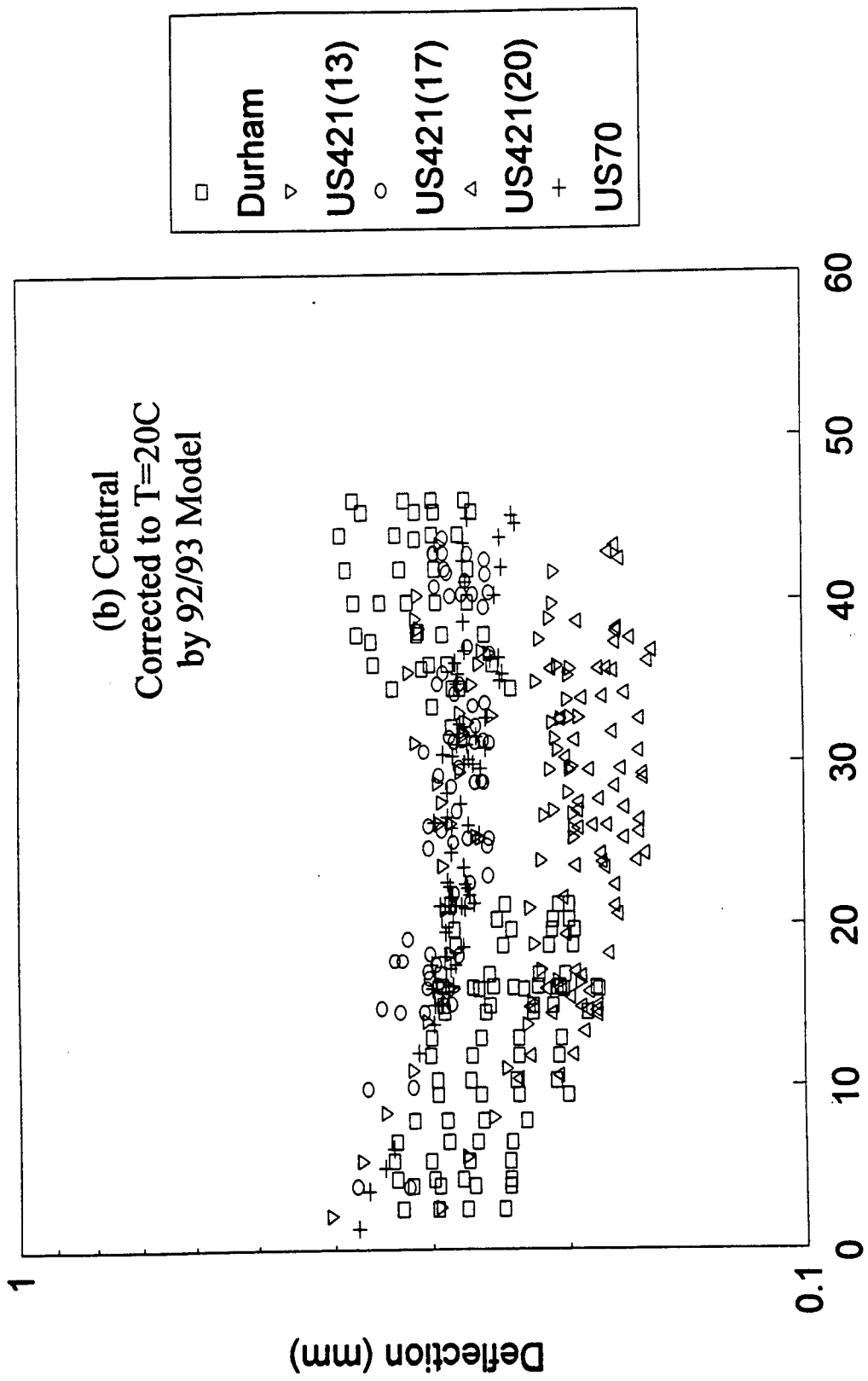

Figure III.5.4. (Continued); (b) central region.

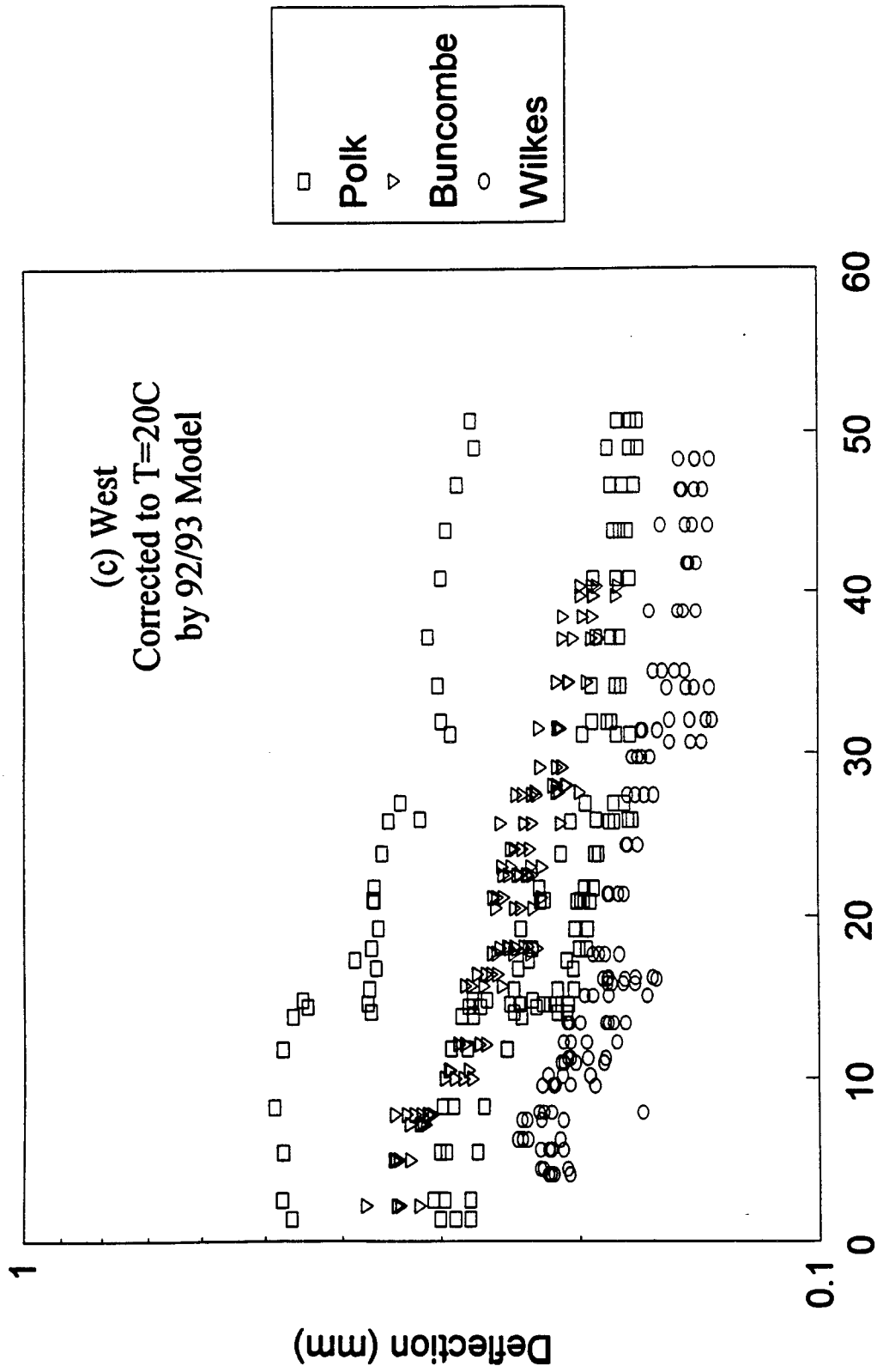

Figure III.5.4. (Continued); (c) west region.

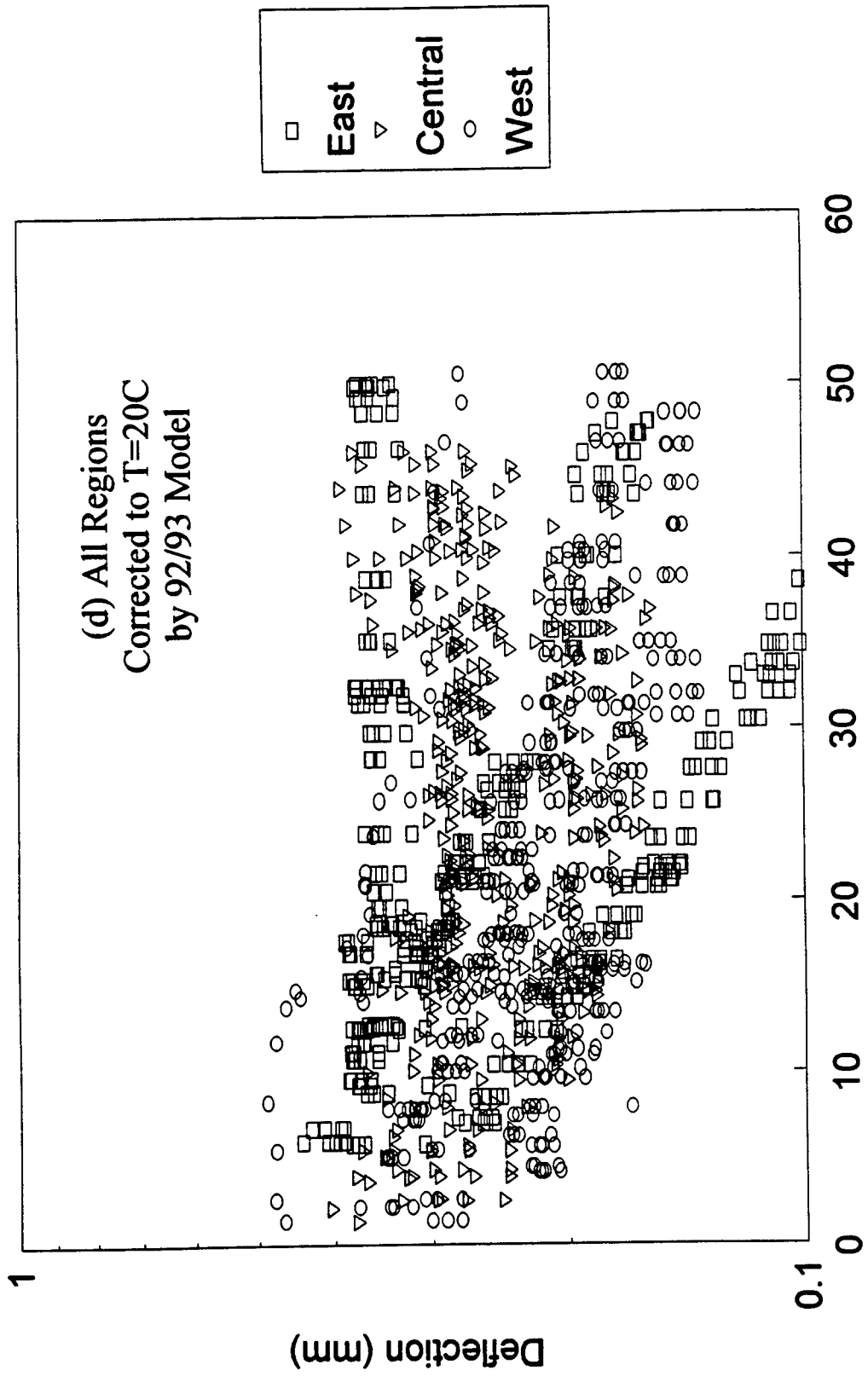

Figure III.5.4. (Continued); (d) all regions.

Overall, the corrections are not satisfactory except for a few sites. The corrections are especially poor for the sites with thick AC layer (e.g., New Hanover, Carteret, and the three western sites). It is believed that the 92/93 model overly accounts for the effects of AC thickness and thus overcorrects the deflections of thick pavements. The quality of correction for central region sites are better than the other two regional sites, as the model was developed using the data from the central sites except Durham site. Even though the Durham site consists of a relatively thick AC layer, the corrections were fairly good, which can be understood considering the fact that the mixture used in Durham site has unusually high viscosity and requires more correction than the normal mixture.

Definitely, there needs an improvement of the 92/93 deflection correction model. We shall make an improvement of the model by considering the following three approaches as have been considered for the modulus correction: (III.1) regionalize the model; i.e., find a C-value for use within each of the three regions of the state, (III.2) find a representative C-value for statewide use, and (III.3) develop an analytical correction procedure for each mixture type and pavement profile. These three approaches will be described in the next three subsections.

III.5.3. Regional Model - New Empirical Deflection-Correction Models Based on Regional Field Data

Assuming that similar mixture types are used in pavement construction within each region, one can develop a regional empirical model based on the observation of the field data obtained from sites within that particular region. Again, utilizing the linear

relationship between log w and T, one can adopt the deflection correction factor of the form (III.28). A proper C-value for each region is already given in Table III.5.1.

The moduli were corrected according to (III.22) and (III.28) with the respective C-value for each region and are presented in Figures III.5.5(a)-(d). The quality of correction has significantly improved over the 92/93 model. For Durham site, the new regional model fails to correct the deflections adequately because of the unusual mixture properties.

III.5.4. Statewide Model - A New Empirical Deflection-Correction Model Based on Statewide Field Data

A statewide empirical model is obtained based on the similar procedure to the regional model except that a different C-value that can better represent the entire state is used. The statewide empirical model for three different thicknesses of AC layer are graphically shown in Figures III.5.6(a) and (b) on the semi-log and the linear scale, respectively, in comparison with the 92/93 model.

The deflections corrected according to the new statewide model are given in Figures III.5.7(a)-(d). Generally, corrections are more or less similar to those made by regional models, even though the correction quality is inferior to that of the respective regional model.

III.5.5. Analytical Model - A New Analytical Deflection-Correction Model Based on Individual Mixture Properties and Forward Deflection Analysis

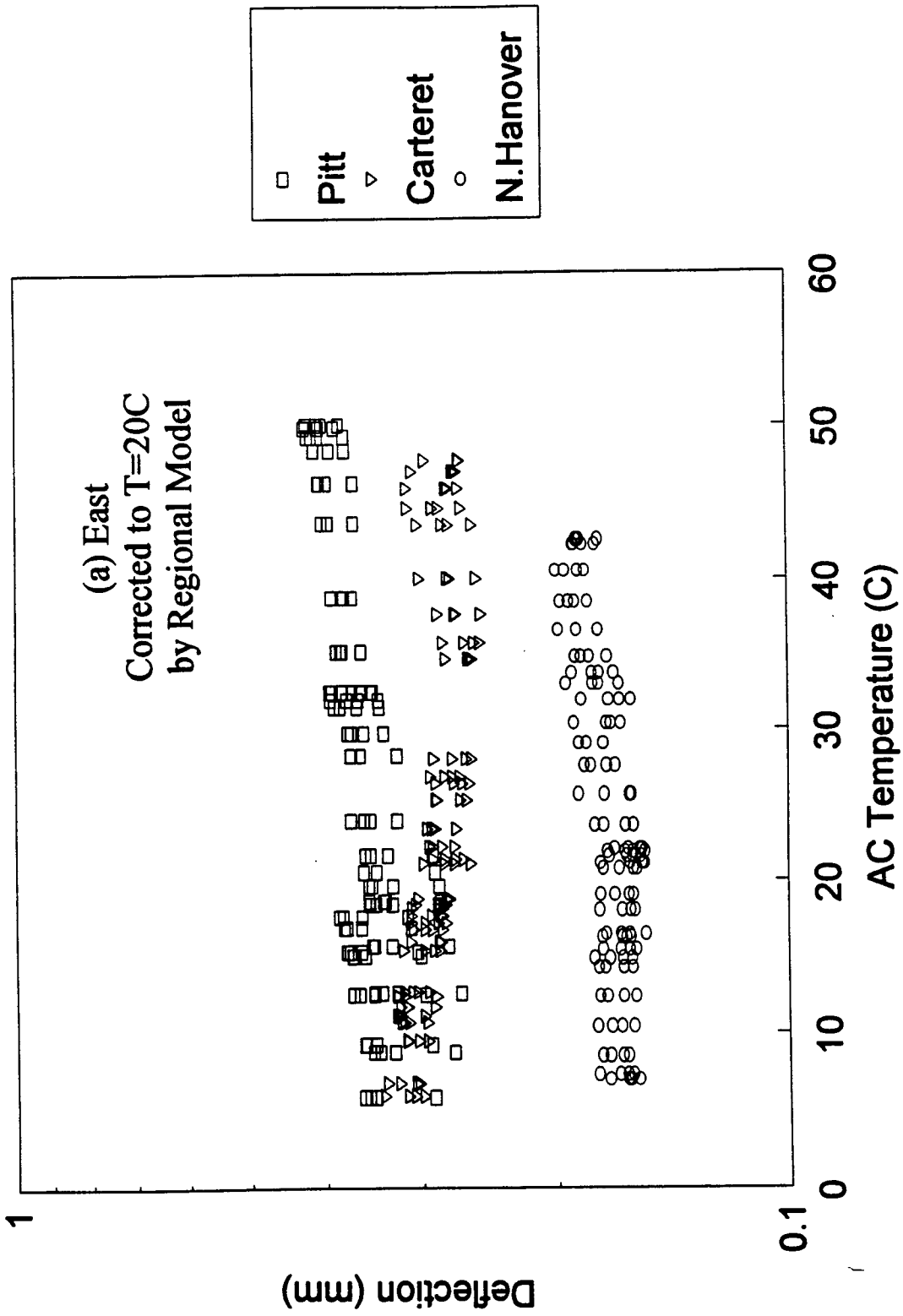

Figure III.5.5. Temperature-corrected deflections using the regional empirical models; (a) east region.

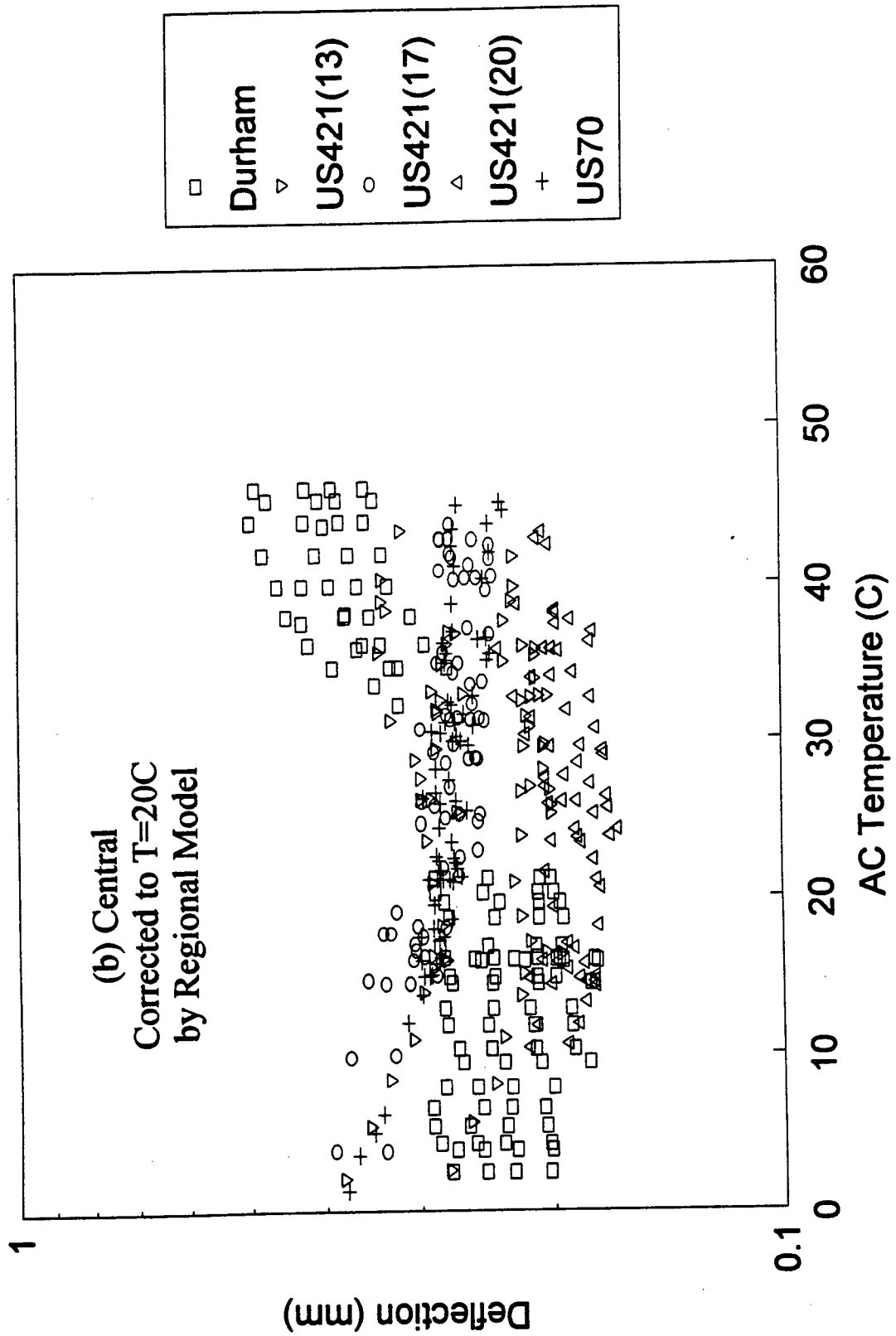

Figure III.5.5. (Continued); (b) central region.

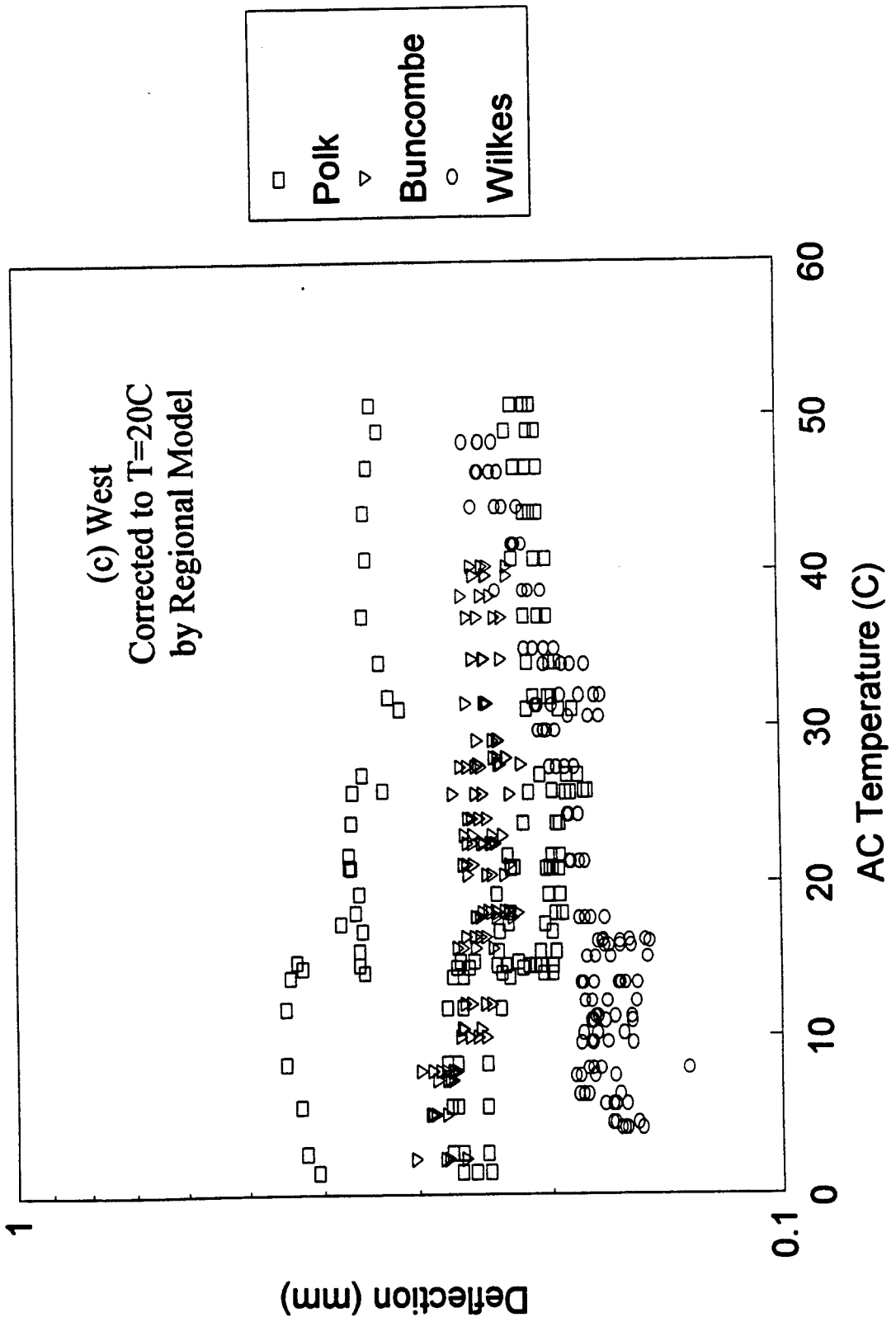

Figure III.5.5. (Continued); (c) west region.

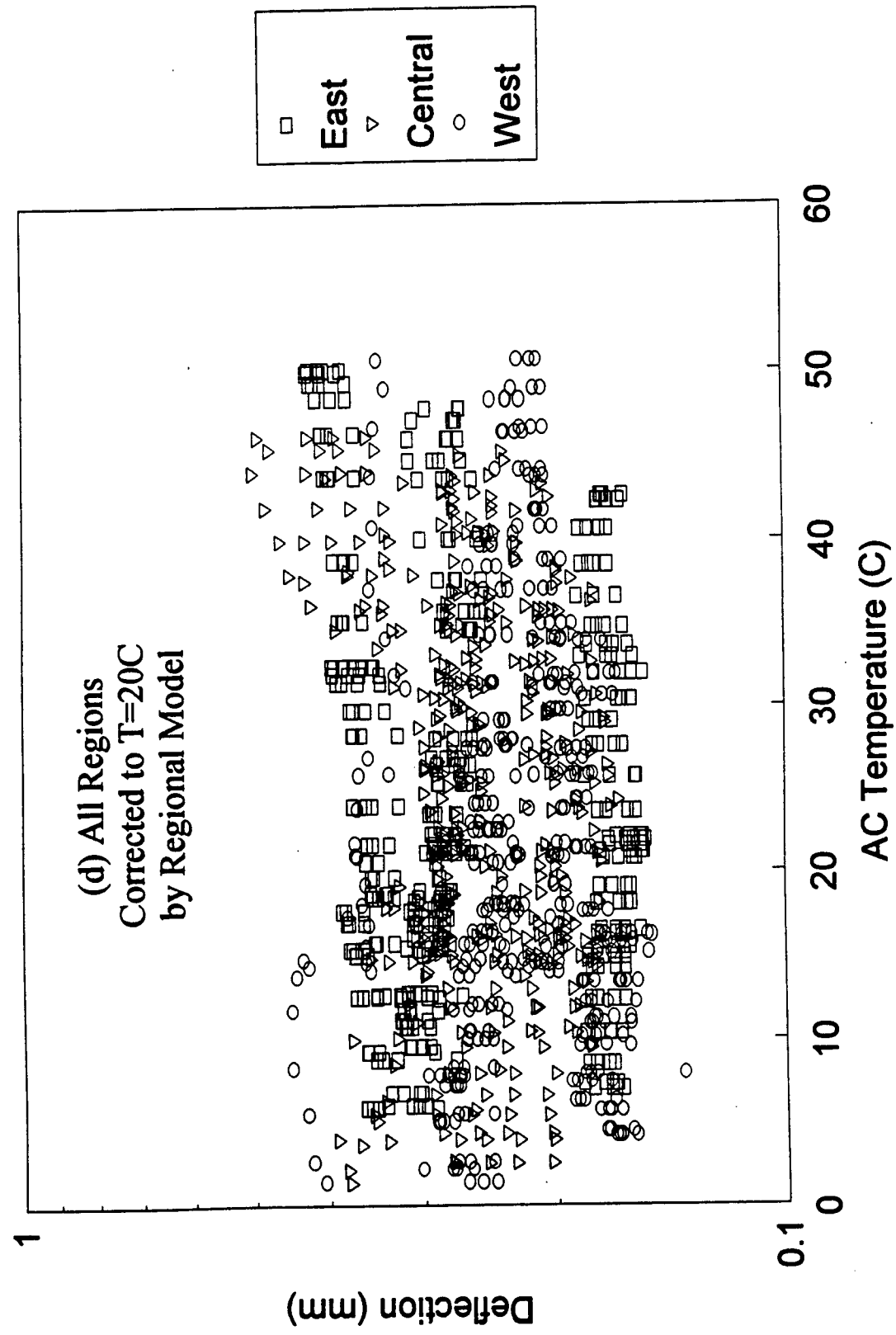

Figure III.5.5. (Continued); (d) all regions.

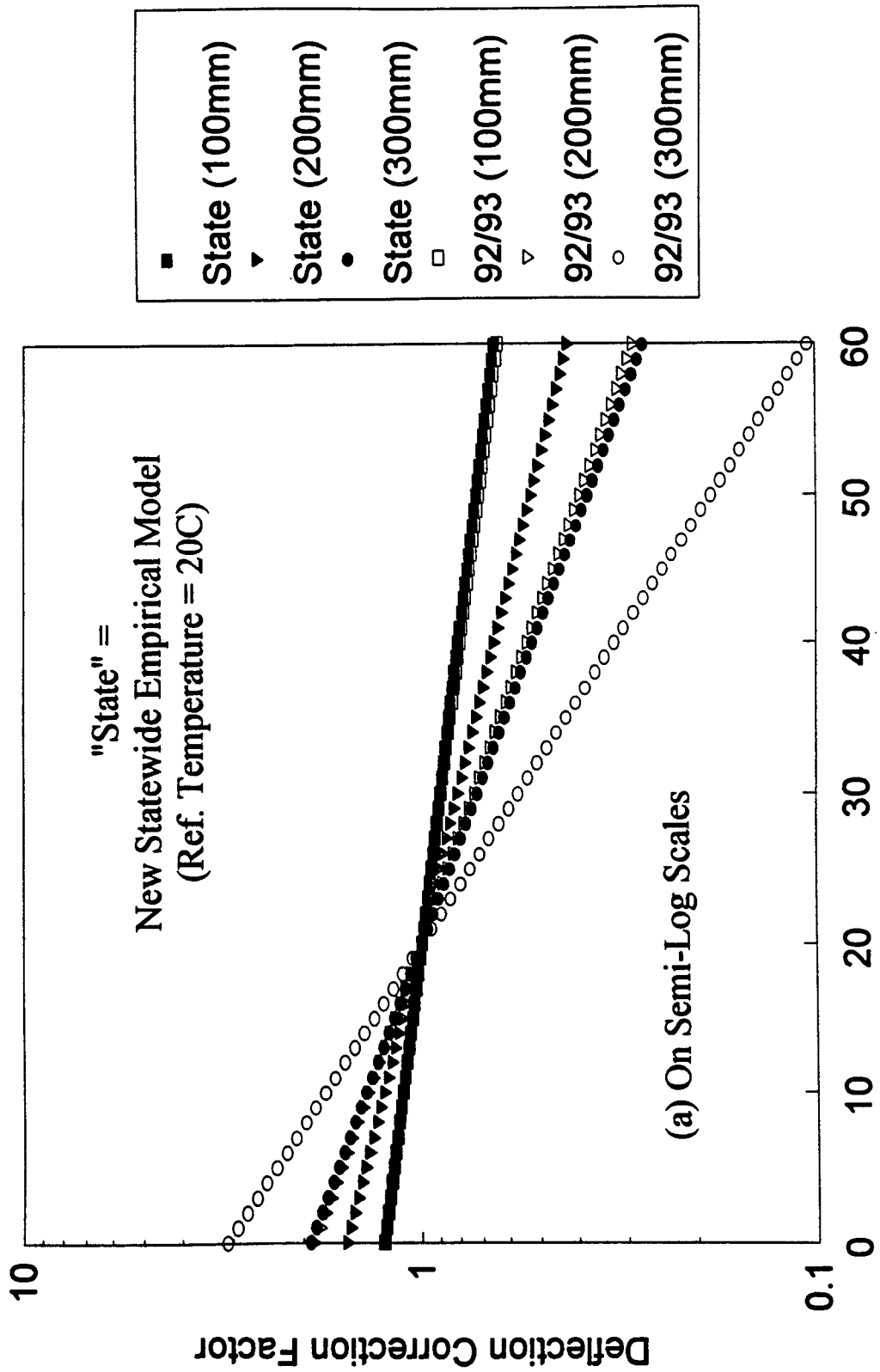

Figure III.5.6. The temperature correction factors for center peak deflections from the statewide empirical model for three different AC layer thicknesses; (a) on the semi-log scales.

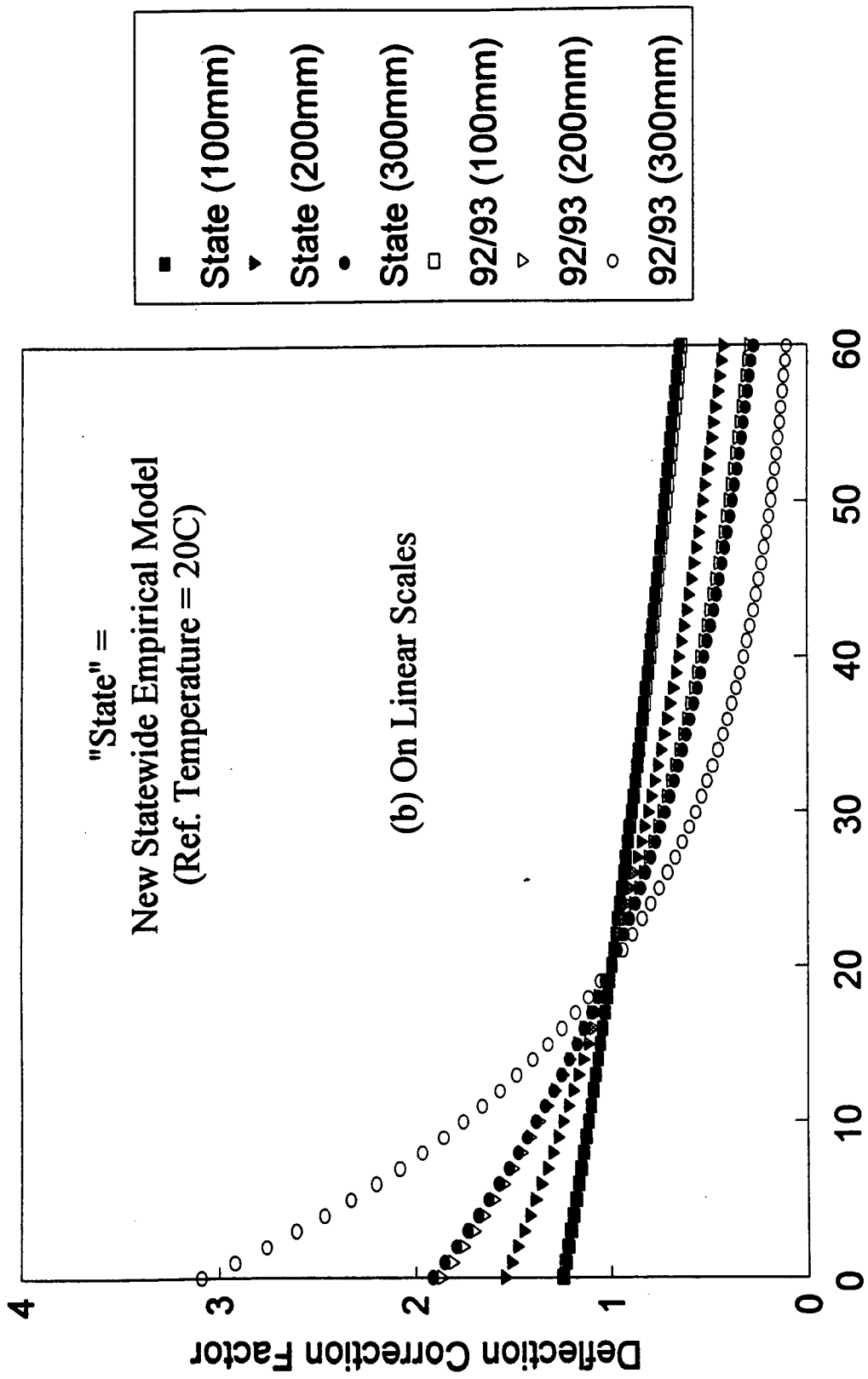

Figure III.5.6. (Continued); (b) on the linear scales.

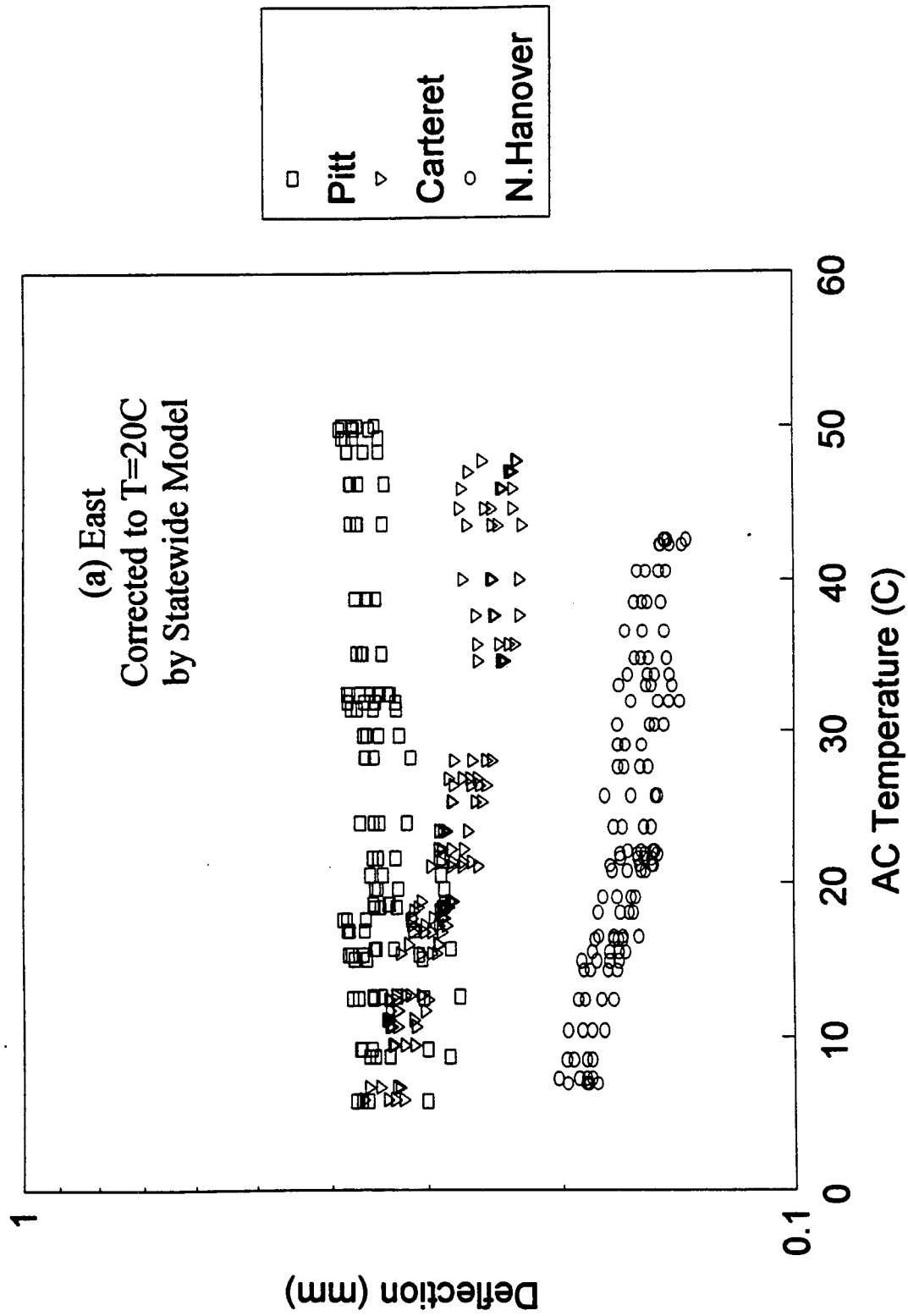

Figure III.5.7. Temperature-corrected deflections using the statewide empirical model; (a) east region.

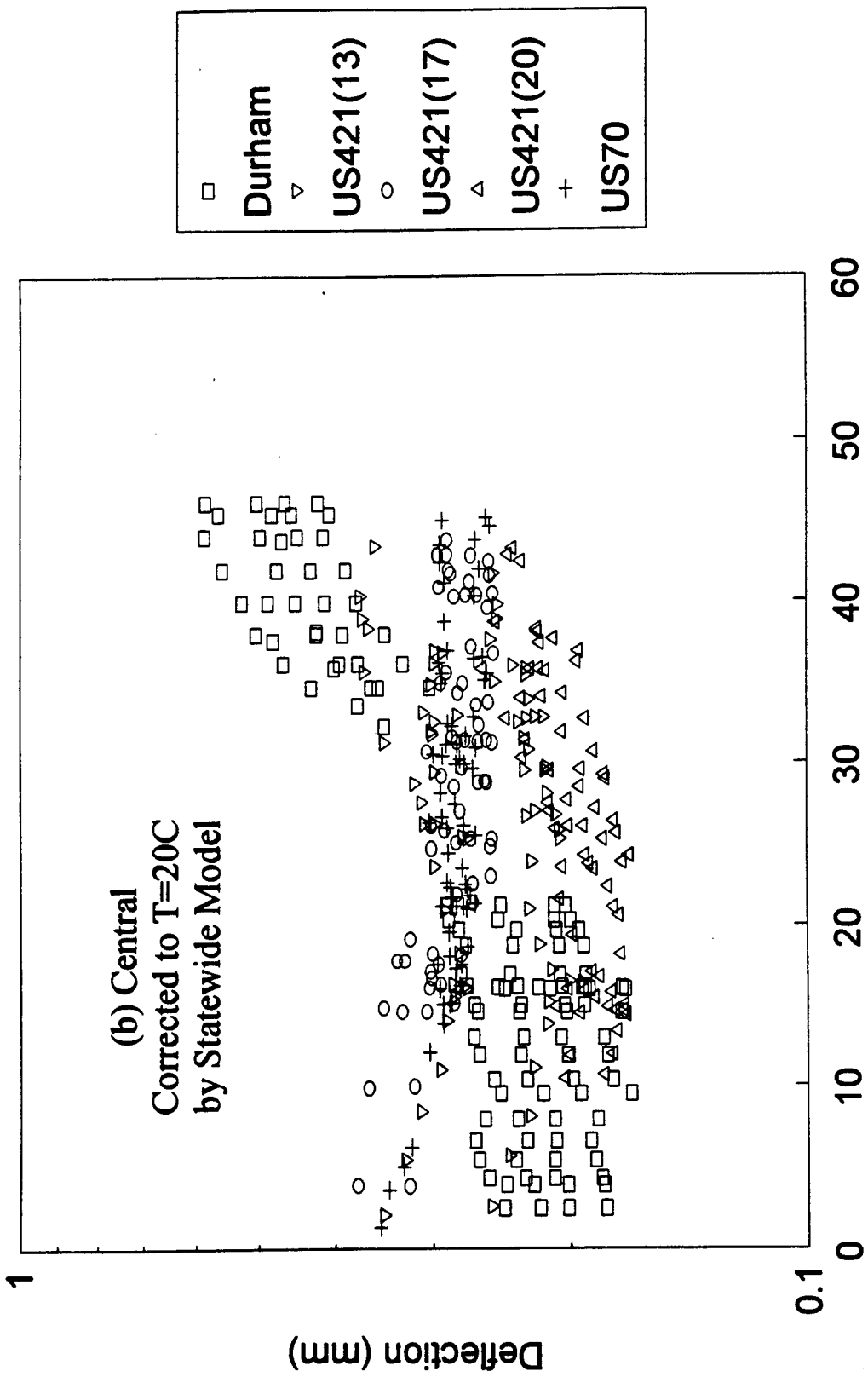

Figure III.5.7. (Continued); (b) central region.

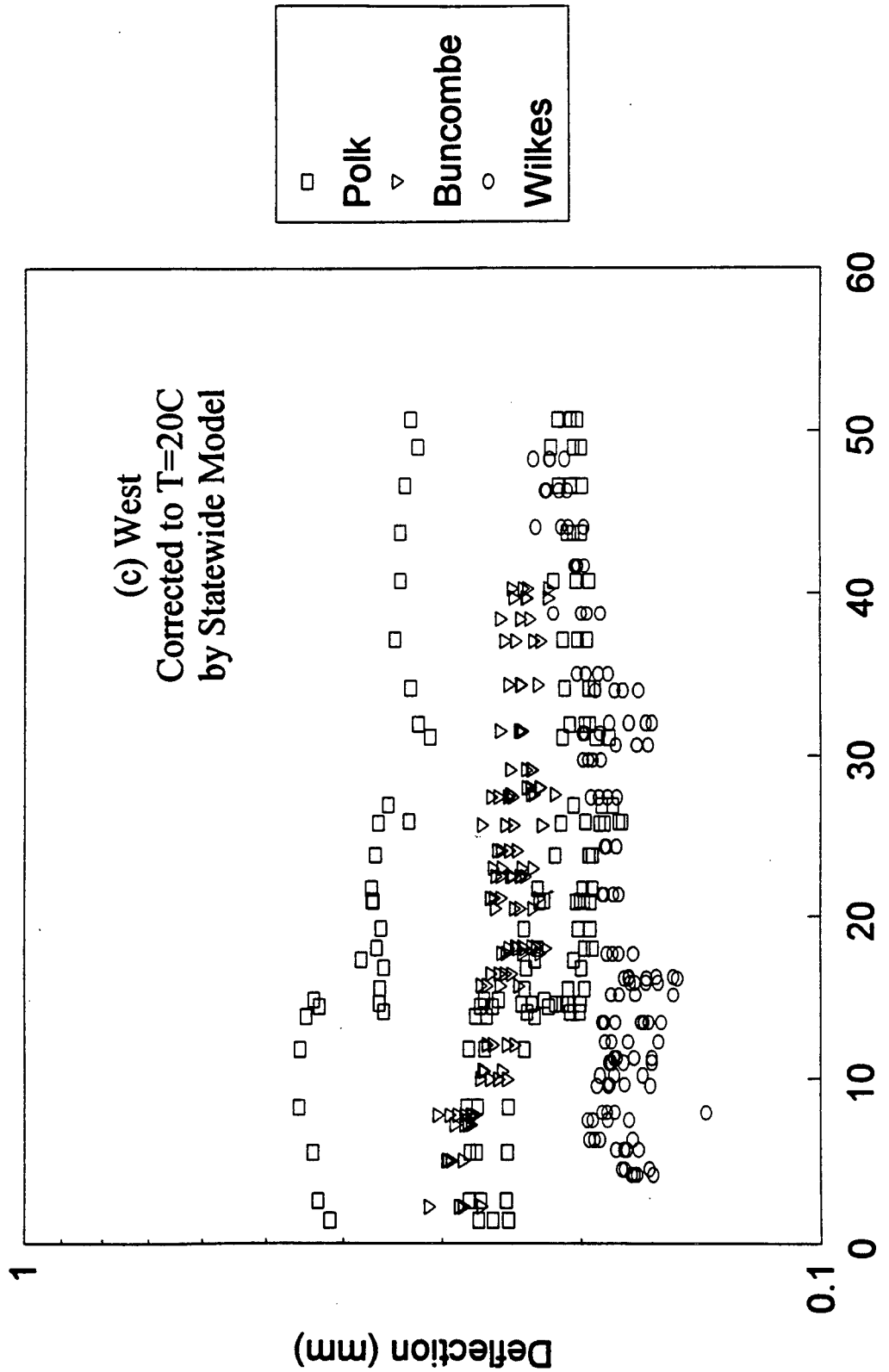

Figure III.5.7. (Continued); (c) west region.

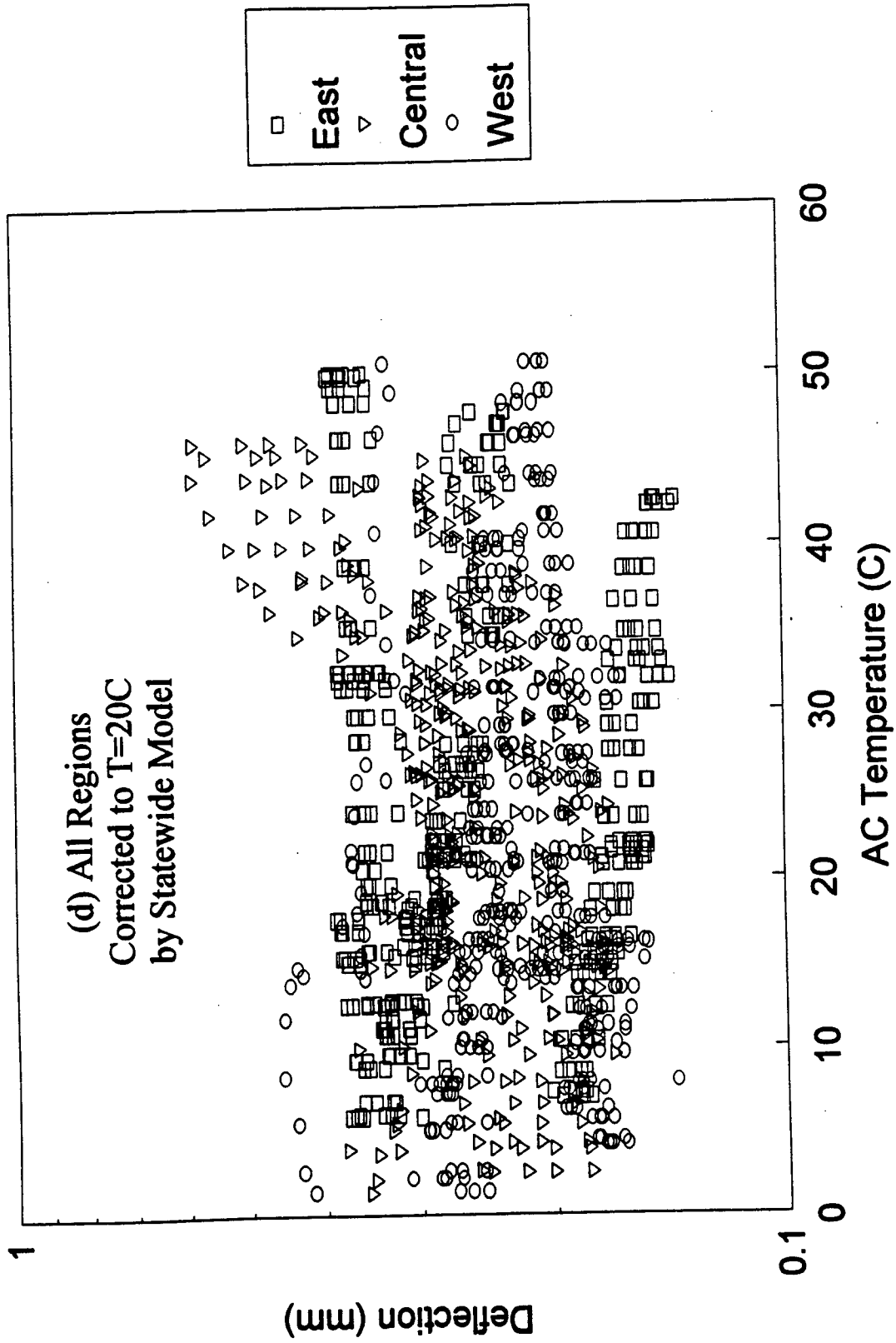

Figure III.5.7. (Continued); (d) all regions.

The theoretical determination of deflection correction factors is more complicated than the corresponding modulus correction factors because one needs to deal with the entire pavement system rather than dealing with only the AC layer properties. Deflections are obtained only through solving a boundary value problem that involves the material properties of each layer, geometric parameters (e.g., layer thicknesses and dimensions of the loading plate), and the loading conditions. Analytical procedures for solving the layered viscoelastic system that simulates the typical flexible pavement system subjected to traffic loads at different temperatures are detailed in Appendix B.

According to the procedure given by Elliott and Moavenzadeh (1971), the deflection at any position on or within the pavement system can be determined by the linear superposition integral (III.6). The unit deflection function $w_H(t)$ in (III.6) can be obtained by solving the corresponding *elastic* layered system with AC layer modulus of E(t) and subjected to the unit step loading, q(t) = 1. A detailed procedure to determine $w_H(t)$ is also given in Appendix B.

One can define theoretical correction factor by substituting (III.6) into (III.23) with the physical times in (III.6) replaced with the reduced times defined by (III.21), i.e.,

$$\lambda_w = \frac{\int_0^{t_1} w_H(\xi_0 - \xi'_0)\frac{dq(\tau)}{d\tau}d\tau}{\int_0^{t_1} w_H(\xi - \xi')\frac{dq(\tau)}{d\tau}d\tau} \qquad \text{(III.30)}$$

where t_1 is taken to be 0.015 second as discussed before, ξ_0 and ξ are as defined by (III.21), and ξ'_0 and ξ' are defined by the following:

$$\xi'_0 = \frac{\tau}{a_T(T_0)} \quad \textit{and} \quad \xi' = \frac{\tau}{a_T(T)}. \qquad \text{(III.31)}$$

The loading function q(t) for a typical FWD device can be represented approximately by a haversine function with a period of 0.03 second and the loading amplitude q_0 as follows:

$$q(t) = q_0 \sin\frac{2\pi}{0.03}t \qquad \text{(III.32)}$$

A loading amplitude of q_0 = 0.5662 MPa (equivalent to 9000 lbs of load on a 5.9 inch-radius loading plate) was used in our analysis.

The theoretical temperature-deflection correction factor (III.30) requires the determination of the unit deflection function $w_H(t)$ and subsequent evaluation of the convolution integral, which may be too laborious to be implemented for routine analysis. However, a simplified correction factor with reasonable accuracy can be derived based on the so-called *quasi-elastic* method. According to the quasi-elastic method, the viscoelastic input-response relationship (III.1) can be approximated and reduced to

$$R(t) \cong R_H(t)I(t) \qquad \text{(III.33)}$$

Equation (III.33) indicates that the current response is approximately obtainable by the current input multiplied by the current value of the unit response function. For a linear elastic system, (III.33) is the exact relationship. Based on (III.33), the numerator and the denominator in (III.30) are reduced to $w_H(\xi_0)q(t_1)$ and $w_H(\xi)q(t_1)$, respectively, and the temperature-deflection correction factor can be simplified to

$$\lambda_w = \frac{w_H(\xi_0)}{w_H(\xi)} \qquad \text{(III.34)}$$

where the reduced times ξ_0 and ξ are again defined by (III.21). The quantities $w_H(\xi_0)$ and $w_H(\xi)$ in (III.34) can directly be obtained by solving the corresponding layered elastic system (e.g., using ELSYM5) with AC modulus values of $E(\xi_0)$ and $E(\xi)$, respectively. It

is to be noted that (III.34) takes the same form as (III.20); however, one may not expect any closed-form relationship between λ_E and λ_w, because while λ_E is simply the ratio of AC moduli at two different temperatures λ_w is the ratio of the deflections at these temperatures that depend not only on the AC modulus but on the moduli of other remaining layers and the thicknesses of all the layers involved.

The analytical correction factors given by (III.34) for the three test sites from which field cores were retrieved and tested are graphically shown in Figures III.5.8(a)-(c) in comparison with the empirical models discussed above. It is seen that the analytical model is not necessarily in a linear function of the temperature as in the empirical models. As in the case of moduli corrections, greatest deviation of the analytical model from the new empirical models is observed in Durham site which has unusual mixture properties.

The deflections corrected by the analytical correction factors in comparison with the empirical models are presented in Figures III.5.9(a)-(c) for each site considered. Overall, the corrections were improved by using the analytical model, especially for the Durham site. In order to compare the qualities of corrections between different models, the slope of the straight-line fit of log w(corrected) versus T data was computed for each model used (and indicated in Figure III.5.9(a)-(c)). The negative slopes indicate that the model overcorrects the deflections and the positive slopes for undercorrections; the perfectly ideal model will results in a slope of zero. It is seen that the analytical model does not correct the deflections perfectly; in fact, in the case of Wilkes site, the statewide empirical model corrected the deflections better than the analytical model. However, this particular finding should not be used as the criterion for devaluating the analytical model.

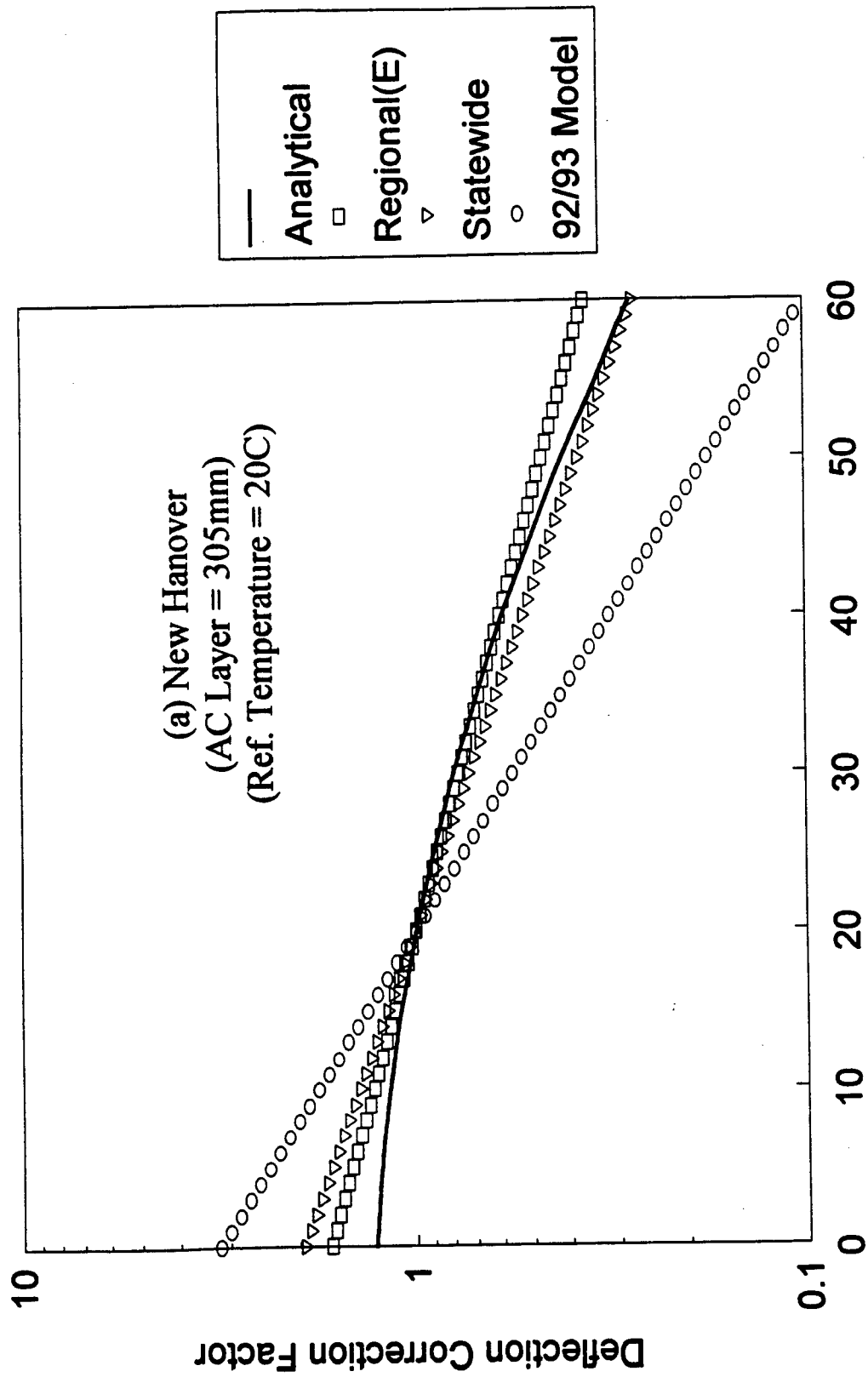

Figure III.5.8. The temperature correction factors for center peak deflections from new analytical model in comparison with the empirical models; (a) New Hanover.

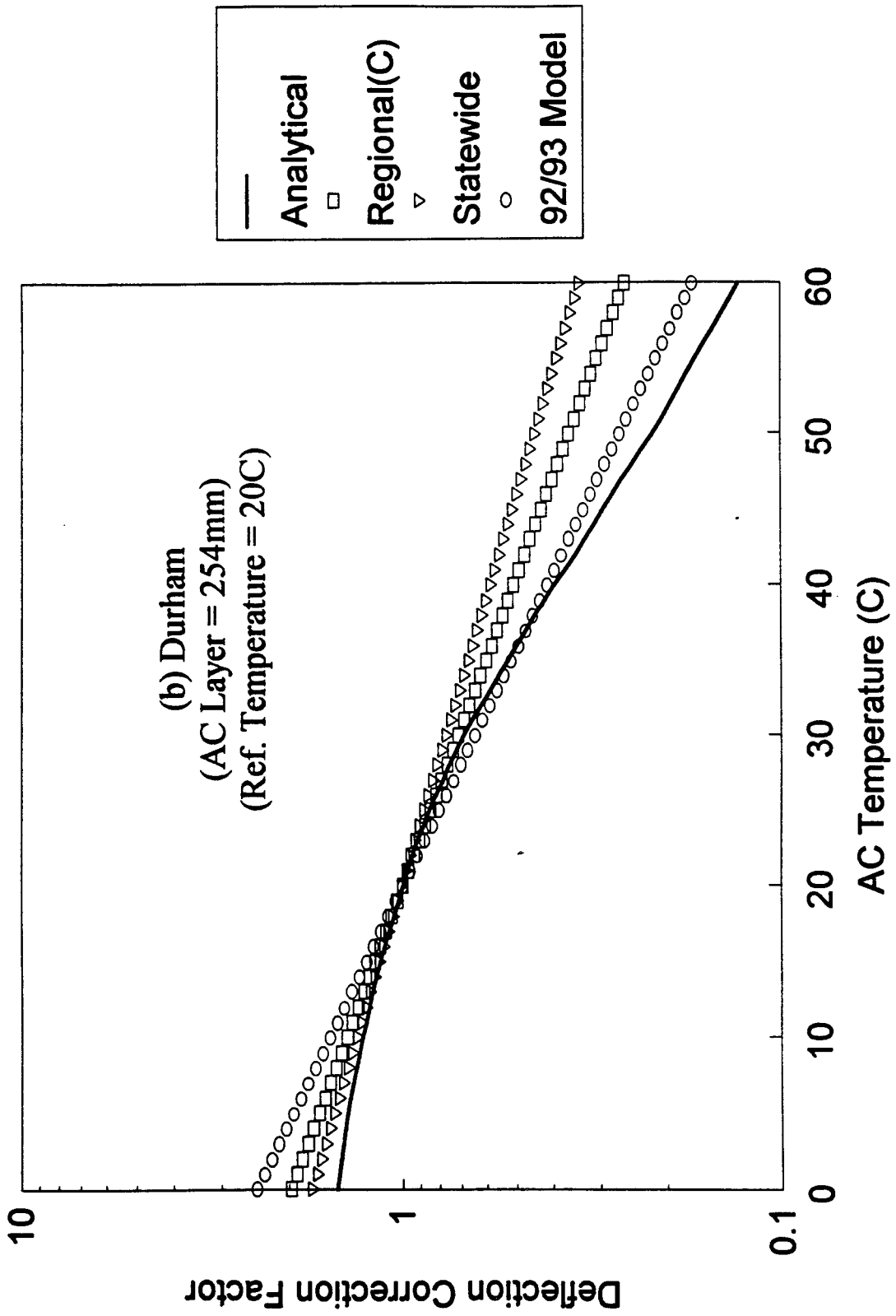

Figure III.5.8. (Continued); (b) Durham.

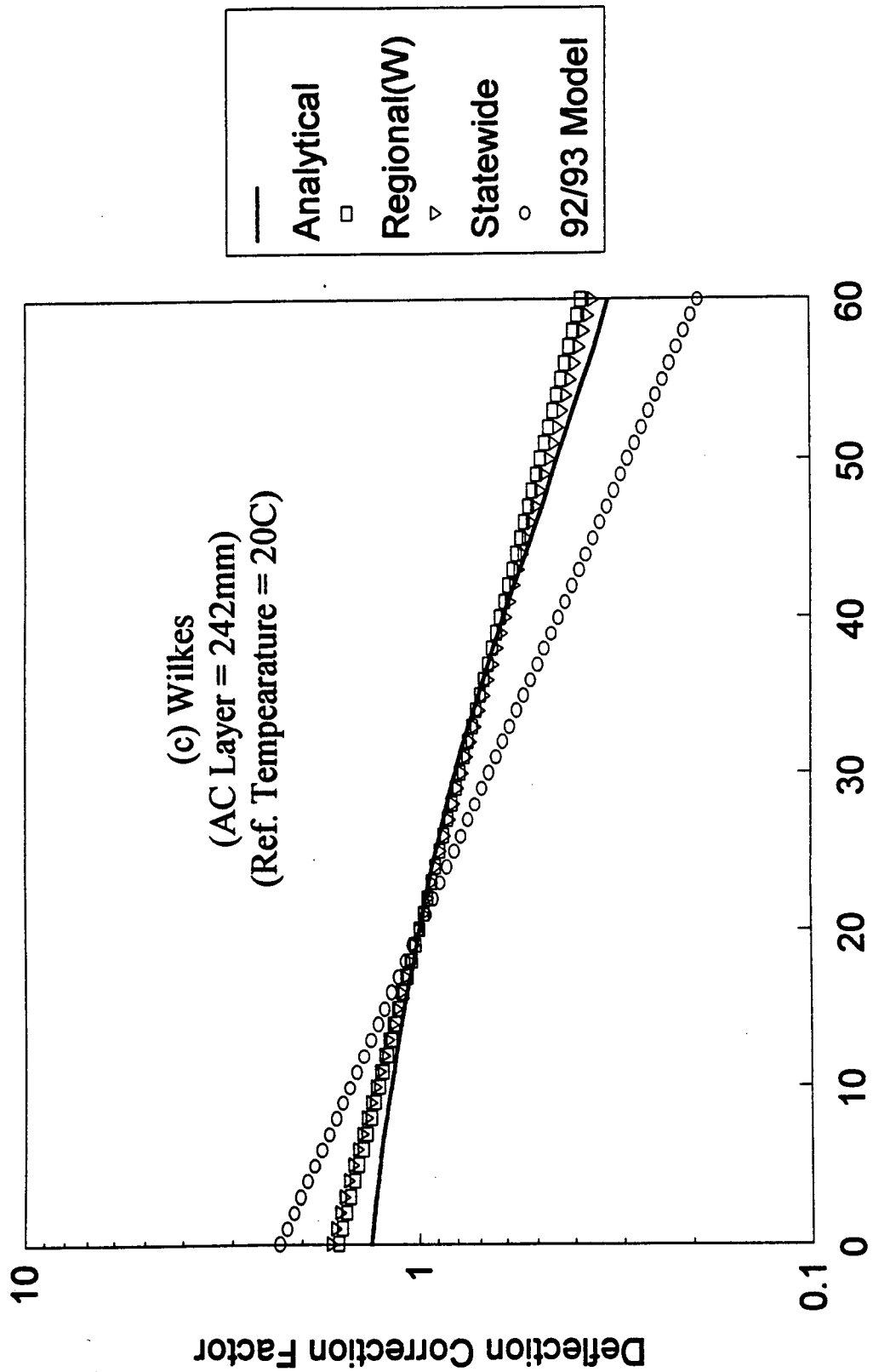

Figure III.5.8. (Continued); (c) Wilkes.

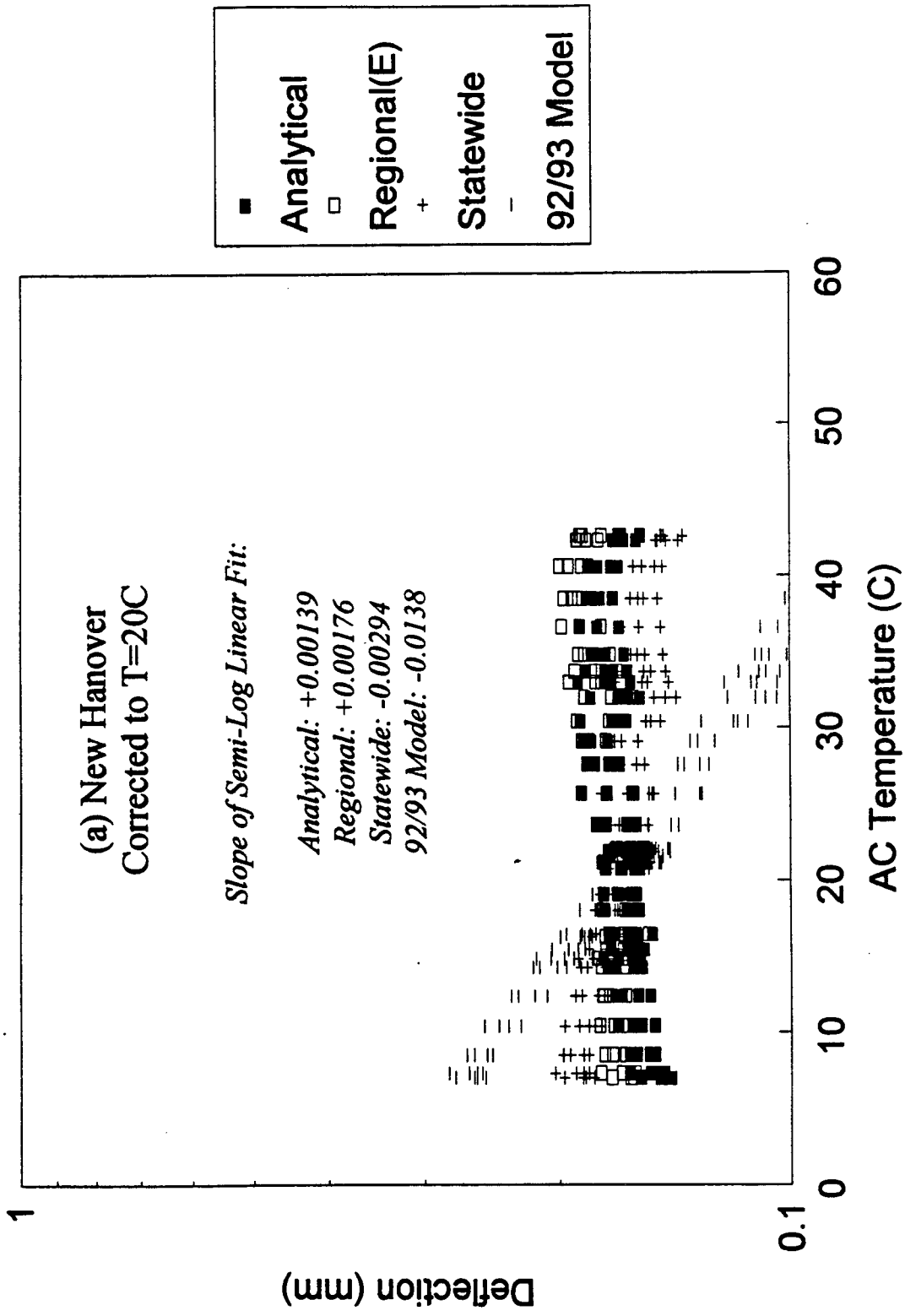

Figure III.5.9. Temperature-corrected deflections using new analytical model in comparison with the empirical models; (a) New Hanover.

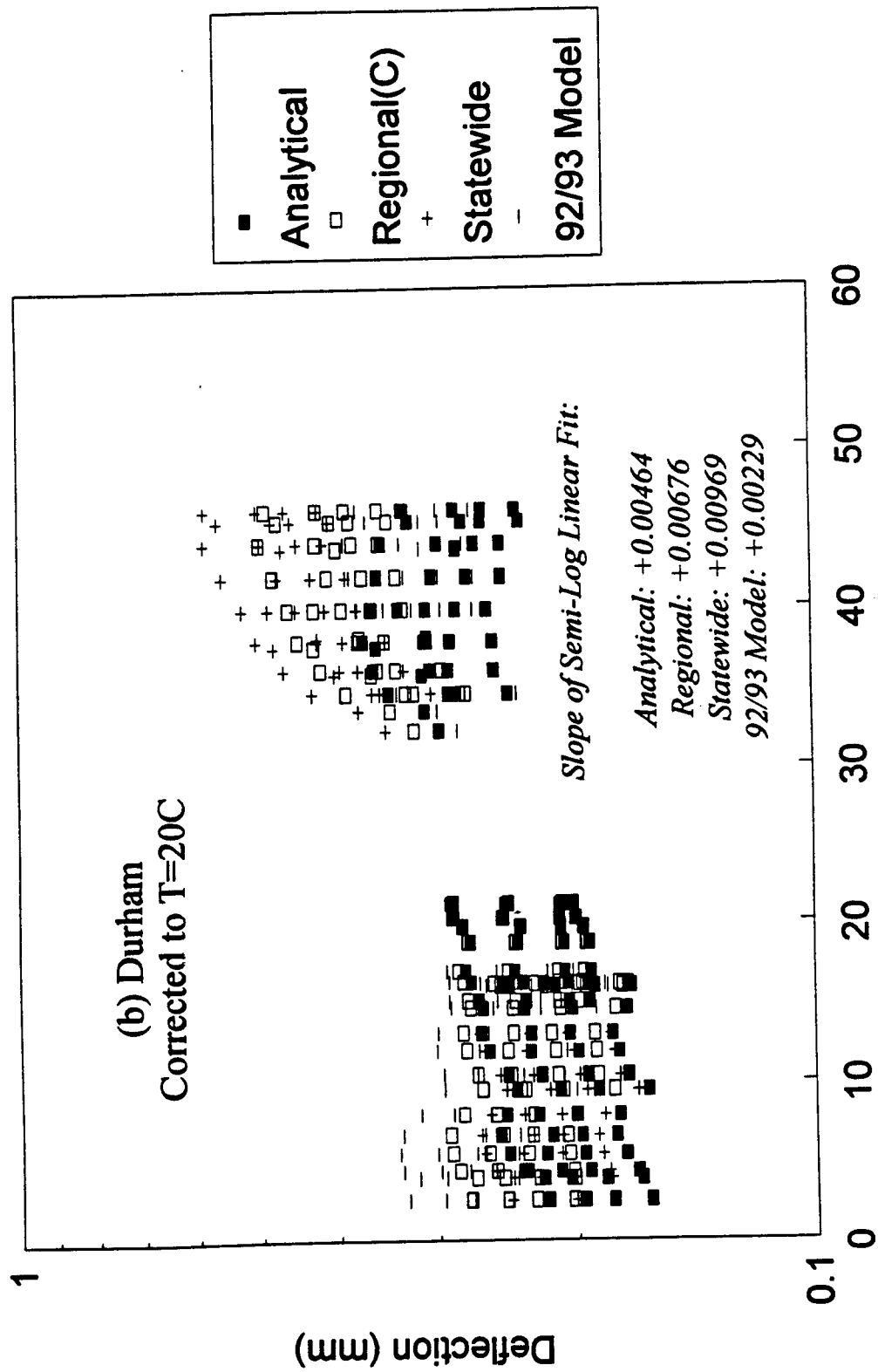

Figure III.5.9. (Continued); (b) Durham.

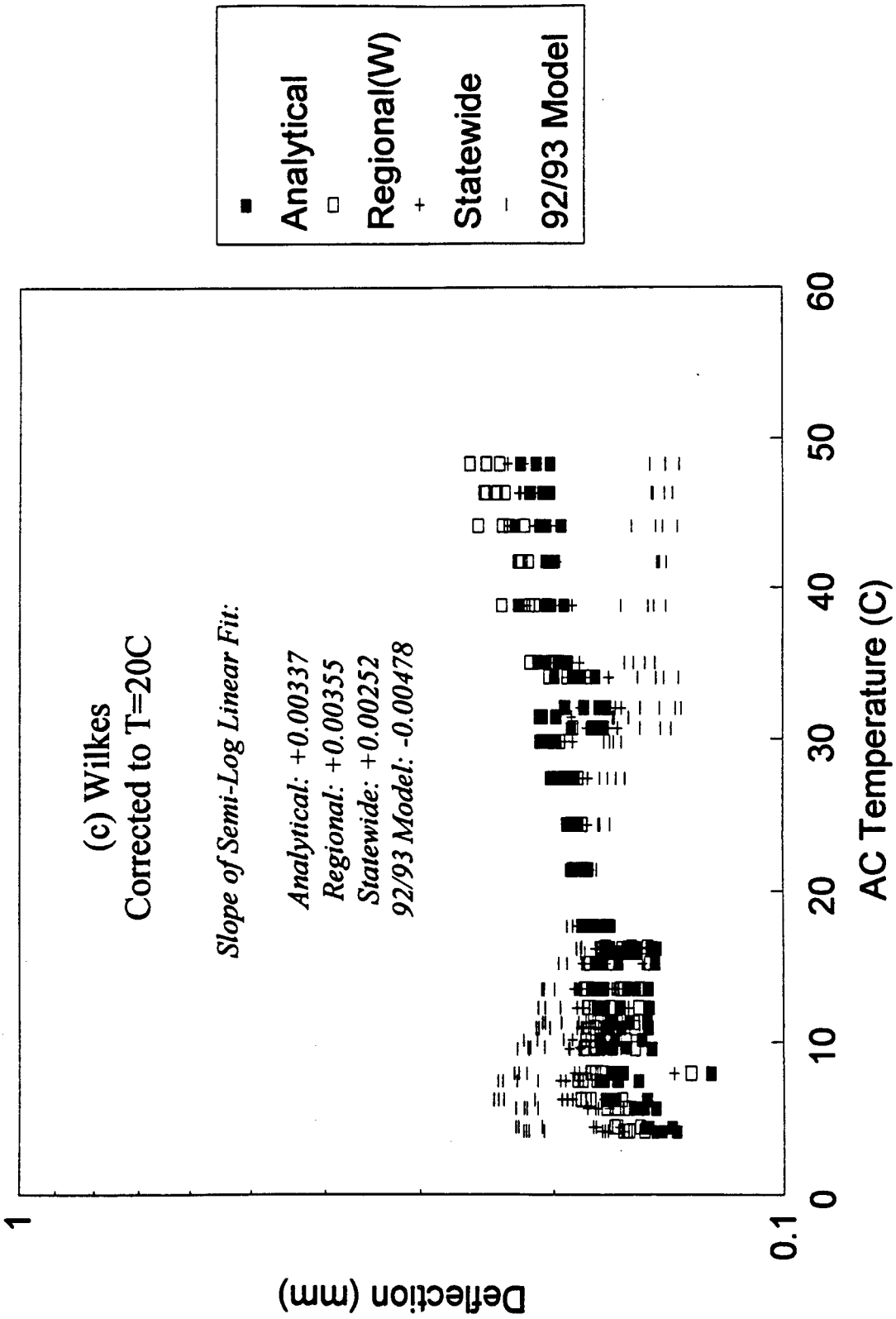

Figure III.5.9. (Continued); (c) Wilkes.

Again, the value of the analytical model lies in the fact that it can account for the individual mixture properties and the individual pavement section profile.

As mentioned before the correction of deflections is more complicated than the correction of moduli because of the involvement of parameters other than AC moduli. The deflections are normally obtained through solving a boundary value problem that simulates the actual pavement system subjected to a specified loading condition. Since the temperature effects on the deflection of an asphalt pavement is a result of changes in AC modulus due to temperature changes, an analytical procedure for temperature correction of deflections require the understanding of how the changes in AC modulus affects the changes in deflection. We took the approach of analyzing the layered viscoelastic system under different temperature levels based on a simple quasi-elastic method.

III.6. Conclusions and Findings

Based on the results of both phenomenological and analytical studies on temperature corrections of AC backcalculated moduli and FWD center peak deflections, the following conclusions are made:

1. The 92/93 empirical models, developed based on the field data obtained within the central region of North Carolina, have been tested against new field data obtained from three representative regions within the state and found to work relatively good for modulus corrections but not adequate enough for deflection corrections.

2. New regional empirical models (for east, central, and west regions of North Carolina, respectively) for both modulus and deflection corrections have been developed

based on a statistical analysis of field data from each respective region. The models corrected both moduli and deflections fairly effectively except for the sites with asphalt mixtures exhibiting unusual thermo-mechanical properties.

3. New statewide empirical models for both modulus and deflection corrections have been developed based on a statistical analysis of the entire field data obtained within North Carolina as part of the 92/93 and the current projects. The models corrected both moduli and deflections fairly effectively except for the sites with asphalt mixtures exhibiting unusual thermo-mechanical properties. The statewide models take the same forms as those of regional models both for modulus and deflection corrections. Roughly, the statewide models render temperature corrections of similar quality to those of regional models except for the sites with unusual thermo-mechanical properties, for which the corresponding regional model works better. The statewide model also takes the same form as that of the 92/93 model for modulus correction; only a different but improved model coefficient is used for the new statewide model. Overall, the new statewide empirical models yield results more accurate than the 92/93 models but still less accurate than the new analytical models.

4. New analytical models for both modulus and deflection corrections have been developed based on the theory of linear viscoelasticity and the time-temperature superposition principle and make use of the thermo-mechanical properties of the individual mixtures. In addition, the analytical deflection correction requires a forward deflection analysis of layered viscoelastic system. The advantage of the analytical models is that they explicitly account for the properties of the individual mixture (and the specific pavement profile for the case of deflection corrections), and hence it improves quality of

corrections. However, it requires individual mixture properties (and a forward deflection analysis of the pavement section for the case of deflection corrections), which may be costly and time-consuming for routine implementation.

III.7. Recommendations

Based on considerations of both accuracy and practicality, the following recommendations in relation to temperature-modulus and temperature-deflection corrections are made.

Use the statewide empirical correction models for moduli and/or deflection corrections if the mixture properties are not available and if the mixture properties are not believed to be unusual. Following the new statewide empirical model, the backcalculated AC moduli at an arbitrary temperature T can be corrected to a reference temperature T_0 (e.g., 20°C) by $E_{T_0} = \lambda_E E_T$ with $\lambda_E = 10^{0.0262(T-T_0)}$ ($\lambda_E = 10^{0.0145(T-T_0)}$ when the temperatures are in Fahrenheit). Also, following the new statewide empirical model, the FWD center peak deflections at an arbitrary temperature T can be corrected to a reference temperature T_0 (e.g., 20°C) by $w_{T_0} = \lambda_w w_T$ with $\lambda_w = 10^{-4.65x10^{-5} h_{AC}(T-T_0)}$ where h_{AC} is the thickness of the AC layer in mm and the temperatures are in Celsius. ($\lambda_w = 10^{-1.02x10^{-6} h_{AC}(T-T_0)}$ where h_{AC} is the thickness of the AC layer in inches and the temperatures are in Fahrenheit).

However, it needs to be warned that, when mixture properties are much different from the normal mixtures in North Carolina (e.g., modified mixtures, stone-matrix asphalt mixtures, etc.), this empirical model may lead to erroneous correction. In this

case, obtaining thermomechanical properties of mixtures (i.e., relaxation modulus and shift factor) and using the analytical procedure described in this report is strongly recommended.

III.8. Implementation and Technology Transfer Plan

The temperature prediction and correction procedures developed in this research can be readily implemented to routine deflection analysis at NCDOT. A FORTRAN program, PD.FOR, has been developed to automatically perform the temperature prediction analysis and is available to NCDOT. Input parameters necessary to run this program include:

1. the maximum air temperature of D-1 day,
2. the minimum air temperature in the morning of D day,
3. cloud conditions of D-1 day, and
4. pavement surface temperatures in D day prior to FWD testing.

The input parameters 1 through 3 can be obtained from local newspapers or nearby weather stations. The pavement surface temperatures prior to FWD testing needs to be measured by an FWD operator, starting as early in the morning as possible at intervals of 30 minutes. When FWD tests did not begin in a particular section until afternoon, despite beginning testing on the roadway in the morning, it is recommended to use the surface temperature data collected in the morning from other pavements.

For the correction of moduli and deflections, the new statewide model is recommended. This model can be easily implemented in the deflection analysis spreadsheet program that is currently used by the Pavement Management Unit of

NCDOT. It needs to be warned that, when mixture properties are much different from the normal mixtures in North Carolina, the statewide model may lead to erroneous correction.

REFERENCES

Acum, W. E. A. and Fox, L. (1951). Computation of road stresses in a three-layer elastic system, *Geotechnique*, **2**, 293-300.

Asphalt Institute (1982). Research and Development of the Asphalt Institute's Thickness Design Manual (MS-1), 9th ed., Research Report No. 82-2.

Ashton, J. E. and Moavenzadeh, F. (1968). Linear viscoelastic boundary value problems, *J. Engineering Mechanics*, ASCE, **94**, 117-136.

Baltzer, S. and Jansen, J. M. (1994). Temperature correction of asphalt-moduli for FWD-Measurements. Proc. 4th International Conference on Bearing Capacity of Roads and Airfields, Vol. 1, Minneapolis, MN.

Barksdale, R. G. (1971). Compressive stress pulse times in flexible pavements for use in dynamic testing, *Highway Research Record*, **345**, Highway Research Board, 32-44.

Biot, M. A. (1958). Linear thermodynamics and the mechanics of solids, Proc. *3rd U. S. National Congress of Applied Mechanics*, 1.

Burmister, D. M. (1943). The theory of stresses and displacements in layered systems and applications to the design of airport runways, *Proceedings*, Highway Research Board, **23**, 126-144.

Burmister, D. M. (1945). The general theory of stresses and displacements in layered soil systems I, II, III, *J. Applied Physics*, **16**, 84-94, 126-127, 296-302.

Carslaw, H. S. and Jaeger, J. C. (1959). *Conduction of Heat in Solids*, Oxford at the Clarendon Press, London.

Chou, Y. T. and Larew, H. G. (1969). Stresses and displacements in viscoelastic pavement systems under a moving load, *Highway Research Record*, **282**, Highway Research Board, 25-40.

CRC. (1984). *Standard Mathematical Tables*, 27th ed., CRC Press Inc., Boca Raton, FL.

Dempsey, B. J., Herlache, W. A. and Patel, A (1986). Climatic-materials-structural pavement analysis program, *Transportation Research Record* **1905**, TRB, Washington, D.C.

Dempsey, B. J., Herlache, W. A., and Patel, A. J. (1993). Design and performance of flexible pavements, *Transportation Research Record* **1095**, TRB, Washington, D.C.

Elliott, J. F. and Moavenzadeh, F. (1971). Analysis of stresses and displacements in three-layer viscoelastic systems, *Highway Research Record*, **345**, Highway Research Board, 45-57.

Ferry, J. D. (1980). *Viscoelastic Properties of Polymers*, John Wiley & Sons, Inc., New York.

Greenberg, M. D. (1978). *Foundations of Applied Mathematics*, Prentice-Hall Inc., Englewood Cliffs, N. J.

Huang, Y. H. (1969). Computation of equivalent single-wheel loads using layered theory, *Highway Research Record*, **291**, Highway Research Board, 144-155.

Huang, Y. H. (1973). Stresses and strains in viscoelastic multilayer systems subjected to moving loads, *Highway Research Record*, **457**, Highway Research Board, 60-71.

Huang, Y. H. (1993). *Pavement Analysis and Design*, Prentice-Hall Inc., Englewood Cliffs, N. J.

Johnson, A. M. and Baus, R. L. (1992). Alternative method for temperature correction of backcalculated equivalent pavement moduli. *Transportation Research Record*, **1355**, Transportation Research Board, Washington, D. C.

Jones, A. (1962). Tables of stresses in three-layer elastic systems, *Bulletin 342*, Highway Research Board, 176-214.

Kenis, W. J. (1977). Predictive design procedures, a design method for flexible pavements using the VESYS structural subsystem, *Proc., 4th International Conference on the Structural Design of Asphalt Pavements*, **1**, 101-147.

Kopperman, S., Tiller, G. and Tseng, M. (1986). *ELSYM5, Interactive Microcomputer Version, User's Manual*, Report No. FHWA-TS-87-206, Federal Highway Administration.

Kim, Y. R., Bradley, O. H., Lee, Y.-C., and Inge, E. H. (1995). *Asphalt Paving Material Properties Affected by Temperature*. Final Report Submitted to NCDOT and FHWA (Report No. FHWA/NC/95-001). Center for Transportation Engineering Studies, North Carolina State University, Raleigh, NC.

Kim, Y. R., Hibbs, B. O. and Lee, Y. C. (1995a). Temperature correction of deflections and backcalculated moduli, *Transportation Research Record*, **1473**, Transportation Research Board, 55-62.

Kim, Y. R. and Lee, Y.-C. (1995). Interrelationships among stiffnesses of asphalt-aggregate mixtures. *AAPT*, **64**, 575-609.

Kim. Y. R. and Little, D. N. (1990). One-dimensional constitutive modeling of asphalt concrete, *J. Eng. Mech.*, ASCE, **116(4),** 751-772.

Leaderman, H. (1943). *Elastic and Creep Properties of Filamentous Materials and Other High Polymers,* The Textile Foundation, Washington, D. C.

Lee, E. H. (1955). Stress analysis in viscoelastic bodies, *Quarterly of Applied Mathematics,* **13,** 183.

Love, A. E. H. (1927). *Mathematical Theory of Elasticity,* 4th ed., Cambridge University Press, New York.

Lytton. R. L., Germann, F. P., Chou, Y. J. and Stoffels, S. M. (1990). Determining asphaltic concrete pavement structural properties by nondestructive testing (NCHRP Report 327), *Transportation Research Board,* Washington, D. C.

Lytton, R.L., F.P. Germann, Y.J. Chou, and S.M. Stoffels, Determining asphaltic concrete pavement structural properties by nondestructive testing, *National Cooperative Highway Research Program Report* No. **327**, Transportation

Magnuson, A. H., Lytton, R. L., and Briggs, R. C. (1991). Comparison of computer predictions and field data for dynamic analysis of falling weight deflectometer data, *Transportation Research Record,* **1293,** Transportation Research Board, Washington, D. C., 61-71.

Moavenzadeh, F., Soussou, J. E., Findakly, H. K. and Brademeyer, B. (1974). *Synthesis for rational design of flexible pavements,* Part 3, *Operating Instructions and Program Documentation,* Reports Prepared for FHWA under Contract FH 11-776.

Morland, L. W. and Lee, E. H. (1960). Stress analysis for linear viscoelastic materials with temperature variation, *Trans., Society of Rheology,* **4,** 233.

Pagen, C. A. (1965). Rheological response of bituminous concrete, *Highway Research Record*, **67**, Highway Research Board, 1-26.

Park, S. W., Kim, Y. R., and Schapery, R. A. (1996). "A viscoelastic continuum damage model and its application to uniaxial behavior of asphalt concrete." *J. Mechanics of Materials* (in press).

Park, S. W. and R. A. Schapery (1994), A thermoviscoelastic constitutive equation for particulate composites with damage growth, *Proc. 1994 Joint Army-Navy-NASA-Air Force (JANNAF) Structures and Mechanical Behavior Working Group Conference*, Chemical Propulsion Information Agency, Baltimore, MD, 131-144.

Park, S. W. and R. A. Schapery (1996), A viscoelastic constitutive model for particulate composites with growing damage, *Int. J. Solids and Structures* (in press).

Pagen, C. A. (1965). Rheological response of bituminous concrete, Highway Research Record, **67**, Highway Research Board, 1-26.

Peattie, K. R. (1962). Stress and strain factors for three-layer elastic systems, *Bulletin 342*, Highway Research Board, 215-253.

Perloff, W. H. and Moavenzadeh, F. (1967). Deflection of viscoelastic medium due to moving load, *Proc., 2nd International Conference on the Structural Design of Asphalt Pavements*, University of Michigan, 269-276.

Read, W. T. (1950). Stress analysis for compressible viscoelastic materials, *J. Applied Physics*, **21**, 671.

Schapery, R. A. (1974). Viscoelastic behavior and analysis of composite materials, *Composite Materials*, Chap. 4, **Vol. 2**, G. P. Sendeckyj Ed., Academic Press, 85-168.

Schwarzl, F. and Staverman, A. J. (1952). Time-temperature dependence of linear viscoelastic behavior, *J. Applied Physics*, **23**, 838.

Shao, L., Park, S. W., and Kim, Y. R., (1997). A simplified procedure for prediction of asphalt pavement subsurface temperatures based on heat transfer theories". Submitted to TRB 76th nnual Meeting, 1997, Washington, D.C.

Sips, R. (1951). General theory of deformation of viscoelastic substances, *J. Polymer Science*, **9**, 191.

Solaimanian, M. and. Kennedy, T. W., (1993) Predicting maximum pavement surface temperature using maximum air temperature and hourly solar radiation, paper number 930671, TRB 72nd Annual Meeting, Washington, DC., 1993

Ullidtz, P. (1987). *Pavement Analysis*, Elsevier, New York.

Williams, M. L., Landel, R. F. and Ferry, J. D. (1955). *J. Am. Chem. Soc.*, **77**, 3701.

Yoder, E. J., and Witczak, M. W. (1975). *Principles of Pavement Design*, Wiley, New York.

Reproduced by NTIS

National Technical Information Service
Springfield, VA 22161

This report was printed specifically for your order from nearly 3 million titles available in our collection.

For economy and efficiency, NTIS does not maintain stock of its vast collection of technical reports. Rather, most documents are printed for each order. Documents that are not in electronic format are reproduced from master archival copies and are the best possible reproductions available. If you have any questions concerning this document or any order you have placed with NTIS, please call our Customer Service Department at (703) 605-6050.

About NTIS

NTIS collects scientific, technical, engineering, and business related information — then organizes, maintains, and disseminates that information in a variety of formats — from microfiche to online services. The NTIS collection of nearly 3 million titles includes reports describing research conducted or sponsored by federal agencies and their contractors; statistical and business information; U.S. military publications; multimedia/training products; computer software and electronic databases developed by federal agencies; training tools; and technical reports prepared by research organizations worldwide. Approximately 100,000 *new* titles are added and indexed into the NTIS collection annually.

For more information about NTIS products and services, call NTIS at 1-800-553-NTIS (6847) or (703) 605-6000 and request the free *NTIS Products Catalog,* PR-827LPG, or visit the NTIS Web site **http://www.ntis.gov**.

NTIS
Your indispensable resource for government-sponsored information—U.S. and worldwide

U.S. DEPARTMENT OF COMMERCE
Technology Administration
National Technical Information Service
Springfield, VA 22161 (703) 605-6000